université de bretagne occidentale

THÈSE / UNIVERSITÉ DE BRETAGNE OCCIDENTALE

sous le sceau de l'Université européenne de Bretagne

pour obtenir le titre de

DOCTEUR DE L'UNIVERSITÉ DE BRETAGNE OCCIDENTALE

Mention : Chimie Marine

École Doctorale des Sciences de la Mer

présentée par

Fabien Quéroué

Préparée à l'Institut Universitaire Européen de la Mer (IUEM) en cotutelle avec l'University of Tasmania (UTAS)

Au sein du Laboratoire des sciences de l'Environnement MARin (LEMAR), Unité Mixte de Recherche (UMR 6539), Institute for Marine and Antarctic Studies (IMAS) et l'Antarctic Climate & Ecosystems Cooperative Research Centre (ACE CRC)

Trace metals distributions in the Southern Ocean: Kerguelen Plateau process study

Soutenue le 23 Septembre 2014 devant le jury composé de :

Rapporteurs

Catherine JEANDEL
HDR, Directrice de Recherche, LEGOS, UMR 5566, CNRS/IRD/CNES/UPS, Université de Toulouse, Observatoire Midi-Pyrénées, Toulouse

Peter J STATHAM
Professor of Marine Biogeochemistry, Ocean Biogeochemistry Research Group, Southampton UK

Examinateurs

Stéphane BLAIN
Professeur, Laboratoire d'Océanographie Mircrobienne (LOMIC), UMR 7621 CNRS UPMC, Banyuls sur mer

Alessandro TAGLIABUE
Associated professeur, Dept. of Earth, Ocean and Ecological Sciences, School of Environmental Sciences, University of Liverpool, Liverpool UK

Andrew BOWIE
Directeur de thèse, Antarctic Climate & Ecosystems Cooperative Research Centre, University of Tasmania, Hobart AUS (TAS)

Géraldine SARTHOU
Directrice de these, HDR, Directrice de Recherche CNRS,, Laboratoire des Sciences de l'Environnement MARin

Eva BUCCIARELLI
Maître de conférences, Co-Directrice scientifique de thèse, Laboratoire des Sciences de l'Environnement MARin

Table of content

Table of figures

Table of tables

Acknowledgements

First and foremost I would like to thank my supervisors, Andy Bowie, Géraldine Sarthou, Delphine Lannuzel, Pier van der Merwe, Ashley Townsend and Eva Bucciarelli. I'm very grateful for the opportunity you gave me and for all the expertise you shared with me and your patience. It was a fantastic PhD. It was a great journey. I spent such great time with you at sea, in the lab, on element2 (I did it and I kept my curly hairs!!!! I did it Ash), at the office, out of the office, on the mountain, mountain biking (Thanks Pier for this nice crash with your camera! Every one saw it after my defence), skiing, playing chess, playing volleyball and badminton, fishing, dancing, cleaning, filling, lifting all sorts of bottles or tubes and empties them also.

I would like to thank Peter Statham, Catherine Jeandel, Alessandro Tagliabue, Stéphane Blain, Andrew Bowie, Géraldine Sarthou and Eva Bucciarelli, members of my jury, for their useful comments and critics on my work in order to improve my thesis.

I would like to thank Andrew Bowie, Stéphane Blain, Bernard Quéguiner, Catherine Jeandel, Sophie Cravatte, Gérard Eldin, Alexandre Ganachaud, chief scientists of the GP13, KEOPS2 and PANDORA cruises. Thanks for the opportunity you gave me. I would like to thank also the captains and the crews involved in these cruises.

I would like to thank Hélène Planquette for her support and comments on my PhD.

During these 3 cruises, I was involved in 3 different TMR teams so thanks to the entire members! Thanks to everyone who shared with me a bit of time in the van. I would like to thank also my cabin mates!!! Thato, Bruno and Max!!! Thanks to all the scientists I met at sea.

I must thank the incredible staff at ACE CRC, IMAS, and LEMAR for the help and fantastic work they do. Thanks a lot Wen, Kate, Heidi, Denbeigh, Gene and Anne-So. It was fantastic to work with you and thanks for your contribution to make ACE CRC, IMAS and LEMAR nice places to work.

I thank also my office mates! Thomas, Marie, Julia, Violette, Rachel, Manon, Ami, Nathalie, Rob, Axel, Manu, Julie, Jorge, Luiz, Molly, Anna, Mana, Tank. I know that's difficult to stay calm when I'm furious in front of my computer so thank you for not throwing me out. I would like to thank you for all your support during this PhD and also for all the great moments we shared in and out of work. This PhD has been incredible because of you

guys. Thanks Manu for the place you gave me in your shared house, for the rides we shared even if I did not manage to convert you into a cyclist!!! Thanks Rob for your support in and out of the office. Thanks for teaching me how to catch abalones! Thanks for all your tips about Tassie. Thanks Tank for all your support in the office, for your company when we went at the Ocean Science meetings and thanks for all the discussion we had about data acquisition, treatment and publishing.

I would like to thank Thibault Wagener, who answered a very important call, the call, and sorry but I'm still do not smoke!!!

Yann, thanks for all your support. You were a supervisor when I started college and you were here all the way through my life up to the PhD! Unbelievable!!!

I would like to thank all the volleyball players I played with. Even opponents, I loved to block your attacks and smashed the ball as a middle player. It was great to release the pressure on the field. Sorry if I returned to my first sport, cycling. It was so much fun to get back to it with your help Pier. Thanks a lot. It was great to go down the Mt Wellington (for sure the uphill part was fun but a little bit less enjoyable).

My family, Papa, Maman, Florent. You believed in me. Followed me in Tassie. Helped me all the way through my studies. You were always here when I needed. Hopefully Skype was here when I was in Tassie. I love you. Dad now you have to translate to Mum!!

Thanks, JJ, Liliane, Benjamin, Elodie, Raphael, who support me at the beginning of my studies in Rennes. I spent 3 incredible years with you and if I had to do it again, I will. Thanks a lot, I enjoyed it!!! But next time please don't wake me up with a bucket full of water!

I would like to thank Marie-André, Thierry and Morgane for all the great moment we shared and the great support.

The last but not the least, Magaly, I would like to tell you that I'm very grateful for your permanent and lovely support, you believed in me and followed me for a year in Tassie. Thanks for helping me drying all these tubes!!! I love you.

PS: I would like to thank also my computer, the dissolved Fe FIA, my multi-element manifold and the ELEMENT2 as they stayed alive until the end of my PhD!!!! I won't thank the rail of the tram!!! You failed to kill me 8 months ago… But I want to thank here my helmet and the company MET, which built it, for the great work the do for cyclist safety!!! You saved my life!!! Please ride safely, ride with your helmet!!!

Chapter I

Introduction

1 Scientific context

The atmospheric concentration of carbon dioxide (CO_2) is of a great interest for scientists since the largest contribution to Earth total radiative forcing is caused by the increase in the atmospheric concentration of CO_2 since 1750 (IPCC 2013). Indeed, from 1750 to 2011, anthropogenic CO_2 emissions have released 555 gigatons of carbon (GtC) that accumulated within different ecosystems and mainly in the atmosphere (240 GtC), 160 GtC have accumulated in natural terrestrial ecosystems and 155 GtC have been taken up by the ocean (IPCC 2013). Two processes lead to the transfer of CO_2 from the atmosphere to the ocean: the physical and the biological carbon pumps (Fig. I.1).

First, the physical carbon pump is initialized by the surface ocean, which constantly exchanges gases and heat with the low atmosphere. The solubility of CO_2 in seawater increases when temperatures decrease. Thus, in the high latitudes, low temperatures, strong winds, and waves favour the transfer of CO_2 into the ocean. Then, CO_2 is exported beneath the ocean surface via the sinking of the cold CO_2-rich waters. This physical removal of CO_2 is also called the "solubility pump". When these cold waters return to the surface ocean and warm up again, they release CO_2 to the atmosphere. Secondly, the organic biological carbon pump is initialized in the surface ocean by phytoplankton, which assimilates carbon (C) via photosynthesis, converting CO_2 and water in organic matter and oxygen (Fig. I.1). This process removes aqueous CO_2 from the euphotic layer, where light penetrates sea surface, and leads to the storage of around 20% of the surface C inventory in the ocean interior (Laws et al., 2000; Falkowski, 2002). In addition, C can also be fixed by corals, foraminifera, coccolithophore or mollusk and crustacean as calcium carbonate to form protective coating or shells, however, this process is counter balanced by the production of carbonic acid, which increase the concentration of CO_2 in seawater initiating a diffusive flux of CO_2 from the ocean to the atmosphere, the so called carbonate counter pump. These are the reasons why the biological pump of C is a key regulator of the global C cycle. In its absence, atmospheric CO_2

concentration would increase by approximately 50 % (200 ppmv), a considerable fraction compared to the present ~ 400 ppmv (Falkowski, 2002).

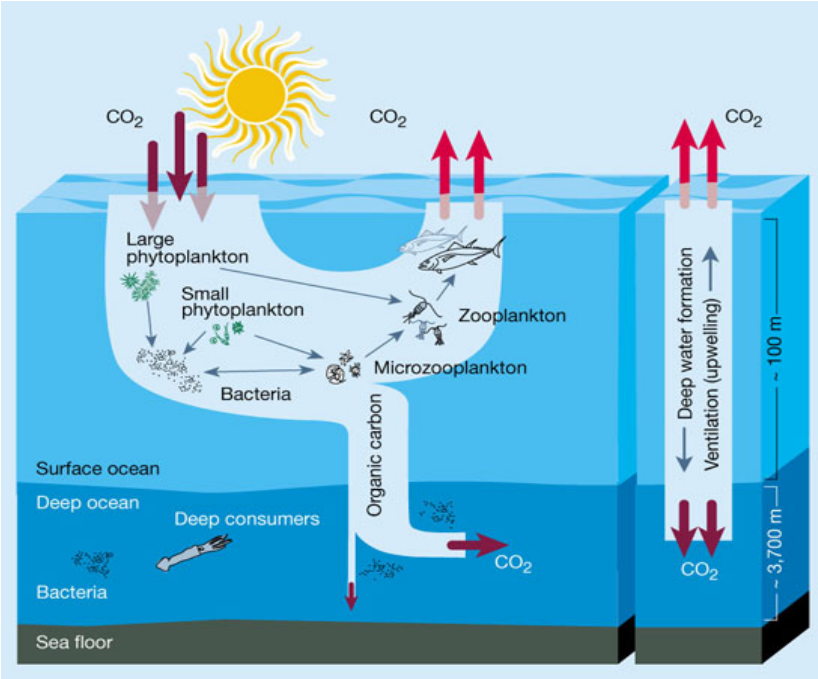

Figure I.1 Schematic of the biological (left) and physical (right) pumps of carbon from Chisholm (2000)

2 Importance of trace metals for the biological activity

Over the past few decades it has been widely demonstrated that trace metals play a fundamental role in marine biogeochemical cycles and are particularly important for primary production (Group, 2007). The biological demand of trace metals is almost three orders of magnitude lower than macro-nutrients such as phosphorus (Twining and Baines, 2013) and as such these elements are therefore called micro-nutrients. Trace metals are required in many metabolic processes and iron (Fe) is the most important amongst them (Table I.1). It is required for numerous metabolic processes and plays a particularly important role in electron transport in photosynthesis (Geider et al., 1993). This metal is also found in enzymes required for N_2 fixation, nitrate and nitrite reduction, reduction of reactive oxygen species, conversion of hydrogen peroxide to water and disproportionation of superoxide to hydrogen peroxide and O_2 (Sunda, 1989; Twining and Baines, 2013). Due to its very low concentrations in open ocean surface waters, taken together with its physiological function and in particularly its regulation of the nitrogen fixation by diazotrophs in nutrient poor low latitude regions, Fe has

been shown to control primary productivity in ≈ 50% of the World's ocean (Moore et al., 2004; Moore et al., 2009; Boyd and Ellwood, 2010). This is notably the case in High Nutrient Low Chlorophyll (HNLC) areas, term used to describe regions of the World's ocean where the plant biomass is low relative to the nutrient stocks. These regions cover 25 % of the World's ocean and are located in the equatorial Pacific Ocean, the subarctic Pacific Ocean and the Southern Ocean, the latest being the largest (de Baar et al., 2005).

Other trace metals such as manganese (Mn), cobalt (Co), nickel (Ni), copper (Cu) and cadmium (Cd) have not been studied as extensively, but they also play key roles in many essential cellular cycles and may (co)-limit marine primary productivity (Morel and Price, 2003; Twining and Baines, 2013). Metals such as Mn (Peers and Price, 2004; Wolfe-Simon et al., 2006), Cu and Ni (Nuester et al., 2012; Ho, 2013) are used as co-factors in the formation of superoxide dismutase (SOD) (Wolfe-Simon et al., 2005), which are important enzymes for the defence of cells against harmful reactive oxygen species. Manganese is also needed in photosystem II for the oxidation of water during photosynthesis (Sunda et al., 1983). Cobalt has important biological implications as it is at the centre of the vitamin B12, which is synthesised by bacteria and assimilated by eukaryotic phytoplankton (Croft et al., 2005; Bertrand et al., 2007). Nickel is required in urease, an enzyme that hydrolyses urea to provide nitrogen (N) to algal cells (Price and Morel, 1991; Morel et al., 2003). Copper limitation can be linked to Fe limitation, because of the replacement in the photosynthetic apparatus of Fe-rich cytochrome c6 by Cu-containing plastocyanin (Peers and Price, 2006), and of the use of a multi-copper oxidase in some phytoplankton Fe transport systems (Maldonado et al., 2006; Peers and Price, 2006). Under low zinc (Zn) conditions, Cd- and Co-containing carbonic anhydrase (CA) (Lane and Morel, 2000; Lane et al., 2005; Park et al., 2007; Xu and Morel, 2013), an enzyme catalysing the conversion of bicarbonate to carbon dioxide, can be substituted for Zn-containing CA for some biological functions (Price and Morel, 1990). Manganese, Co, Ni and Cu can therefore (co)-limit phytoplankton growth in the ocean (Price and Morel, 1991; Sunda and Huntsman, 1995; Saito et al., 2002; Peers and Price, 2004; Peers et al., 2005; Peers and Price, 2006; Saito and Goepfert, 2008; Ho, 2013). Lead (Pb) is the only non-bioactive studied trace metal passively removed from the dissolved phase by passive adsorption and bio-accumulated.

Table I.1 Enzyme and enzyme cofactor containing trace metals and their biological function from Twining and Baines (2013).

Fe	Cytochromes	Electron transport in photosynthesis and respiration
	Ferredoxin	Electron transport in photosynthesis and N fixation
	Other Fe-S proteins	Electron transport in photosynthesis and respiration
	Nitrate and nitrite reductase	Conversion of nitrate to ammonia
	Chelatase	Porphyrin and phycobiliprotein synthesis
	Nitrogenase	N fixation
	Catalase	Conversion of hydrogen peroxide to water
	Peroxidase	Reduction of reactive oxygen species
	Superoxide dismutase	Disproportionation of superoxide to hydrogen peroxide and O_2
Mn	O2-evolving enzyme	Oxidation of water during photosynthesis
	Superoxide dismutase	Disproportionation of superoxide to hydrogen peroxide and O_2
	Arginase	Hydrolysis of arginine to ornithine and urea
	Phosphotransferases	Phosphorylation reactions
Ni	Urease	Hydrolysis of urea
	Superoxide dismutase	Disproportionation of superoxide to hydrogen peroxide and O_2
Cu	Plastocyanin	Photosynthesis electron transport
	Cytochrome oxidase	Mitochondrial electron transport
	Ascorbate oxidase	Ascorbic acid oxidation and reduction
	Superoxide dismutase	Disproportionation of superoxide to hydrogen peroxide and O_2
	Multicopper ferroxidase	High-affinity transmembrane Fe transport
Co	Vitamin B12	C and H transfer reactions
Cd	Carbonic anhydrase	Hydration and dehydration of carbon dioxide

3 Trace metal cycle

3.1 The trace metal chemical speciation

3.1.1 Inorganic speciation

Trace metals are typically present as free ions or as oxides/hydroxides in seawater. Iron is found as free Fe^{2+}, which is more soluble than the oxidized form Fe^{3+} (Table I.2). Fe^{2+} is

rapidly oxidized by oxygen or hydrogen peroxide, which leads to the dominance of Fe^{III} state in seawater (Millero et al., 1987; Moffett and Zika, 1987; Millero and Sotolongo, 1989).

Table I.2 Inorganic Fe speciation in seawater at pH = 8 from de Baar and de Jong (2001). Fractions less than 0.001 are not given.

Species	Fraction (%)	Species	Fraction
Fe^{2+}	75.84	Fe^{3+}	2.9×10^{-9}
$FeHCO_3^+$	0.54	$FeCl^{2+}$	
$FeCO_3$	22.58	$FeCl_2^+$	
$Fe(CO3)^{2-}$	0.05	FeF^{2+}	
$FeOH^+$	0.099	FeF_2^+	
$Fe(OH)_2$		FeF_3	
		$FeSO_4^+$	
		$FeOH^{2+}$	3.66
		$Fe(OH)_3$	91.81
		$Fe(OH)_4^-$	4.53

Cobalt is also found as Co^{II} and Co^{III} oxidation state. Co^{II} is the dominant form even if less thermodynamically stable (Turner et al., 1981; Ćosović et al., 1982; Donat and Dryden, 2001). Co^{III} oxydes or hydroxydes are almost insoluble (Moffett and Ho, 1996). Copper can be found as inorganic Cu^{II} only, however this state has been found to be toxic to some marine phytoplankton while free cadmium, Cd^{II} showed to be not as toxic as free Cu (Brand et al., 1986). Manganese exists as three inorganic oxidation states Mn^{II}, Mn^{III} and Mn^{IV}. Mn^{II} is the most soluble and dominating oxidation state in seawater (Tebo et al., 2007). It mainly forms complex with chloride $MnCl^+$ and to a lower extent with sulphate and carbonate (Byrne et al., 1988). In surface water, photochemical and microbial processes strongly influence the distribution of dissolved Mn reducing particles and increasing Mn^{2+} concentrations (Sunda and Huntsman, 1990; Sunda and Huntsman, 1994). Nickel is predominantly present as Ni^{2+} free ion or as $NiCl^+$ complex (Byrne, 2002). Lead is mostly present in seawater as $PbCl_4^{2-}$ but is also found as $PbCl_3OH^{2-}$ (Byrne, 2002).

3.1.2 Organic speciation

Trace metals are known to be organically chelated to organic ligands. The formed complexes reduce the transfer from the dissolved phase to the particulate phase by precipitation or scavenging. Over 99.7 % of dissolved Fe is chelated by organic ligands (Gledhill and Van den Berg, 1994; Rue and Bruland, 1995; Gledhill and Buck, 2012).

Manganese is also found chelated with organic ligands and especially in hypoxic environments (Trouwborst et al., 2006; Duckworth et al., 2009) and in pore water (Madison et al., 2013; Luther III et al., 2015). Manganese can compete with Fe for the same organic ligands, notably siderophores, biogenic chelating agents produced by microbes and plants to increase the bioavailability of micronutrients (Kraemer, 2004; Duckworth et al., 2009). Cobalt is also found in complexes with organic ligands, the most important form in the dissolved phase (Saito and Moffett, 2001; Ellwood et al., 2005) and affecting both its bioavailability and solubility (Moffett and Ho, 1996; Ellwood and van den Berg, 2001; Saito and Moffett, 2001; Ellwood et al., 2005). While Cu^{2+} is toxic to some marine phytoplankton (Brand et al., 1986), it has been suggested that phytoplankton can produce organic compounds that chelate Cu^{2+} reducing the overall copper toxicity (Moffett and Brand, 1996). Surface dissolved Cu has been found to be 99.7% complexed with strong organic ligands (Coale and Bruland, 1988). Dissolved Ni can also be found as organically complexed in seawater from 35 to over 90 % by strong ligands (Donat et al., 1994; Xue et al., 2001; Ndung'u et al., 2003; Turner and Martino, 2006). Lead has also been found in organic complexes (50%) in the Eastern North Pacific (Capodaglio et al., 1990).

3.2 The trace metal physical speciation

The physical speciation is a continuous size scale separating multiple phases characterized by the filter size used to dissociate the different fractions of the sampled seawater. The particulate phase (pTMs) represents the fraction larger than 0.2 µm (Fig. I.2). The dissolved fraction represents the fraction smaller than 0.2 µm and is generally more concentrated than the particulate fraction. The colloidal phase is within both previous categories as it represents the fraction between 1 µm and 0.01 µm (Fig. I.2). Within the dissolved phase, two additional fractions can be dissociated to better describe this phase, the soluble fraction below 0.02 µm and the nanoparticles between 0.1 µm and 0.005 µm.

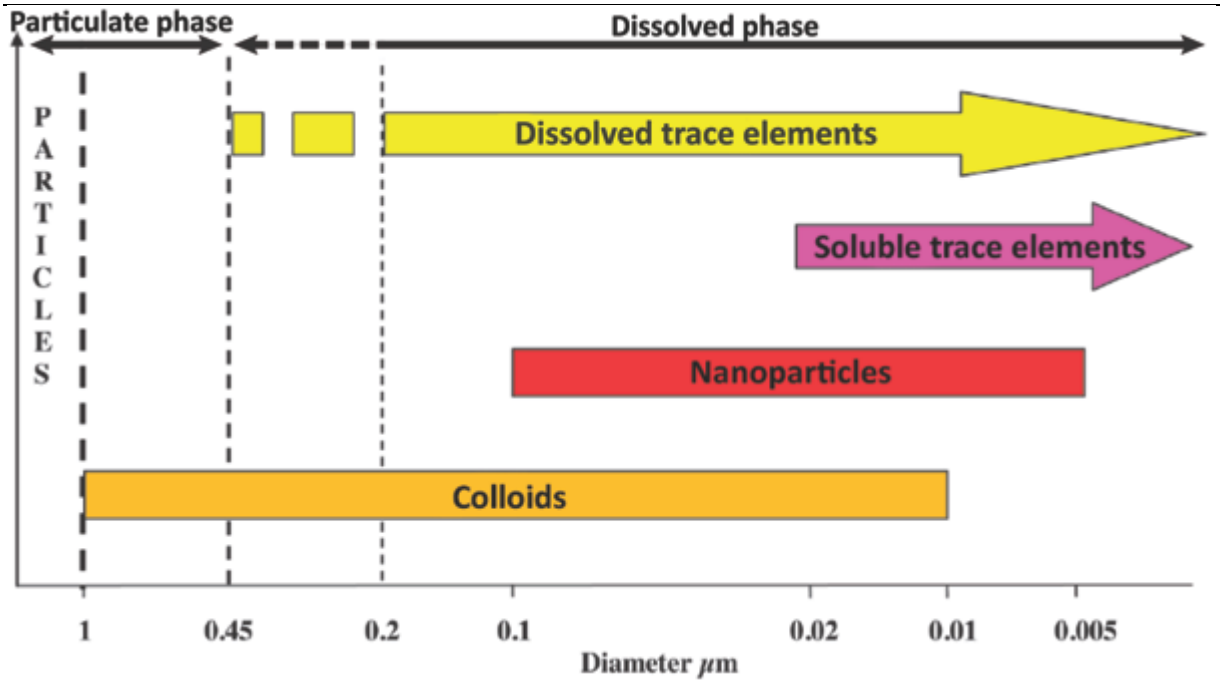

Figure I.2 Schematic of trace metal size fractions. Figure adapted from Raiswell and Canfield (2012).

3.3 Sources of trace metals

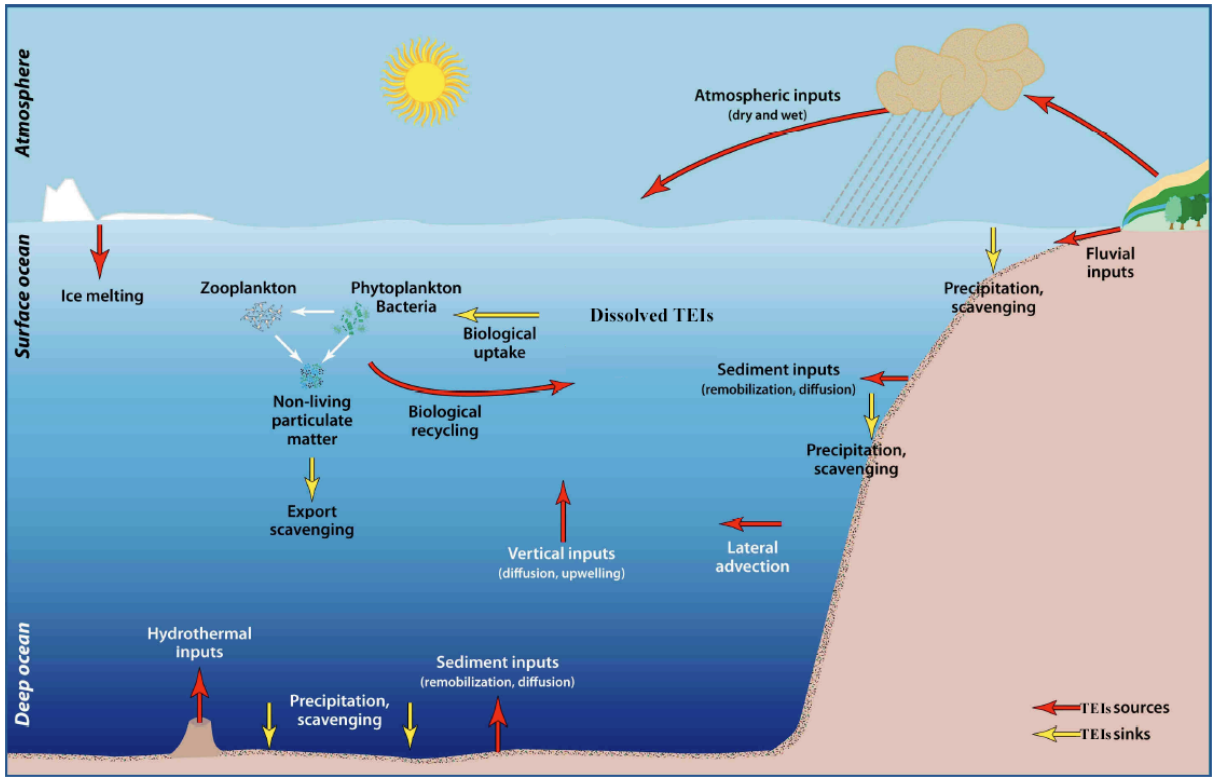

Figure I.3 Schematic of trace metals sources and sinks and recycling processes in the ocean adapted from Sarthou (2009)

3.3.1 Riverine inputs

The Amazon and the large Asian rivers such as the Yang Tsé Kiang provide a large amount of lithogenic material to coastal waters either in the dissolved or the particulate phase (Milliman and Meade, 1983; Chester, 2009). The overall riverine discharge has been estimated to about 16 10^{15} g y^{-1} of particulate materials and 4.6 10^{15} g y^{-1} of dissolved metals (Degens et al., 1991). Rivers have been shown to be important sources of dissolved iron (dFe) to the World's oceans, except for the remote open ocean, displaying high dFe concentrations in freshwaters, around (on average) 720 nmol L^{-1} (Chester, 1990; de Baar and de Jong, 2001). The dFe river inputs to estuaries have been estimated at about 26 10^{9} g y^{-1} (de Baar and de Jong, 2001). For coastal environments, river inputs have been considered as the main source of Fe (Guieu and Martin, 2002). However, 90 % of dFe do not leave the estuary due to flocculation with organic matter and subsequent precipitation in the salinity gradient (Chester, 2009). On the other hand nanoparticles (≈ 5 nm) attached to sediment grains may escape the estuarine removal process and as suspended load to enrich the dissolved phase out of the estuary (Raiswell et al., 2006). Riverine fluxes of Fe to the coastal environment have been estimated to be 2 orders of magnitude higher than the Mn flux and 3 orders of magnitude higher than Co, Ni, Cu, Cd, Pb fluxes (Yeats and Bewers, 1985).

3.3.2 Atmospheric inputs

Atmospheric deposition is a major source of dissolved trace metals to the World's open oceans (Duce and Tindale, 1991; Jickells, 1995; Ussher et al., 2013; Wuttig et al., 2013). Aerosols can reach the troposphere where they are transported rapidly and over long distances. However, the transport distance depends on the rate of gravitational settling and particle size (Maring et al., 2003; Kallos et al., 2006). TM can be deposited to the surface ocean by dry or wet deposition. Although anthropogenic influence can occur due to the combustion of fossil fuel or biomass burning, most of the aerosols are of natural origin (Boyle, 2001; Jickells and Spokes, 2001; Jickells et al., 2005; Boyle et al., 2014). The main sources are deserts from North Africa (Sahara), Patagonia, the southern regions of Africa, Mongolia or Australia (Prospero et al., 2002; Mahowald et al., 2005; Ginoux et al., 2012). Additional possible aerosol sources are likely to be from extra-terrestrial origin and have been suggested to be as large as the aeolian dust inputs (Johnson, 2001; Plane, 2012).

As shown Fig. I.4, atmospheric dust fluxes are spatially and temporally highly variable especially in regions prone to alternating wet and dry seasons. Most of the dust deposition is observed in the northern hemisphere (Fig. I.4) and almost 80 % of the deposition in the World's Oceans occur during wet events (Fan et al., 2006).

The type of deposition (wet or dry), the presence of organic ligands, primary production, the source of aerosol and atmospheric chemistry may change the flux of dissolved TMs from atmospheric sources (Desboeufs et al., 2001; Bonnet and Guieu, 2004; Journet et al., 2008). Iron, Mn and Pb are amongst the main TMs for which dissolved distribution can be influenced by dust deposition (Boyle et al., 2005; Jickells et al., 2005; Boyle et al., 2014). With regards to Fe and Mn this is due to their abundance in the Earth's crust, 5 % and 1 % respectively (Taylor and McLennan, 1985; Taylor and McLennan, 1995; McLennan, 2001) and with regards to Pb, this is due to its anthropogenic source (see text below). The remoteness of the Southern Ocean from dust source leads to low atmospheric fluxes (Jickells et al., 2005). However, local dust inputs were observed in areas close to South Africa (Boyé et al., 2012), Crozet Island (Planquette et al., 2007; Castrillejo et al., 2013) and in the Drake passage (Klunder et al., 2013). The main uncertainty lies on the solubility of these aerosols when they enter seawater. A wide range of solubilities have been observed in the literature from 0.001 % to 90 % (Bonnet and Guieu, 2004; Jickells et al., 2005; Mahowald et al., 2005; Baker et al., 2006; Fan et al., 2006; Wagener et al., 2008) (Bonnet and Guieu, 2004; Desboeufs et al., 2005; Sedwick et al., 2007; Journet et al., 2008; Schroth et al., 2009; Boyd et al., 2010; Schulz et al., 2012), due to various processes such as the dust source, natural vs anthropogenic knowing that anthropogenic solubility is higher (Spokes et al., 1994; Desboeufs et al., 2005; Sedwick et al., 2007), mineralogy (Journet et al., 2008), the particles size and concentration (Bonnet and Guieu, 2004; Hand et al., 2004; Mackie et al., 2005; Baker and Jickells, 2006), UV light levels (Zhu et al., 1997) or cloud pH (Spokes et al., 1994; Mackie et al., 2005) amongst them.

Lead (Pb) is a key element used to trace anthropogenic sources of trace metals to the ocean. The main source of Pb into the ocean is wet or dry atmospheric deposition. Historically Pb has reached the atmosphere mainly after combustion of leaded gasoline, coal fired power stations, refineries/smelters, lead-acid batteries, fertilisers and pesticides. However the phase-out of leaded gasoline in the developed countries of northern hemisphere commenced in the 1970's, with surface ocean Pb concentrations subsequently decreasing

(Boyle et al., 1994; Wu and Boyle, 1997). Recently, 3D maps of the Atlantic Ocean (GEOTRACES Intermediate Data Product 2014) revealed high dPb concentrations in waters collected at 1000 m deep, fingerprinting the high Pb inputs to the North Atlantic from North America and Europe when the use of leaded gasoline was still important (Fig. I.5a). These water masses with high dPb concentrations also exhibit high Pb isotopic ratios ($^{206}Pb/^{207}Pb$) (Noble et al., 2014) due to higher values associated with US and European leaded gasoline (Boyle et al., 1994). In some regions such as South Africa, surface seawater still shows elevated dPb concentrations, which is thought to be due to atmospheric inputs from the African continents and late phase out of leaded gasoline (Witt et al., 2006; Boyé et al., 2012)(Fig. I.5b). In the North and central Indian Ocean, extremely high dPb concentrations are due to the recent and rapid industrialization of India, South Asia and Oceania and the late phase out of leaded gasoline (Boyle et al., 2014; Echegoyen et al., 2014). In the Southern Ocean, relatively low dPb concentrations were observed probably due to the remoteness from industrial areas (Echegoyen et al., 2014). However, in areas such as Crozet Island, south of Africa and south of Australia, enhanced surface concentrations were observed probably due to local atmospheric deposition (Boyé et al., 2012; Castrillejo et al., 2013).

With regards to Co, Shelley et al. (2012) showed that in Sargasso Sea, despite significant Fe atmospheric inputs, no significant trend was observed for Co due to relatively modest input in early summer, which could be more significant in late summer. Indeed dust loading from Sahara is higher in late summer compared to preceding months (Shelley et al., 2012). Similarly, in the subtropical domain of the Atlantic sector of the Southern Ocean, unlike Fe (Chever et al., 2010a), no significant atmospheric input of Co were observed (Bown et al., 2011). To our knowledge, no specific studies of Ni, Cu, Cd atmospheric input in the open ocean has been conducted recently, presumably due to their negligible continental crust relative abundance (Taylor and McLennan, 1985; Taylor and McLennan, 1995; McLennan, 2001).

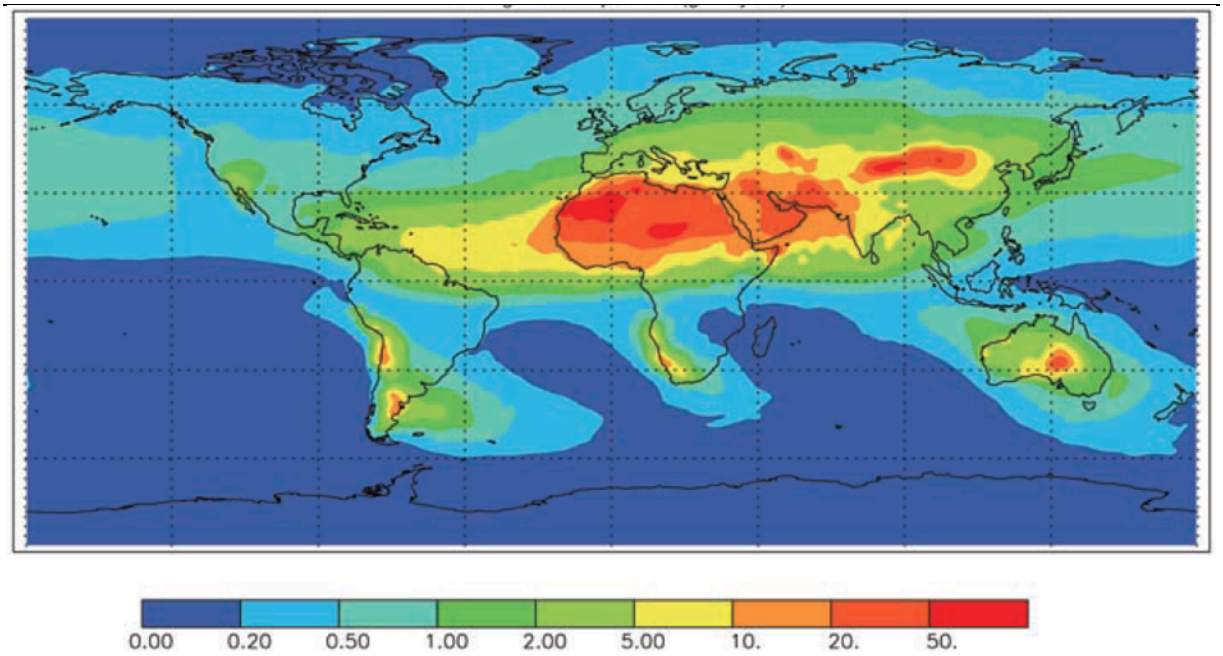

Figure I.4 Dust fluxes to the World's Oceans based on a composite of three published studies (Mahowald and Luo, 2003; Tegen, 2003; Ginoux et al., 2004) in g m^{-2} y^{-1} from Jickells et al. (2005).

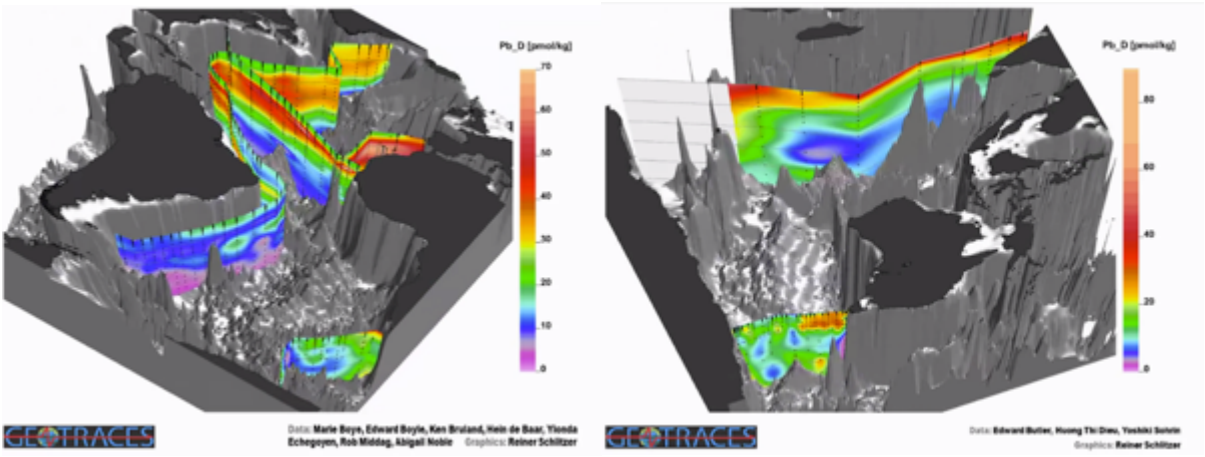

Figure I.5 Three dimensional representation of the dPb in the Atlantic and the Atlantic sector of the Southern Ocean (left) and the Indian and Southern Oceans (right) (Schlitzer, 2014).

3.3.3 Sediment inputs

Sediment resuspension and associated pore-water release are important sources of dissolved Fe and Mn (Elrod et al., 2004; Blain et al., 2008b; Lohan and Bruland, 2008; Dulaiova et al., 2009; Ardelan et al., 2010; Nielsdóttir et al., 2012; Hatta et al., 2013; Measures et al., 2013). Moore and Braucher (2008) showed that sedimentary dFe input could be as large as atmospheric one. Two processes supply dissolved trace metals from the

sediment to the benthic boundary layer (BBL), reductive dissolution and the non-reductive release. The later can mobilize trace metals after particle resuspension and subsequent particle dissolution and is favoured in oxic BBL with low organic matter degradation. The former involves degradation of sinking organic matter by bacteria or other micro or macro organisms. During degradation, Fe and Mn are reduced and transferred to pore-waters. Anoxic/suboxic conditions in the sediment are crucial to mobilize Fe and Mn and increase the dFe and dMn concentrations in pore-waters (Homoky et al., 2011). The input of dFe and dMn to the BBL is possible only if the sediment oxic layer is relatively thin to avoid back precipitation.

Iron stable isotopes ($\delta^{56}Fe$) are key tools to differentiate between the non reductive release and the reductive dissolution of Fe. Negative $\delta^{56}Fe$ values are associated with a reductive dissolution while positive ones with a non-reductive release (Radic et al., 2011; Homoky et al., 2013; Conway and John, 2014; Labatut et al., 2014).

The transport of water masses, which interacted with the BBL, by lateral advection or vertical mixing extends the enriched area beyond areas directly influenced by sediment resuspension (de Baar et al., 1995; Lam and Bishop, 2008).

In addition, high dCo concentrations in deep water masses have already been attributed to sediment resuspension (Noble et al., 2008; Bown et al., 2011; Bown et al., 2012; Noble et al., 2012). Furthermore, in the Southern Ocean, over the Kerguelen plateau, high dCo concentrations were observed due to lateral advection of water masses transporting sedimentary materials from Heard Island (Bown et al., 2012). High dCo concentrations has also been observed in deep waters of the Atlantic Ocean due to the lateral advection of Antarctic bottom water and dissolution of particulate material during its transport (Dulaquais et al., 2014).

Recently, Jacquot and Moffett (2014) observed a marked increase of dCu concentration in bottom waters presumably due to sediment remobilization and associated organic ligand input.

To our knowledge, no previous studies have reported sedimentary input of Ni or Cd.

3.3.4 Hydrothermalism

Dissolved Fe and Mn are commonly enriched at mid-oceanic ridges (Boyle et al., 2005; Tagliabue et al., 2010; Klunder et al., 2011; Wu et al., 2011; Nishioka et al., 2013; Saito et al., 2013; Hawkes et al., 2014). While most of the TMs are thought to be lost during rapid cooling

of hot water, increase in pH and precipitation, the formation of complexes with organic ligands reduces precipitation and allows the vertical and horizontal fluxes of Fe and Mn to extend to surrounding waters (Statham et al., 2005; Bennett et al., 2008). Iron and Mn hydrothermal contribution to the deep and intermediate waters of the World's Oceans was re-evaluated after the discovery of long range spreading hydrothermal plumes and showed that hydrothermalism is the most important source of Fe for 23% of the world's oceans (Tagliabue et al., 2014). However its impact on carbon export is limited to regions where inputs occur in shallow waters, or close to upwelling to bring Fe to surface water and subsequently enhance the primary production (Tagliabue et al., 2014). The impact of hydrothermal activity is influenced by ocean mixing, scavenging processes and organic complexation (Bennett et al., 2008; Tagliabue et al., 2010).

Hydrothermal vent fluids are characterized by a light signature of the Fe stable isotopes (δ^{56}Fe) (Sharma et al., 2001; Beard et al., 2003; Severmann et al., 2004; Bennett et al., 2008; Rouxel et al., 2008). Over the mid-Atlantic ridge (MAR), Conway and John (2014) identified a hydrothermal dFe source by measuring stable Fe isotopes. The light signature of samples from the TAG hydrothermal field allowed for the quantification of the hydrothermal source which was not significant for this cross Atlantic transect (Conway and John, 2014). Furthermore, Saito et al. (2013) observed elevated dFe and dMn concentrations over the MAR due to slow-spreading hydrothermal vents during the CoFeMUG cruise (Fig. I.6). High dFe and dMn concentrations were also observed over the Triple Bouvet Junction in the Southern Ocean by Middag et al. (2011a) and Klunder et al. (2011) (Fig. I.6). In addition to Fe and Mn, Cd has been measured in this areas but no dCd inputs were concurrently observed (Abouchami et al., 2014; Baars et al., 2014; Conway and John, 2015). The analysis of dCd and Cd stable isotopes (δ^{114}Cd) by Conway and John (2015) revealed that over the MAR, hydrothermal vent inputs were not a significant source of dCd and may even act as a sink of dCd by particulate scavenging. Over the MAR, during the CoFeMUG cruise, Noble et al. (2012) did not observe any particularly high dCo or total dissolved Co. With regards Cu and Pb, hydrothermal plumes remove Cu and Pb from dissolved phase by scavenging (Jacquot and Moffett, 2014; Noble et al., 2014). To our knowledge, no recent studies have reported Ni concentrations in waters surrounding hydrothermal plumes during a transect or process study.

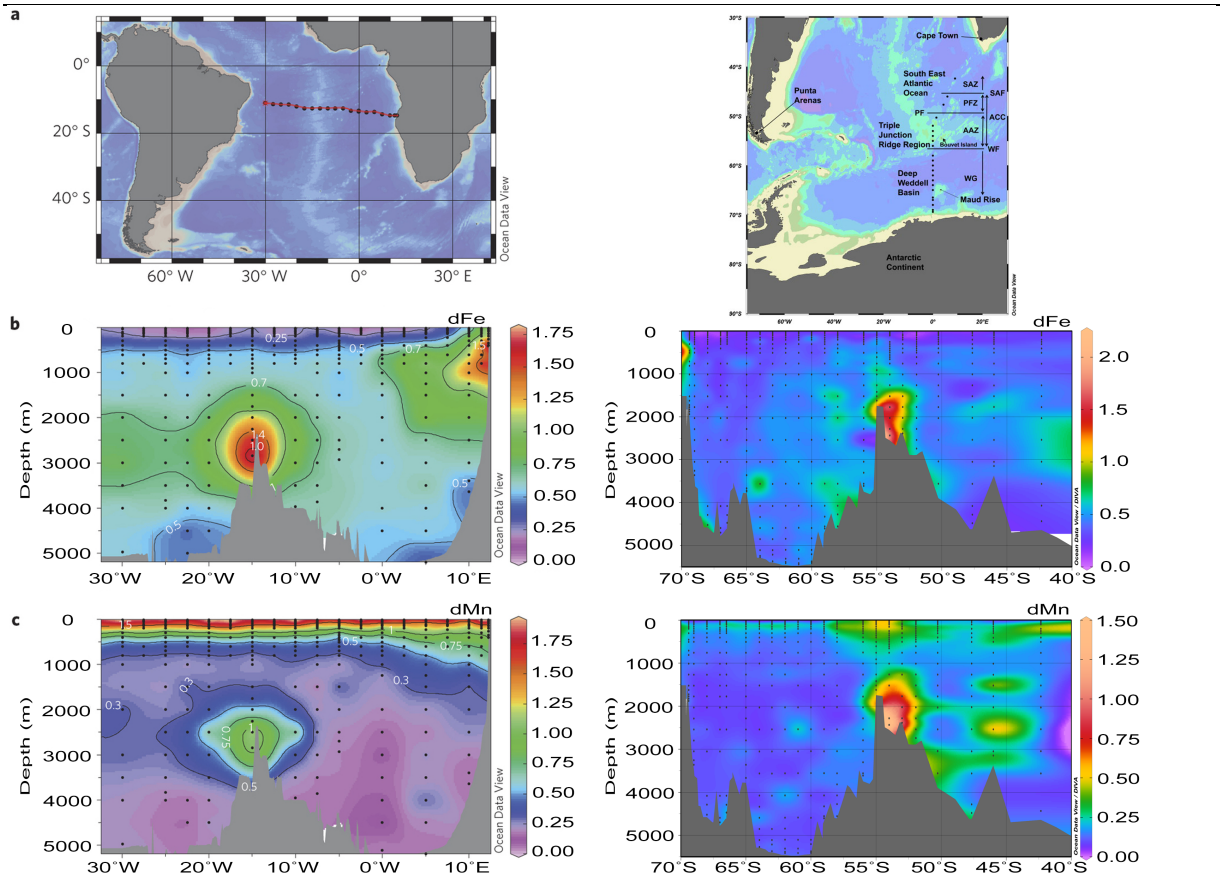

Figure I.6 Map of the CoFeMUG (a left) and ANT-XXIV-3 cruises (a right) with observed dFe (b) and dMn distributions (c). Figures and data from Saito et al. (2013), Middag et al. (2011a) and Klunder et al. (2011).

3.3.5 Glaciers, icebergs and melting sea ice

Glacier meltwaters can be a significant source of TM in surface polar oceans (Statham et al., 2008; Gerringa et al., 2012; Bhatia et al., 2013). In the Southern Ocean, it has been shown that the Pine Island Glacier meltwaters supplied high dFe, up to 150 km away from the glacier (Gerringa et al., 2012). The concentrations observed in this region were considered maximum, because the Fe-binding ligands were saturated (Thuróczy et al., 2012). This major input supplied enough dFe to sustain the development of a phytoplankton bloom for 73 days (Alderkamp et al., 2012), and with more intense lateral advection could influence an area up to 300 km away from the glacier. In Greenland, Statham et al. (2008) and Bhatia et al. (2013) observed very high dFe concentrations in glacier meltwaters, which represent an important additional source of Fe in HNLC region where meltwaters are directly injected in the productive area.

Free drifting icebergs can also be potential sources of Fe as Fe that is incorporated within their basal layer may often be derived from mechanical erosion of bed rock (Smith et al., 2007; Lin et al., 2011; Smith Jr, 2011; Lin and Twining, 2012). Within icebergs and in surrounding seawater, Fe organic ligands were also found in higher concentration compared to remote seawater, which might affect the Fe bioavailability and reduce the loss of Fe by scavenging (Lin and Twining, 2012). Raiswell et al. (2006), using a global model, showed that sediment delivered by icebergs is a significant source of iron to the open oceans, beyond the continental shelf. During the Last Glacial Maximum (LGM), the increase of drifting iceberg would have increased by a factor of three the iron flux from drifting icebergs and enhanced surface primary production, leading to subsequent atmospheric CO_2 drawdown. To our knowledge no other dissolved trace metals study other than Fe have been studied in water surrounding an iceberg or in an iceberg.

It has been shown that dFe is enriched in Antarctic sea ice at levels up to 3 orders of magnitude higher than in surrounding waters (Grotti et al., 2005; Lannuzel et al., 2007; Lannuzel et al., 2008; van der Merwe et al., 2009; Lannuzel et al., 2010; Lannuzel et al., 2011; van der Merwe et al., 2011; de Jong et al., 2013). When sea ice melts, it releases Fe and organic matter such as exopolysaccharides (EPS), which may increase Fe solubility and bioavailability in seawater (van der Merwe et al., 2009; Hassler et al., 2011). While sea ice is not a new source of Fe on a seasonal time scale, it acts as a temporary storage medium, concentrating dFe from the water column during autumn/winter and releasing it in spring at a time ideal for phytoplankton blooms. In the Antarctic marginal ice zone (which represents 40% of the Southern Ocean), sea ice is the main source of Fe to surface waters in spring (Lannuzel et al., 2007; Lannuzel et al., 2008; Statham et al., 2008). Melting sea ice is however not a significant source of other TMs such as Mn, Cu and Cd (Lannuzel et al., 2011). Fitzwater et al. (2000) did not showed significant enhancement of dissolved Cu, Ni, Co or Cd in the Ross sea while high dFe concentration, potentially from meltwaters inputs, were observed. To our knowledge dissolved Pb has not been studied in such environment.

3.4 Sinks of trace metals

3.4.1 Biological uptake

As shown earlier (section 2), all discussed metals except Pb are essential for phytoplankton growth due to their importance in a range of diverse metabolic processes. In

the Southern Ocean, Mn, Co, Ni, Cu and Cd are generally linearly correlated with macronutrients in the upper water column due to their role as micronutrients (Ellwood, 2008; Lai et al., 2008; Middag et al., 2011a; Boyé et al., 2012; Butler et al., 2013; Castrillejo et al., 2013). The biological uptake of trace metals influences their distribution in the water column, with regional and taxonomic differences on micro- to macro-nutrient uptake ratios (Twining and Baines, 2013). For that reason in addition to low inputs, biologically active trace metals such as Fe, Mn, Co, Ni, Cu and Cd show relatively low dissolved concentrations in Southern Ocean surface waters. Abouchami et al. (2011) showed that in the Southern Ocean, phytoplankton biogeography might control the distribution and the isotopic ratios of Cd isotopes ratios. During biological uptake, light isotopes are favoured during the assimilation, leaving a heavy isotopic signature in the dissolved phase except for Ni isotopes (Cameron and Vance, 2014).

3.4.2 Particle scavenging

Trace metals are prone to passive adsorption onto particles and subsequent removal from the euphotic layer during sinking, a phenomenon known as scavenging. Manganese is one of the most susceptible metals to particle scavenging (Sunda and Huntsman, 1994). Manganese often exhibits scavenged type distributions with high concentrations in the euphotic layer due to photoreduction (Sunda and Huntsman, 1994), atmospheric inputs (Baker et al., 2006; Wuttig et al., 2013), and/or fluvial inputs (Aguilar-Islas and Bruland, 2006). However Mn is insoluble in oxygenated water and is scavenged leading to a sharp decrease in subsurface concentrations (Sunda and Huntsman, 1994). Iron, Co and Pb are also subject to scavenging (Bruland and Lohan, 2003; Noble et al., 2008; Noble et al., 2012; Echegoyen et al., 2014). To our knowledge, Ni, Cu, and Cd never showed a scavenged type vertical distribution, presumably due to their biological uptake and regeneration (section 3.5).

3.5 Recycling of trace metals

Micronutrients are regenerated through bacterial decomposition, dissolution, or heterotrophic assimilation in the water column (Bruland and Lohan, 2003). Several studies have shown that grazers can rapidly regenerate Fe from ingested prey into the dissolved phase (Hutchins et al., 1993; Hutchins and Bruland, 1994; Barbeau et al., 1996; Chase and Price, 1997; Barbeau et al., 2001; Xu and Wang, 2003; Zhang and Wang, 2004; Sarthou et al., 2008). Assimilation of Fe by bacteria and subsequent viral induced lysis may also play a

critical role in Fe recycling (Gobler et al., 1997; Maranger et al., 1998; Poorvin et al., 2004; Mioni et al., 2005). Fe regeneration could account for half of the Fe demand in fertilized regions (Sarthou et al., 2008) and up to 90% in HNLC areas(Poorvin et al., 2004). It has been demonstrated that in the upper 200 m, Ni from sinking diatoms can be remineralized faster than Fe (Twining et al., 2014). In surface waters, krill and whales faeces can act as local Fe fertilizers to the Southern Ocean, by successive bioaccumulation in the food chain (from diatom to krill and from krill to whales) and eventually contribute to enhance local primary productivity (Tovar-Sanchez et al., 2007; Nicol et al., 2010; Smith et al., 2013; Ratnarajah et al., 2014). In the Atlantic sector of the Southern Ocean, Middag et al. (2011a) evidenced for the first time a significant relationship between dMn and macronutrients in the upper water column above a subsurface dMn maximum attributed to remineralization. Cobalt was also shown to be significantly remineralized in the Pacific Ocean, the subtropical domain of the Atlantic sector of Southern Ocean and the North Atlantic Ocean (Noble et al., 2008; Bown et al., 2011; Dulaquais et al., 2014). In addition, Jacquot and Moffett (2014) and Heller and Croot (2014) showed that high dCu concentration in the Atlantic Ocean or the Atlantic sector of the Southern Ocean were due to the remineralization of particulate Cu (pCu). The loss of pCu due to remineralization by micro-grassers is still to elucidate in the northeast subarctic Pacific Ocean (Semeniuk et al., 2015). Finally, Cd distributions are highly influenced by remineralization, leading to a strong relationship between Cd and PO_4 (Cullen, 2006; Boyé et al., 2012; Castrillejo et al., 2013; Abouchami et al., 2014; Baars et al., 2014).

4 Studies of High Nutrient Low Chlorophyll (HNLC) regions

4.1 Artificially fertilized area

The importance of Fe for marine ecosystems has been highlighted by artificial fertilisation experiments (FeAXs) in HNLC waters. The first experiment was conducted in east equatorial Pacific Ocean (IronEx-1) in 1993 (Martin et al., 1994; Coale et al., 1998) and led to an increase in primary productivity from 21 % to 31 % within 3 days following the introduction of 450 kg of Fe in the area (added as dissolved ferrous sulphate). However, due to Fe subduction to deeper depth after 4 days, no further fertilisation impact was observed. Since the first FeAXs, 14 additional FeAXs have been carried out (Fig. I.7).

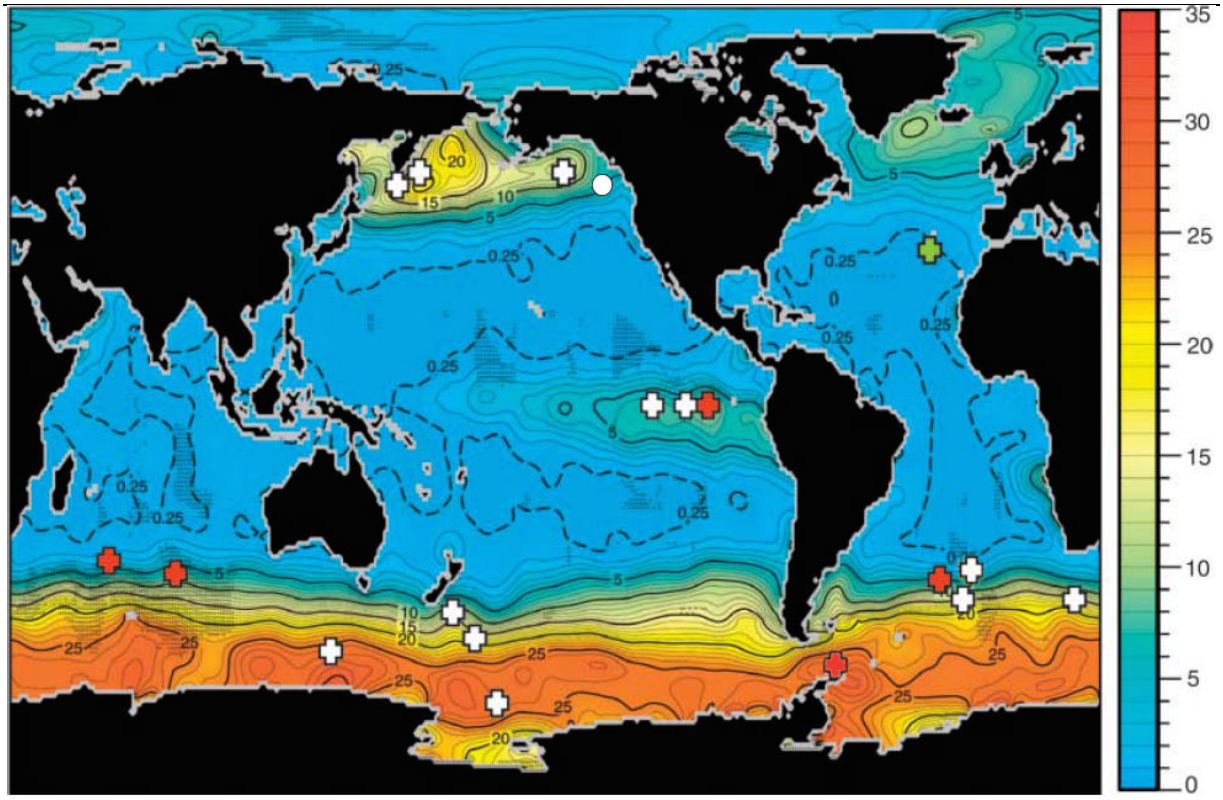

Figure I.7 Annual surface mixed-layer nitrate concentrations in units of µmol L^{-1}. FeAXs (white crosses) and FeNXs (red crosses) location. The green cross represent a FeAXs location with additional P enrichment study, although this location was actually in the eastern Mediterranean Sea and not in the Atlantic Ocean as shown on the map (updated from Boyd et al. (2007). The white circle represent the location of the controversial commercially Fe enrichment experiment (Haida Salmon Restoration Corporation).

One unequivocal result from the FeAXs is that primary production was enhanced after Fe addition (Boyd et al., 2007). However, issues were raised on the effect of the increased primary production on the carbon sequestration efficiency (the fraction of carbon exported to the deep ocean), the effect on the ecosystems and if these effects are transient or sustained.

The major findings of artificial fertilisation experiments could not be extrapolated to larger spatial and time scale due to the low spatial resolution (few hundreds of kilometres) and short time scale (weeks) of these experiments. In the subarctic Pacific, the SERIES FeAXs showed an enhancement of higher trophic levels (Tsuda et al., 2006) as for 3 additional FeAXs (IronEX II, EIFEX and SEEDS) (Boyd et al., 2007).

4.2 Naturally fertilized areas

To study the sustained effect of Fe fertilisation, some regions naturally fertilized by Fe have been identified and studied (FeNXs). In the Southern Ocean, 5 regions have been studied in detail: the polar front in the Atlantic sector (de Baar et al., 1995), the Ross sea (Smith Jr et al., 2012), the Scotia sea (Dulaiova et al., 2009; Ardelan et al., 2010; Nielsdóttir et al., 2012; Hatta et al., 2013; Measures et al., 2013), Crozet Island (Pollard et al., 2009; Planquette et al., 2011) and the Kerguelen Plateau (Blain et al., 2007). Each year, primary production is locally enhanced at these 5 sites (Sullivan et al., 1993; Holm-Hansen et al., 2004; Blain et al., 2007; Pollard et al., 2007a). However, these studies showed varying phytoplankton blooms and carbon sequestration efficiencies. Morris and Charette (2013) showed that in areas influenced by natural Fe fertilization in the Southern Ocean, the export efficiency, known as the exported C to added Fe ratio, is 3 fold higher than in not fertilized areas. Resuspension of sediments derived from the continental shelves and entrainment in the mixed layer have been proposed as fundamental Fe sources in these regions. Only a small number of studies have reported the concentrations of other trace metals, such as dissolved Mn (dMn). In the Scotia Sea, the study of the dMn and dFe relationship allowed the identification of anoxic or suboxic diagenesis as the major source of dFe to shelf surface waters compared to atmospheric or upwelling inputs (Hatta et al., 2013; Measures et al., 2013). Around Crozet Islands, Castrillejo et al. (2013) reported the distributions of dissolved trace metals, Ni, Co, Cd, Pb and Mn amongst them. During this study, the use of several trace metals together allowed the identification of sources, sinks and recycling processes of trace metals. The low concentrations of dMn and dCo in deep waters were attributed to sinking of particles and scavenging. Dissolved Cd, Co and Ni showed significant relationships with macronutrients, therefore highlighting the role of biological uptake and associated remineralization on the distribution of trace metals.

4.3 Kerguelen Island study site

Three cruises including trace metal studies around Kerguelen Island have been conducted to date: ANTARES3 (Oct. 1995), KEOPS1 (Jan.-Feb. 2005), and KEOPS2 (Oct.-Nov. 2011) (Fig.I.8).

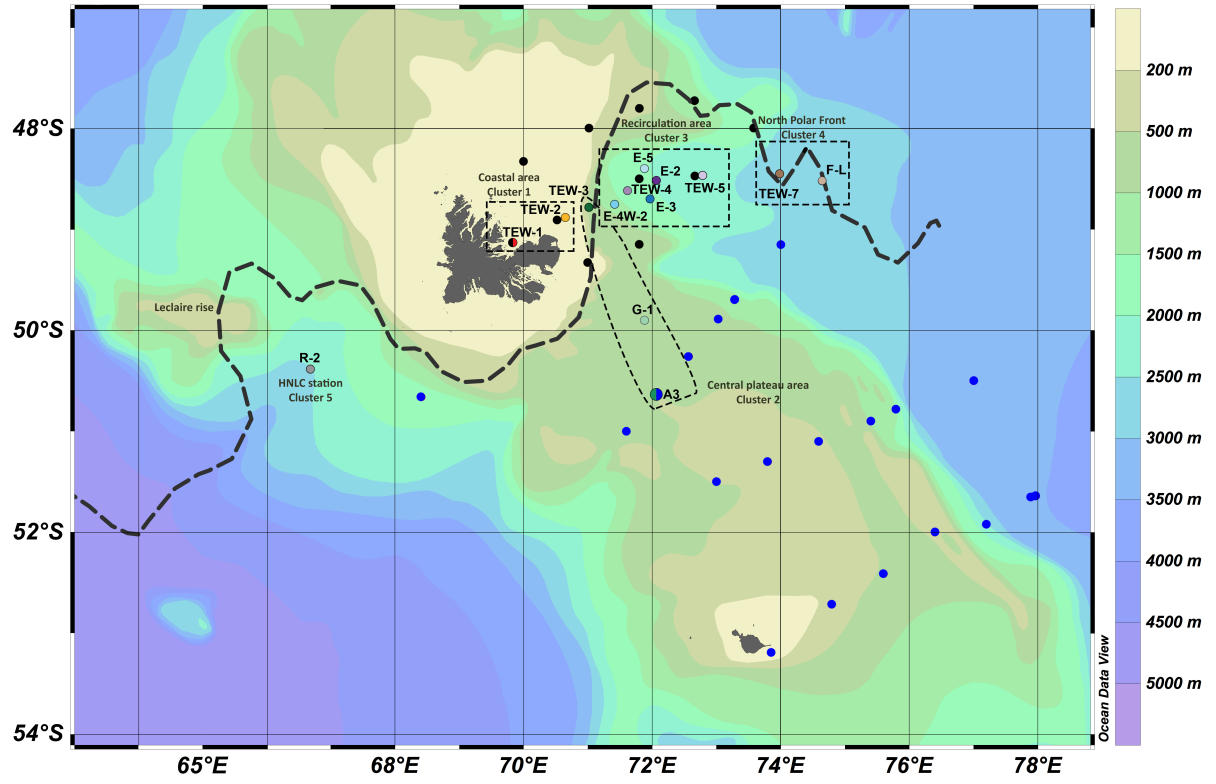

Figure I.8 Map showing the bathymetry of the area and the stations visited during ANTARES3 (black dots; Bucciarelli et al., 2001), KEOPS1 (blue dots; Blain et al., 2008) and KEOPS2 (colored dots). The dashed line represented the approximate location of the Polar Front (200 m) (Park et al., 2014).

KEOPS2 is the second study on the impact of natural Fe fertilization on the biogeochemical cycles around this island area in the Southern Ocean. The first initiative, KEOPS1 (January to February 2005) showed the impact of natural Fe fertilization on the biogeochemical cycle of TMs and the ecosystem. During the first study, Blain et al. (2007) showed the enhancement of the C export by Fe fertilization. The C export efficiency (154 000 mol C (mol Fe)$^{-1}$) (Chever et al., 2010b) was significantly higher than during the CROSEX study (8640 mol C (mol Fe)$^{-1}$) (Pollard et al., 2009) and higher than the efficiency of FeAX (< 25 000 mol C (mol Fe)$^{-1}$) (de Baar et al., 2008a). This result showed that the biological pump of C was intensified due to the regular Fe input in surface waters and subsequent diatom bloom, enhancing primary production and biomass (chla), 4 and 10 fold more important in Fe fertilized region compared to HNLC area respectively (Blain et al., 2007; Armand et al., 2008; Mosseri et al., 2008). This was highlighted by a pCO_2 decrease 2.5 fold

higher than during FeAX (Jouandet et al., 2008). However many questions remained unanswered, which were to be considered further during KEOPS2.

During KEOPS1, the study of the biogeochemical cycle of Fe highlighted the pathways of natural Fe fertilization, however, the supply of Fe from below was not sufficient to meet the biological Fe demand in surface waters. One of the main objectives of the KEOPS2 cruise was then to better assess the Fe and other TM sources in this fertilized area, including in the particulate phase. KEOPS2 has focused on the impact of the different sources of TM on metal uptake ratios and whether processes such as nitrification and ammonium regeneration in surface waters are of importance in sustaining phytoplankton primary production. The central issue of KEOPS2 has been to understand the processes involved in carbon export to depth and how the natural Fe fertilization influences this export. The different pathways of organic matter through the water column have been studied. The aim has been to observe the influence of the fertilization on the biogeochemical cycles and the ecosystems diversity and their impact on the carbon biogeochemical cycle. The deployment of sediment traps at different locations; depths and bloom stages has focused on the study of the biogeochemical cycle of particulate fraction of TMs and the processes involved in carbon export.

KEOPS2 complemented the KEOPS1 cruise by increasing the spatial resolution of the KEOPS program visiting the northern part of the plateau and the bloom area offshore. Furthermore, this second visit has provided a better temporal understanding of the processes involved in the natural Fe fertilization as the second visit occurred in the early stage of the phytoplankton bloom. The aim has been to build seasonal budget of different chemical elements that has required a proper description of the variability of the mixed layer depth especially in the early stage of the bloom when the mixed layer was shallow. This has allowed the evaluation of the mixed layer variability impact on the biogeochemical cycles of TMs and phytoplankton bloom.

The ANTARES3 and KEOPS1 studies reported trace metal distributions around Kerguelen Island. Iron was studied during ANTARES3 and KEOPS1 while Mn distributions was studied during ANTARES3 only and Co during KEOSP1 only. Over the plateau, high dFe, dMn and dCo concentrations revealed the relevance of shelf processes in fertilizing the phytoplankton bloom area. Results also revealed that lateral and vertical transport of Fe enriched water masses were crucial to sustain the bloom offshore. Bucciarelli et al. (2001) was the first to show clear evidence of dFe and dMn increases in the northern part of the

Kerguelen Plateau. This study showed that Fe and Mn sedimentary sources were transported offshore by lateral advection. During KEOPS1 the southern part of the Kerguelen Plateau showed a clear dFe increase in deep waters above the plateau (Blain et al., 2008b). Dissolved Co distribution revealed the importance of basalt sources (Bown et al., 2012). These sources were found to be higher than the biological uptake of Co.

These studies, however, remain focused on one or two trace metals. A multi-element study, such as that completed during CROZEX (Castrillejo et al. 2013), should be a powerful tool not only to better understand the oceanic distributions of several distinct metals, but also to identify tracers of specific sources, sinks and recycling processes.

5 Aims of this PhD

The overall aim of this thesis is to study the biogeochemical cycles of key trace metals in a naturally-Fe fertilized area of the Southern Ocean: the Kerguelen Plateau. Extensive datasets on the distribution of key trace metals in this region are scarce, due in large part to the challenges of sampling and analysing such contamination-prone metals. The first objective of this PhD is therefore to develop a fast and sensitive method for the simultaneous analysis of multiple trace metals in seawater. The 2nd objective is then to evaluate the distributions, sources and sinks of Fe and other key trace metals in the early stage of the recurrent phytoplankton bloom east of the Kerguelen Plateau. This crucial data will finally allow us to use the key bioactive trace metals (Mn, Co, Cu, Ni, Cd) and a tracer of anthropogenic inputs (Pb) to trace the Fe biogeochemical cycle around Kerguelen Island. From this PhD work, two key questions should then be able to be addressed:

1. What were the distributions, sources and sinks of Fe and other key trace metals in the early stage of the recurrent phytoplankton bloom east of the Kerguelen Plateau?

2. Can other trace metal distributions help us to better constrain the Fe cycle in this complex region?

This PhD project was conducted within the framework of a GEOTRACES approved process study: the KEOPS2 project. GEOTRACES is an international program, which focuses on studying marine biogeochemical cycles of TMs. The program is focused around three main goals (Boyle, 2001; Bruland and Lohan, 2003; Boyle et al., 2014):

- To study the biogeochemical cycles of TMs within the global ocean, identifying and quantifying sources, sinks and the physical, chemical, and biological processes controlling their distributions.
- Anticipate the response of biogeochemical cycles to global change
- Understand the processes, which control the concentrations of TMs used for proxies of the past environment.

This PhD will address the first objective of the GEOTRACES programme

The layout of this manuscript is as follows:

- Chapters 2 and 3: Methodological advances

The first objective of this thesis was to develop an analytical technique to simultaneously analyse multiple trace metals. The method required high sensitivity for sub-nanomolar samples, low sample volumes (< 30 mL) and high sample throughput (typically 24 samples per station). Flow Injection Analysis (FIA) has been extensively used in the IUEM and ACE CRC laboratories, and can be adapted to measure Mn, Al and Fe in marine samples by using different reagents and detectors (see Fe-FIA methods in Chapter 2). Flow Injection Analysis can be operated at sea and therefore allows real-time measurements. However, the technique is single element and time intensive. Recent technological advances have resulted in several publications focusing on multi-element methods using ICP-MS instrumentation stimulating further developments of this highly promising analytical method (Sohrin et al., 2008; Milne et al., 2010; Biller et al., 2012; Lagerstrom et al., 2013). The 1st objective of this PhD project was to adapt the multi-element method presented in Milne et al. (2010) to measure simultaneously dissolved Mn, Co, Ni, Cu and Cd (Chapter 3). The new method has been published in Analytical Methods in 2014 and will be used in conjunction with the FIA to obtain the dissolved Fe data presented in chapters 4 and 5.

- Chapter 4. Dissolved Fe cycle during KEOPS2

This chapter will focus on the distributions, sources and sinks of dissolved Fe in the vicinity of Kerguelen Plateau. More specifically, the objective of this chapter is to increase our understanding of the processes, which drive the seasonal phytoplankton bloom in the vicinity of Kerguelen Plateau. The KEOPS2 project occurred in late spring while KEOPS1 occurred in summer, and by combining data from both cruises we can gain insight into the seasonal progression of dissolved Fe. This chapter is published in the Biogeosciences KEOPS2 special issue.

- Chapter 5. Dissolved TM cycles during KEOPS2

This chapter will focus on the distributions, sources and sinks of dissolved Mn, Co, Ni, Cu, Cd and Pb in the vicinity of Kerguelen Plateau. Chapter 5 will constitute the first dataset to document and discuss such a wide range of key trace metals in a natural fertilization study. This chapter will be submitted to a peer-reeviewed journal following completion of this thesis.

- Chapter 6. Conclusion and future work

The last chapter of this thesis will use the information gained in chapters 4 and 5 to compare the sources of Fe to the sources of other trace metals, as a way to fingerprint the Fe cycle. Chapter 6 will also suggest future directions for international programs such as GEOTRACES to increase the spatial and temporal resolution of dissolved TM studies.

Chapter II

Materials, methods and Fe FIA analysis procedure

1 Clean workspace and labware

Iron is the fourth most abundant element in the continental crust (Taylor, 1964), which means that it is a ubiquitous element in our daily lives. Not only Fe, but also Mn, Co, Ni, Cu, Cd and Pb are omnipresent. However, concentrations of these elements are extremely low in the open ocean and research groups around the world have needed to develop protocols, tools and expertise to avoid potential contaminations issues arising from sample handling, laboratory environment, air quality or the required sampling tools (Bruland et al., 1979; de Baar et al., 2008b; Cutter and Bruland, 2012).

During my PhD, laboratory work was undertaken in the field (conducted in a containerized clean laboratory under high-efficiency particulate air (HEPA) conditions (Fig. II.1)), in a clean room at LEMAR laboratory (class 10,000), and in a laboratory at IMAS or ACE-CRC where class 100 laminar flow hoods (AirClean 600 PCR workstation, AirClean System, or ADS VSM 12 CA, ADS Laminaire) were used for the handling of all samples and reagents. For reagent preparation and labware cleaning, ultra high purity water (resistivity: UHP > 18 MΩ cm) was supplied from a Barnstead International, NANOpure DIamond polisher, fed by a Diamond RO, reverse osmosis system coupled with an additional 3 stage pre-filter. Ultra high purity water (resistivity = 18.2 MΩ cm) was also used supplied by a Milli-Q® Direct Water Purification System (Millipore). All sample bottles and pipette tips were acid washed prior to use following recommendations from the GEOTRACES approved methods handbook (Cutter et al., 2010) with slight modification. A brief summary of this acid washing protocol used for dissolved iron sample bottles is outlined below:

- 1 night storage in 2 % v:v detergent bath (DECON or MICRON) in reverse osmosis water (ROW)
- 3 rinses with ROW followed by 1 rinse with distilled water
- 1 week filled with 1 M HCl (reagent grade)

- 3 rinses with distilled water followed by 1 rinse with MQ
- 1 week filled with 0.04 M HCl (Suprapur® MERCK)
- 3 rinses with MQ
- 1 week filled with 0.02 M HCl (Ultrapur® MERCK)
- 3 rinses with MQ

This protocol has been modified compared to the GEOTRACES approved methods handbook (Cutter et al., 2010) due to laboratory space restrictions and the high throughput requirements of our laboratory. Our laboratory protocols have been tested for contamination and compared to GEOTRACES protocols providing similar cleaning efficiency. Sample bottles for the other dissolved trace metal analysis followed strictly the GEOTRACES approved methods handbook (Cutter et al., 2010).

Reagents and samples were prepared or stored in low density polyethylene (LDPE) bottles (Nalgene®) during routine work. Teflon fluorinated ethylene propylene (FEP) bottles (Nalgene®) were used when samples required UV irradiation as these bottles allowed UV transmission without degradation and were still clean enough for trace metal work. Polypropylene (PP) tubes (Technoplas) were used to collect concentrated trace metal samples after the pre-concentration manifold as they integrated with the ICP-MS autosampler and were also clean enough for trace metal work, albeit, with slightly less resistance to concentrated acids.

2 Sampling

Samples were collected between 20 October to 19 November, 2011 on board the R/V *Marion Dufresne* using a trace metal clean rosette (TMR, model 1018, General Oceanics) equipped with twelve, 10 L, externally closing, Teflon-lined, Niskin-1010X bottles mounted on a polyurethane powder-coated aluminium frame specially designed for trace metal work (Bowie et al., 2009) (Fig. II.1). Seawater was sub-sampled for the dissolved trace metals via a Teflon tap connected to acid cleaned 0.2 µm filter cartridges (Pall Acropak and Sartorius SARTOBRAN 300). Two acid cleaned low density polyethylene bottles per sampled depth (60 mL for Fe analysis and 250 mL for Mn, Co, Ni, Cu, Cd and Pb analysis) were rinsed 3 times with, respectively, ~ 20 mL and ~ 80 mL of seawater before final sample collection. Dissolved Fe samples were acidified to pH < 2 using 1 ‰ of concentrated ultrapure

hydrochloric acid (Seastar Baseline, HCl) while for the other elements, samples were acidified to pH =1.8 using 2 ‰ of concentrated ultrapure hydrochloric acid (Seastar Baseline, HCl). The sample bottles were then double bagged and stored at ambient temperature in the dark until analysis. The shallowest sample was collected at 15 m depth in order to avoid contamination from the ship. Samples collected in deep water off the Kerguelen Plateau were collected to a maximum depth of 1300 m (further details on sampling strategy is included in Chapter III).

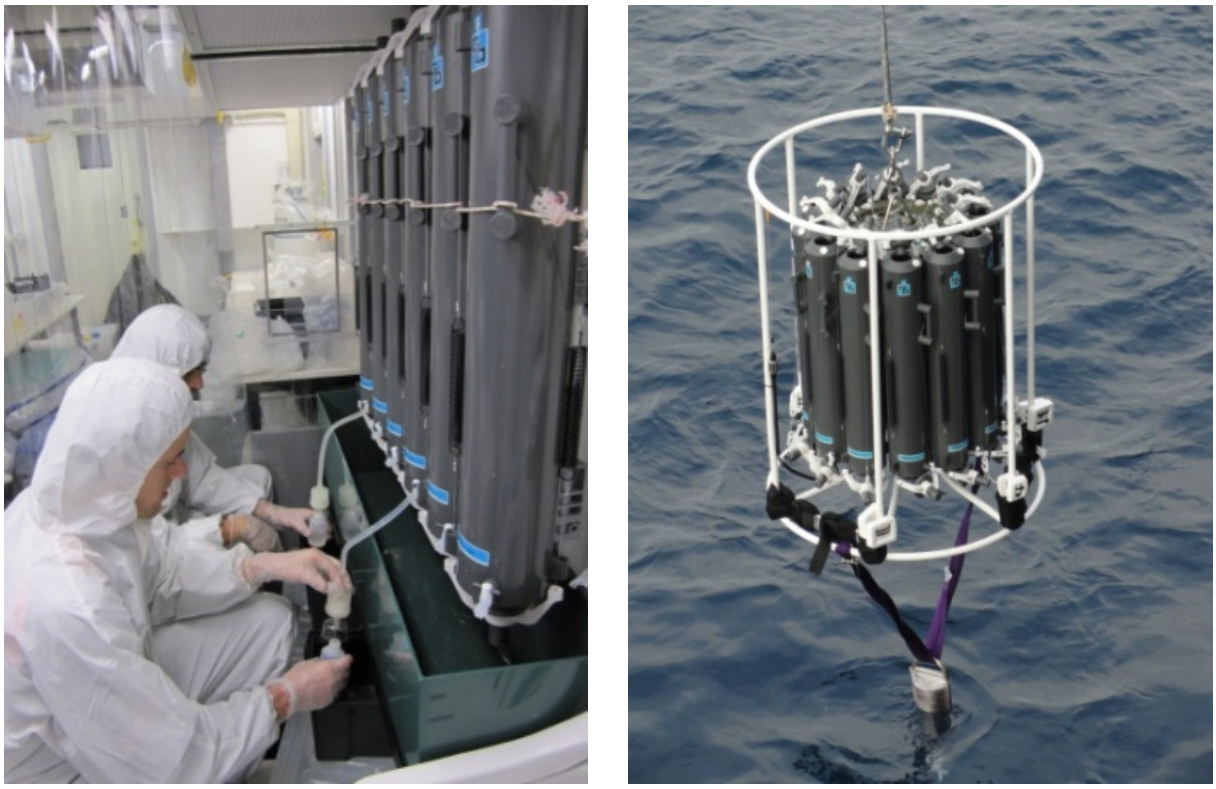

Figure II.1 Left: Trace metal sub-sampling in the containerized clean laboratory. Right: Deployment of the TMR device with an acoustic transponder for ocean bottom estimations.

3 Dissolved iron measurements

3.1 Basics of the method

Dissolved Fe (dFe) was analysed on board at least 24 h after sample collection by flow injection analysis (FIA) with online solid phase extraction onto 8-hydroxyquinoleine (8-HQ) resin and chemiluminescence detection, following a method adapted from Obata et al. (1993) and Sarthou et al. (2003). Sample pre-concentration was required before analysis due to the low dFe concentrations considered. Sample pre-concentration was achieved by firstly

increasing the sample pH to 4.7 by addition of an ammonium acetate buffer (3.5 mol L^{-1}). Then, Fe was pre-concentrated by ion exchange onto a 8-hydroxyquinoleine (8-HQ) resin (loading for 10 s to 120 s) and a rinse of the column by MQ water removed remnant seawater salts from the resin (60 s). A HCl (0.4 mol L^{-1}) eluent solution then allowed the extraction of Fe from the 8-HQ (120 s). The eluent solution was then mixed with luminol ($C_8H_7N_3O_2$), ammonia (NH_3) and hydrogen peroxide (H_2O_2) solutions at an optimum reaction pH of 9.0. The reaction of the luminol was catalysed with H_2O_2 under a basic pH, and the resultant emitted photons were detected by a photomultiplier. The transmitted signal is proportional to the number of photons and hence to the Fe concentration. This reaction is also highly sensitive to temperature changes so a constant temperature of 30 °C was maintained using a thermostatic water bath.

3.2 Reagents

Ammonia. 1 mol L^{-1} ammonium hydroxide solution was prepared by adding 75 mL of concentrated NH_3 (25%) (Suprapur®, Merck) to MQ water to a final volume of 1 L in a LDPE volumetric flask.

Hydrochloric acid. 0.4 mol L^{-1} HCl was prepared by adding 40 mL of concentrated HCl (30%) (Suprapur®, Merck) to MQ water to a final volume of 1 L in a LDPE volumetric flask.

Hydrogen peroxide. 0.7 mol L^{-1} H_2O_2 was prepared by adding 72 mL of concentrated H_2O_2 (30%) (Suprapur®, Merck) to MQ water to a final volume of 1 L in a LDPE volumetric flask.

Luminol. 0.74 mol L^{-1} luminol solution ($C_8H_7N_3O_2$) was prepared by adding 0.13 g of luminol (97 %) and 0.53 g of potassium carbonate Suprapur (K_2CO_3, 3/2 H_2O) (Merck) and 60 µL of triethylentetramine (TETA, 60 %) to MQ water to a final volume of 1 L in a LDPE volumetric flask. This solution was purified by extraction onto an 8-HQ resin.

Ammonium Acetate buffer. An ammonium acetate buffer (CH_3COO^- 3.5 mol L^{-1} and NH_4^+ 4.5 mol L^{-1}) was prepared by adding 48 mL of concentrated CH_3COOH (18 mol L^{-1}) and 103 mL of concentrated NH_3 (11 mol L^{-1}) to UHP water to a final volume of 250 mL in a 250 mL LDPE bottle. The pH of the solution was then adjusted to pH = 9.0 ± 0.2 with either CH_3COOH or NH_3. This solution was purified by three successive extractions onto an 8-HQ resin.

Fe(III) solutions. Fe(III) standard solutions were prepared for the calibration of the method by serial dilution of a 1000 mg.L^{-1} solution of $FeCL_3$, $6H_2O$ (Carlo Erba Reagenti) in acidifed MQ 1 ‰ v:v HCl. A first solution (F1) was prepared by addition of 280 µL of the commercial solution in 50 mL of acidified MQ (final Fe concentration :0.1 m L^{-1}). Two other solutions (F2 and F3) were prepared by adding, respectively, 500 µL and 50 µL of F1 in 50 mL of acidified MQ (final Fe concentration: F2, 1 µmol L^{-1}; F3, 100 nmol L^{-1}). F1, F2 and F3 were prepared weekly. For the calibration, 0.25, 0.50, 0.75 and 1 nmol L^{-1} of Fe were added to one of the surface samples.

3.3 Blank and detection limit

At the start of each FIA analysis day, the pre-concentration sequence was repeated 10 times with a loading time of 10 s using the shallowest sample collected at the station. This was performed to stabilize and condition the manifold and the photomultiplier with low-Fe seawater. In addition, these samples were used for the determination of blanks and detection limits. The aim was to obtain the manifold blank (consisting of all reagents except sample-pH-adjustment reagents) without a significant contribution from the seawater matrix, by using a very short sample load time. Blanks were low enough to allow the determination of dFe in open ocean seawater (0.039 ± 0.014 nmol L^{-1}, n=15). The sample-pH-adjustment reagent (HCl used for the acidification and buffer) blanks were also analysed everyday by adding 2 and 3 times more reagents to the sample. The expectation is for a standard addition type increase in the signal if there is a significant contribution of Fe. Their contribution were below the detection limit of the instrument (3 times the standard deviation of the sample loaded for 10 s: 0.017 ± 0.012 nmol L^{-1}, n=22), and therefore, the method and reagents were deemed suitable for open ocean seawater analysis (Johnson et al., 2007).

3.4 Precision and accuracy

Each collected sample was analysed in triplicate with an average precision of 4.8 % ± 4.6 % (n=149). The North Pacific SAFe Surface (SAFe S) (0.094 ± 0.003 nmol L^{-1} (n=3)) and SAFe Deep D2 (0.95 ± 0.05 nmol L^{-1} (n=3)) dFe measured values were in excellent agreement with consensus values (S1=0.088 ± 0.007 nmol L^{-1} and D2 = 0.88 ± 0.02 nmol L^{-1}; Johnson et al., 2007).

Chapter III

Method development of an offline trace metal extraction of Mn, Co, Ni, Cu, Cd and Pb and SF-ICP-MS detection

1 Introduction

Trace elements in the dissolved phase are at concentrations in the pmol L^{-1} to nmol L^{-1} level so trace metal clean technology has been developed to collect seawater without contamination (de Baar et al., 2008b; Cutter et al., 2010; Cutter and Bruland, 2012; Planquette and Sherrell, 2012). Many single element analytical techniques with adequate detection limits and sensitivities have been developed for the analysis of these samples.

Methods based on chemiluminescence detection (Obata et al., 1993; Bowie et al., 1998; Bowie et al., 2005; Shelley et al., 2010; Durand et al., 2012), fluorescence spectroscopy (Brown and Bruland, 2008; Remenyi et al., 2012), electrothermal atomic absorption spectrometry (ETAAS or GFAAS) (Kremling and Streu, 2001; Ndung'u et al., 2003) and voltammetry (Baars and Croot, 2011; Croot, 2011) have all been used, with offline or online pre-concentration of trace elements. Inductively coupled plasma mass spectrometry (ICP-MS) is a crucial tool for fast and sensitive analysis of multiple trace elements in seawater. Although offering superior sensitivity with ultra-low detection limits, this technique is very sensitive to sample matrix effects arising from the high level of dissolved salts (Rodushkin and Ruth, 1997). Therefore solid phase extractions typically have to be used for analyte pre-concentration and matrix-exclusion prior to ICP-MS analysis.

Different chelating resins have been used such as nitrilotriacetate resin (NTA) (Lohan et al., 2005; Lee et al., 2011), Toyopearl AF-Chelate-650M (Milne et al., 2010), and more recently Nobias-chelate PA1 resin (Biller and Bruland, 2012; Lagerstrom et al., 2013). The NTA uses resin-immobilised nitriloacetic acid functional groups, Toyopearl AF-Chelate-650M resin uses iminodiacetic (IDA) acid functional groups and Nobias-chelate PA1 resin combines ethylenediaminetriacetic (EDTriA) and IDA acids functional groups. The difference between these resins is the denticity between the functional groups. Indeed the IDA functional group is tridentate while the NTA is tetradentate and EDTria is pentadentate. The complex

stability is correlated with the denticity, which means that Nobias Chelate PA1 resins form more stable complexes with metals than NTA type and Toyopearl AF-Chelate-650M resins. Lee et al. (2011) developed a batch extraction method using NTA resin, which involved a complex and lengthy sample handling procedure, considered impractical for our study. The use of chelating columns is therefore more appropriate. The method developed by Lagerstrom et al. (2013) is automated, easy to use, and provides an off-line extraction method with high sample throughput. However, on-line extraction with ICP-MS was not optimal due to the long idle period during the pre-concentration step, which unnecessarily uses ICP-MS time and consumables (e.g. argon consumption, high quality expensive acids), and increases analysis costs significantly. Milne et al. (2010) extracted samples using a very simple manifold, which was easy to use, reproducible, portable and off-line, saving ICP-MS analysis time. Further modifications could be made to this manifold to achieve a completely automated method, with high throughput, and to allow extraction of up to12 samples (usually 1 TMR cast) at a time. The use of only 1 peristaltic pump to carry samples was considered important for operational simplicity, compared to Biller and Bruland (2012) who used a combination of peristaltic pump and argon gas. Biller and Bruland (2012) showed that the Nobias-chelate PA1 resin had a better recovery for Mn compared to the Toyopearl AF-Chelate-650M. To allow for quantification of mono-isotopic elements like Mn and Co, they moved away from the isotope dilution technique used by Milne et al. (2010) and employed a standard addition calibration protocol, which significantly simplified the analysis and reduced the analytical time and expense.

In this work, we adapted the offline matrix separation and pre-concentration system presented by Milne et al. (2010) using the Nobias resin column and standard addition calibration coupled with Sector Field (SF) ICP-MS detection to measure simultaneously dissolved trace metals (dTM) such as dMn, dCo, dNi, dCu, dCd and dPb in seawater samples. We developed a manifold, which is easy to use, easy to reproduce, automated, low cost and portable, providing off-line extraction capabilities with high sample throughput. This method development has been published in Analytical Methods (Quéroué et al., 2014) and is presented below.

There is no reason why this method could not be applied to Fe and Zinc (Zn), however we found in our lab that blanks and detection limits were better on the FIA for dFe and in the

interest of maintaining the highest possible accuracy, we decided to run dFe samples with the FIA.

2 Method paper

Volume 6 | Number 9 | 7 May 2014 | Pages 2793–3184

Analytical Methods

www.rsc.org/methods

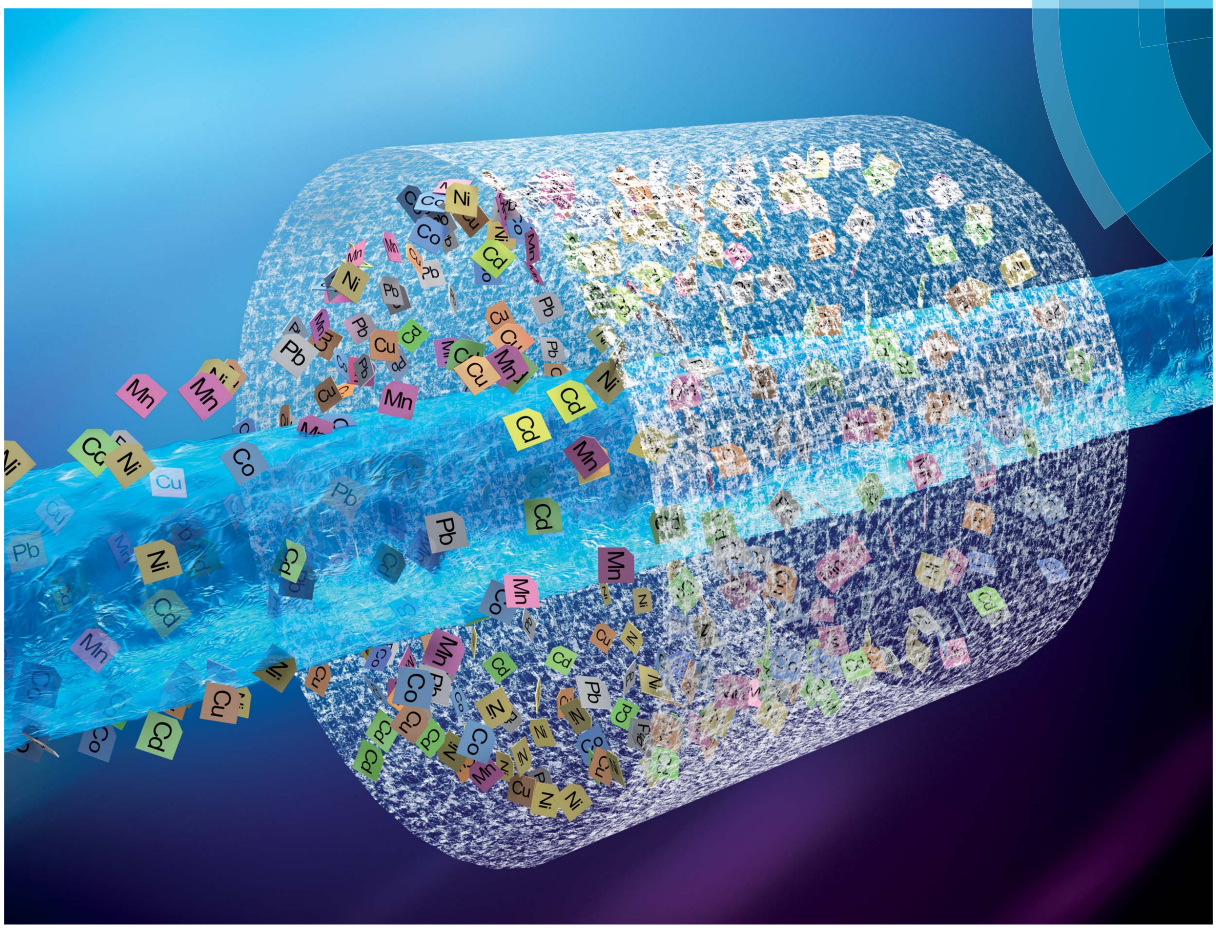

ISSN 1759-9660

ROYAL SOCIETY OF CHEMISTRY

PAPER
Fabien Quéroué *et al.*
Advances in the offline trace metal extraction of Mn, Co, Ni, Cu, Cd, and Pb from open ocean seawater samples with determination by sector field ICP-MS analysis

Fabien Quéroué et al., 2014, Advances in the offline trace metal extraction of Mn, Co, Ni, Cu, Cd, and Pb from open ocean seawater samples with determination by sector field ICP-MS analysis, Analytical methods, 6(7), 2837-2847, 10.1039/c3ay41312h

Chapter IV

A new study of natural Fe fertilisation processes in the vicinity of the Kerguelen Islands (KEOPS2 experiment)

F. Quéroué[1,2,3,4], G. Sarthou[2], H. Planquette[2] F, E. Bucciarelli[1,2], H. Planquette[2] F. Chever[2], P. van der Merwe[2,3], D. Lannuzel[3,4], A. Townsend[5], M. Cheize[2], S. Blain[6,7], F. d'Ovidio[8] and A. Bowie[3, 4]

[1] Université de Bretagne Occidentale, Brest, 29200, France

[2] LEMAR-UMR 6539, CNRS-UBO-IRD-IFREMER, Place Nicolas Copernic, 29280 Plouzané, France

[3] Institute for Marine and Antarctic Studies, University of Tasmania, Hobart, Tas 7001, Australia

[4] Antarctic Climate & Ecosystems Cooperative Research Centre, University of Tasmania, Hobart, Tas 7001, Australia

[5] Central Science Laboratory, University of Tasmania, Hobart, Tas 7001, Australia

[6] Laboratoire Océanographie Biologique de Banyuls sur Mer, Université Pierre et Marie Curie, Paris 06, quai Fontaulé, 66650 Banyuls sur Mer, France

[7] Laboratoire Océanographie Biologique de Banyuls sur Mer, CNRS, Paris 06, quai Fontaulé, 66650 Banyuls sur Mer, France

[8] Sorbonne Universités (UPMC, Univ Paris 06)-CNRS-IRD-MNHN, LOCEAN-IPSL, 4 place Jussieu, 75005 Paris, France

Manuscript published in the special issue of *Biogeosciences* on the KEOPS2 project

Biogeosciences, 12, 3869–3883, 2015
www.biogeosciences.net/12/3869/2015/
doi:10.5194/bg-12-3869-2015

Biogeosciences Open Access

High variability in dissolved iron concentrations in the vicinity of the Kerguelen Islands (Southern Ocean)

F. Quéroué[1,2,3,4], G. Sarthou[2], H. F. Planquette[2], E. Bucciarelli[1,2], F. Chever[2], P. van der Merwe[4], D. Lannuzel[3,4], A. T. Townsend[5], M. Cheize[2], S. Blain[6,7], F. d'Ovidio[8], and A. R. Bowie[3,4]

[1]Université de Bretagne Occidentale, IUEM, 29200 Brest, France
[2]LEMAR-UMR 6539, CNRS-UBO-IRD-IFREMER, Place Nicolas Copernic, 29280 Plouzané, France
[3]Institute for Marine and Antarctic Studies, University of Tasmania, Hobart, TAS 7001, Australia
[4]Antarctic Climate & Ecosystems Cooperative Research Centre, University of Tasmania, Hobart, TAS 7001, Australia
[5]Central Science Laboratory, University of Tasmania, Hobart, TAS 7001, Australia
[6]Laboratoire Océanographie Biologique de Banyuls sur Mer, Université Pierre et Marie Curie, Paris 06, quai Fontaulé, 66650 Banyuls sur Mer, France
[7]Laboratoire Océanographie Biologique de Banyuls sur Mer, CNRS, Paris 06, quai Fontaulé, 66650 Banyuls sur Mer, France
[8]Sorbonne Universités (UPMC, Univ Paris 06)-CNRS-IRD-MNHN, LOCEAN-IPSL, 4 place Jussieu, 75005 Paris, France

Correspondence to: G. Sarthou (geraldine.sarthou@univ-brest.fr)

Received: 28 November 2014 – Published in Biogeosciences Discuss.: 6 January 2015
Revised: 25 April 2015 – Accepted: 12 May 2015 – Published: 25 June 2015

Abstract. Dissolved Fe (dFe) concentrations were measured in the upper 1300 m of the water column in the vicinity of the Kerguelen Islands as part of the second KErguelen Ocean Plateau compared Study (KEOPS2). Concentrations ranged from 0.06 nmol L^{-1} in offshore, Southern Ocean waters to 3.82 nmol L^{-1} within Hillsborough Bay, on the north-eastern coast of the Kerguelen Islands. Direct island runoff, glacial melting and resuspended sediments were identified as important inputs of dFe that could potentially fertilise the northern part of the plateau. A significant deep dFe enrichment was observed over the plateau with dFe concentrations increasing up to 1.30 nmol L^{-1} close to the seafloor, probably due to sediment resuspension and pore water release. Biological uptake was shown to induce a significant decrease in dFe concentrations between two visits (28 days apart) at a station above the plateau. Our work also considered other processes and sources, such as lateral advection of enriched seawater, remineralisation processes, and the influence of the polar front (PF) as a vector for Fe transport. Overall, heterogeneous sources of Fe over and off the Kerguelen Plateau, in addition to strong variability in Fe supply by vertical or horizontal transport, may explain the high variability in dFe concentrations observed during this study.

1 Introduction

Iron (Fe) has been shown to be an essential trace metal controlling phytoplankton growth and primary production in about 50 % of the world's oceans (Moore et al., 2001) including high-nutrient, low-chlorophyll (HNLC) regions. The main sources of Fe in the world's oceans are atmospheric deposition (wet or dry) (e.g. Jickells et al., 2005), sediment resuspension (Lam and Bishop, 2008), pore water release (Elrod et al., 2004), hydrothermal activity (Tagliabue et al., 2010), and remineralisation of organic matter (Ibisanmi et al., 2011). In the Southern Ocean, dust inputs have been considered to be small due to its remoteness from land masses (Wagener et al., 2008; Heimburger et al., 2013), but the other sources of Fe have been shown to induce natural fertilisation in several sites including the Crozet Plateau (Pollard et al., 2009; Planquette et al., 2011), the Scotia Sea (Dulaiova et al., 2009; Ardelan et al., 2010; Nielsdóttir et al., 2012; Hatta et al., 2013; Measures et al., 2013), the Ross Sea (Smith Jr. et al., 2012), and the Kerguelen Plateau (Blain et al., 2007, 2008), all stimulating phytoplankton blooms and enhancing carbon sequestration with varying magnitudes.

During the first KErguelen Ocean Plateau compared Study (KEOPS1), carried out in late austral summer 2005, the im-

Published by Copernicus Publications on behalf of the European Geosciences Union.

pact of natural fertilisation on primary productivity and carbon export was demonstrated in this area (Blain et al., 2007; Savoye et al., 2008). The surface area of the observed phytoplankton bloom was about 45 000 km^2 and led to a carbon sequestration efficiency 18 times higher (Chever et al., 2010) than estimated around the Crozet Islands (bloom area 90 000 km^2) during the CROZEX experiment in the same year (Pollard et al., 2009; Morris and Charette, 2013). A second cruise, KEOPS2 (KErguelen Ocean and Plateau compared Study 2), was designed to study the development of the Kerguelen bloom in early spring 2011 and in the offshore fertilisation area further east. In this paper, we present dissolved Fe (dFe) concentrations clustered into five groups (near-coastal, plateau, recirculation, north of the polar front (PF), HNLC area) and discuss their distributions in relation to potential new and regenerated sources. Where possible, an estimate of the biological uptake of Fe is provided. Finally, dFe data presented in this paper together with particulate Fe data from a closely aligned companion study (van der Merwe et al., 2015) are combined by Bowie et al. (2014) in order to establish short-term Fe budgets at three sites (above the plateau, in the recirculation area, and the HNLC area).

2 Materials and methods

2.1 Study area

During austral spring (7 October–30 November 2011), 149 seawater samples from 15 stations were collected as part of the KEOPS2 oceanographic research cruise (Fig. 1, Table 1) in the vicinity of the Kerguelen Islands in the Southern Ocean (48.40–50.62° S and 66.68–74.65° E). Two stations were sampled over the plateau (A3 and G-1), south of the island. A3 was visited twice, 28 days apart, in the early stage and during the build-up of the spring phytoplankton bloom. An east–west (E-W) transect (from TEW-1 to F-L) was sampled from the Kerguelen coast to offshore waters, and crossed the PF twice. Finally, three additional stations were analysed within a complex system of recirculation located in a stationary meander of the PF (E-3, E-4W-2 and E-5). An open-ocean station (R-2) was located in the HNLC area south-west of the Kerguelen Islands and south of the PF.

2.2 Sampling and analytical methods

Cleaning, sampling, handling, and processing of the samples were conducted using stringent trace metal clean protocols as recommended by the GEOTRACES programme (Cutter et al., 2010; Cutter, 2013). Samples were collected using a trace metal clean rosette (TMR, model 1018, General Oceanics) equipped with twelve 10 L externally closing Teflon-lined Niskin-1010X bottles mounted on a polyurethane powder-coated aluminium frame specially designed for trace metal work (Bowie et al., 2009). Seawater was subsampled for dFe via a Teflon tap connected to acid-cleaned 0.2 µm filter cartridges (Pall Acropak® and Sartorius Sartrobran® 300). Acid-cleaned low-density polyethylene bottles (60 mL) were rinsed three times with ~ 20 mL of seawater before final sample collection. Dissolved Fe samples were acidified to pH ~ 2 using concentrated ultrapure hydrochloric acid (Seastar Baseline, HCl). The sample bottles were then double-bagged and stored at ambient temperature in the dark until analysis. The shallowest sample was collected at 15 m depth in order to avoid contamination from the ship. Samples were collected off plateau to a depth of 1300 m.

Dissolved Fe was analysed on board at least 24 h after collection by means of flow injection analysis (FIA) with online solid-phase extraction onto 8-hydroxyquinoline (8-HQ) resin and chemiluminescence detection, following a method adapted from Obata et al. (1993) (Sarthou et al., 2003). All analyses were conducted inside a class 100 laminar flow hood within a containerised clean laboratory, using high-efficiency particulate air (HEPA) filters. During the cruise, hydrogen peroxide, ammonium acetate buffer, and HCl blanks were consistently below the detection limit (0.017 ± 0.012 nmol L^{-1}, $n = 22$), and therefore the system was deemed suitable for open-ocean seawater analysis (Johnson et al., 2007). Each sample was analysed in triplicate with an average precision of 4.8 % ($n = 149$). The North Pacific SAFe Surface (SAFe S) (0.094 ± 0.003 nmol L^{-1}, $n = 3$) and SAFe Deep D2 (0.95 ± 0.05 nmol L^{-1}, $n = 3$) reference samples were measured for dFe, and the results were in excellent agreement with the consensus values (S1 $= 0.095 \pm 0.008$ nmol L^{-1} and D2 $= 0.96 \pm 0.02$ nmol L^{-1}; Johnson et al., 2007).

Potential temperature (Θ), salinity (S), oxygen (O_2), and beam attenuation data were retrieved from the CTD sensors. We used the data from the CTD casts that were deployed immediately before or after our TMR casts.

3 Results and discussion

3.1 Clustering of stations

The presentation and discussion of results are organised into clusters, which were defined considering the hydrography and the complex regional circulation. Water masses were identified using Θ–S diagrams (Fig. 2).

Cluster 1 includes TEW-1 and TEW-2 stations located at the north-eastern flank of the Kerguelen Islands and north of the PF, with shallow waters (~ 85 m bottom depth), low salinity (33.6–33.8), and low density anomaly (< 27.0 kg m^{-3}). Below the surface mixed layer (SML), the water masses can be defined as subsurface (shelf) waters.

Cluster 2 includes stations located above the central part of the Kerguelen Plateau (A3-1, A3-2, G-1, and TEW-3, bottom depths lower than 600 m), and located south of the PF, with a minimum of temperature around 200 m. At A3-1, stratification had not yet started and surface water temperature

Table 1. Station name, longitude, latitude, sampling date, mixed layer depth (MLD), station bottom depth, location, dissolved iron concentrations (dFe), and standard deviation (SD) during KEOPS2. MLD were estimated using, as a reference, potential densities at both 10 and 20 m. When estimates are different, both values are given.

Station	Long [degrees east]	Lat [degrees south]	Date	MLD [m]	Bot. depth [m]	Depth [m]	dFe [nmol L^{-1}]	SD [nmol L^{-1}]
A3-1	72.06	50.62	20/10/11	164–165	530	45	0.28	0.00
						105	0.40	0.01
						160	0.32	0.02
						340	0.53	0.03
R-2	66.68	50.38	26/10/11	76–95	2500	40	0.09	0.01
						70	0.08	0.01
						100	0.17	0.00
						140	0.18	0.01
						170	0.12	0.01
						200	0.27	0.00
						235	0.26	0.00
						300	0.33	0.01
						350	0.35	0.01
						400	0.38	0.01
						500	0.39	0.01
						700	0.28	0.02
						900	0.28	0.01
						1000	0.31	0.02
						1200	0.30	0.01
						1300	0.32	0.01
TEW-1	69.83	49.13	31/10/11	32–42	86	15	1.82	0.38
						40	2.52	0.12
						50	2.58	0.16
						62	3.82	0.04
TEW-2	70.65	48.88	31/10/11	40–70	85	15	1.26	0.03
						30	1.61	0.02
						40	1.70	0.14
						50	1.80	0.07
						62	1.82	0.01
TEW-3	71.02	48.78	31/10/11	16–94	560	20	0.19	0.02
						40	0.12	0.02
						70	0.09	0.01
						100	0.21	0.00
						150	0.19	0.01
						200	0.19	0.01
						300	0.26	0.01
						400	0.37	0.00
						480	0.52	0.01
TEW-4	71.62	48.62	1/11/11	95	1600	40	0.17	0.02
						70	0.15	0.01
						100	0.20	0.01
						150	0.10	0.01
						200	0.11	0.00
						300	0.21	0.00
						400	0.30	0.00
						500	0.36	0.01
						600	0.39	0.01
						700	0.35	0.01
						1000	0.40	0.00
						1300	0.42	0.01
E-2	72.07	48.52	1/11/11	42–43	2000	40	0.08	0.01
						70	0.08	0.00
						100	0.10	0.00
						150	0.07	0.01
						200	0.18	0.00
						300	0.22	0.01
						400	0.23	0.01
						500	0.28	0.01
						600	0.34	0.01
						700	0.28	0.01
						1000	0.37	0.01
						1300	0.37	0.01
TEW-5	72.78	48.47	1/11/11	22–56	2250	40	0.12	0.01
						70	0.13	0.01
						100	0.16	0.01
						150	0.16	0.02
						200	0.21	0.08
						300	0.30	0.01
						400	0.39	0.01
						500	0.36	0.01
						600	0.31	0.01
						700	0.34	0.01
						1000	0.44	0.01
						1300	0.42	0.01

Table 1. Continued.

Station	Long [degrees east]	Lat [degrees south]	Date	MLD [m]	Bot. depth [m]	Depth [m]	dFe [nmol L^{-1}]	SD [nmol L^{-1}]
TEW-7	73.98	48.45	2/11/11	22–24	2500	20	0.39	0.02
						40	0.22	0.02
						150	0.40	0.04
						200	0.46	0.02
						300	0.46	0.02
						400	0.48	0.02
						1000	0.56	0.01
						1300	0.59	0.02
E-3	71.97	48.70	3/11/11	32–35	1900	20	0.38	0.03
						40	0.31	0.02
						70	0.22	0.01
						100	0.24	0.01
						130	0.24	0.02
						200	0.33	0.01
						300	0.50	0.01
						400	0.46	0.01
						600	0.50	0.02
						800	0.50	0.02
						1000	0.50	0.01
						1300	0.52	0.01
F-L	74.65	48.52	7/11/11	47	2700	20	0.26	0.02
						35	0.17	0.03
						60	0.30	0.00
						100	0.33	0.01
						200	0.48	0.03
						300	0.40	0.03
						400	0.40	0.01
						600	0.56	0.03
						800	0.61	0.02
						1000	0.67	0.03
						1300	0.61	0.05
A3-2	72.05	50.62	16/11/11	123	525	37	0.18	0.02
						70	0.14	0.01
						108	0.14	0.01
						210	0.51	0.01
						300	0.66	0.01
						400	0.81	0.02
						450	1.04	0.00
						480	1.30	0.01
G-1	71.88	49.90	9/11/11	60–68	590	20	0.21	0.04
						40	0.13	0.01
						70	0.23	0.01
						100	0.17	0.01
						150	0.19	0.01
						200	0.18	0.01
						250	0.24	0.01
						300	0.49	0.01
						350	0.67	0.01
						400	0.74	0.02
						500	0.59	0.02
						540	0.99	0.01
E-4W-2	71.42	48.75	18/11/11	26–35	1390	20	0.20	0.01
						40	0.16	0.01
						70	0.15	0.01
						100	0.11	0.00
						150	0.22	0.01
						180	0.28	0.00
						230	0.28	0.01
						300	0.35	0.01
						500	0.41	0.01
						700	0.42	0.01
						900	0.40	0.00
						1100	0.61	0.02
E-5	71.88	48.40	19/11/11	35–41	1920	25	0.06	0.01
						40	0.06	0.00
						70	0.10	0.00
						110	0.08	0.01
						150	0.11	0.01
						200	0.14	0.01
						350	0.23	0.00
						500	0.43	0.01
						700	0.37	0.00
						900	0.34	0.01
						1100	0.40	0.00
						1300	0.39	0.03

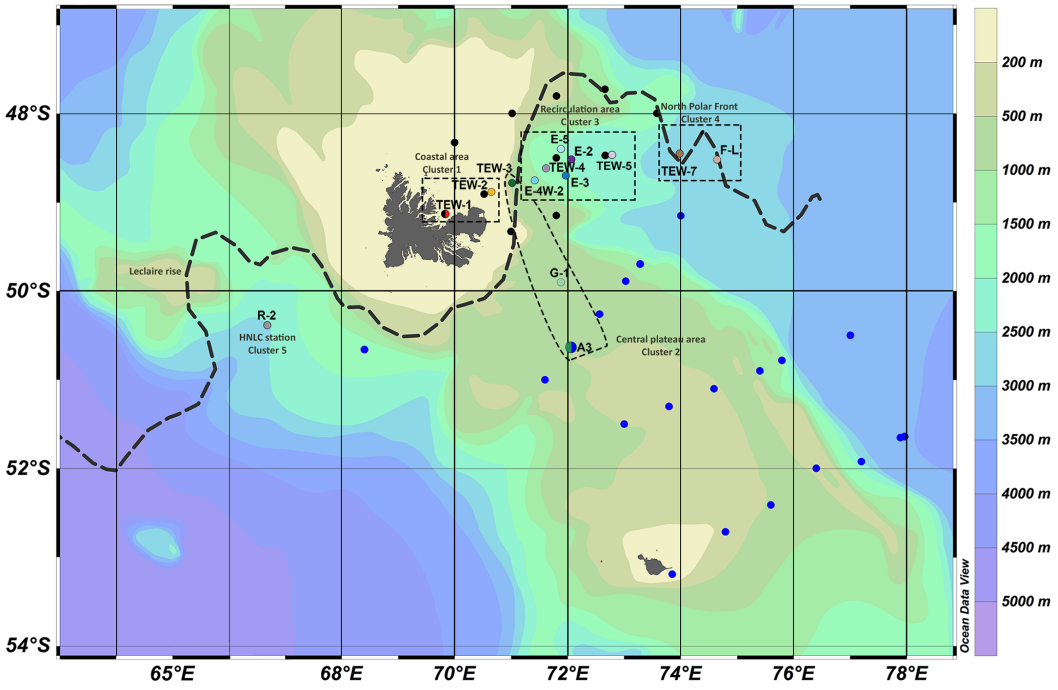

Figure 1. Map showing the bathymetry of the area and the stations visited during KEOPS2 (yellow-orange for cluster 1, green for cluster 2, blue-violet for cluster 3, brown for cluster 4, and grey for cluster 5), KEOPS1 (blue dots; Blain et al., 2008), and ANTARES3 (black dots; Bucciarelli et al., 2001). The dashed line represents the approximate location of the polar front (200 m) (Park et al., 2014).

was low ($\sim 1.7\,^{\circ}$C) and typical of winter conditions. Stations A3-2 and G-1 presented similar water masses (Fig. 2). The SMLs were observed down to 125 and 65 m, respectively. Below, winter water (WW) is encountered with temperatures around 1.7 °C at 225 and 115–210 m, respectively. The inclusion of TEW-3 in cluster 2 is debatable given its location at the plateau edge. Indeed, although TEW-3 can be considered as south of the PF, its location within the polar front jet is likely more correct. However, a structure comparable to A3-1, A3-2, and G-1 was observed below the surface waters with a WW temperature just below 2 °C.

East of the Kerguelen Plateau, the PF presents a permanent meander (Park et al., 2014). This meander delimits a region with a complex circulation including stations TEW-4, E-2, TEW-5, E-3, E-4W-2, and E-5, and is defined as cluster 3. All these stations showed very similar Θ–S profiles (Fig. 2). The warmest sea-surface temperatures were observed at station E-5, due to the decrease in the mixed layer depth (MLD) and progression into summer. Below the surface water (SW), a subsurface temperature minimum (~ 1.7–$1.8\,^{\circ}$C) was observed between 170 and 220 m, characteristic of the WW (Fig. 2). Below, the oxygen minimum around 600–800 m (175 µmol kg^{-1}) can be attributed to the Upper Circumpolar Deep Water (UCDW). Deeper in the water column (below 1300 m), the salinity increased towards a salinity maximum (~ 34.75), indicating the presence of the Lower Circumpolar Deep Water (LCDW).

Stations TEW-7 and F-L (cluster 4), located north of the PF and east of the plateau presented the warmest surface waters of the study (4.2 °C) characteristic of the Subantarctic Surface Water (SASW). The Antarctic Intermediate Water (AAIW) occurred deeper, at 170 (TEW-7) and 290 m (F-L) (Fig. 2). Below the AAIW, the UCDW and the LCDW were encountered.

Station R-2, located in the HNLC area, stands on its own in cluster 5. A salinity minimum (33.78) and a surface temperature maximum (2.0 °C) were observed in the upper 100 m, which is characteristic of the SW (Fig. 2). At 200 m, the temperature minimum (1.6 °C) was indicative of WW. The oxygen minimum (170 µmol kg^{-1}) defined the UCDW. Deeper in the water column (below 1300 m), the salinity increased towards a salinity maximum (~ 34.73) indicating the presence of the LCDW.

3.2 A general overview of dFe distributions

Median dFe concentrations for the different water masses and clusters (2 to 5) are plotted in Fig. 3.

In the surface waters, near-coastal stations presented the highest concentrations (2.10 ± 0.77 nmol L^{-1}). When considering the other stations, the lowest sea-surface concentrations were found at station R-2 (0.09 ± 0.01 nmol L^{-1}), while the highest were observed in cluster 4 (0.26 ± 0.09 nmol L^{-1}). If we compare our results

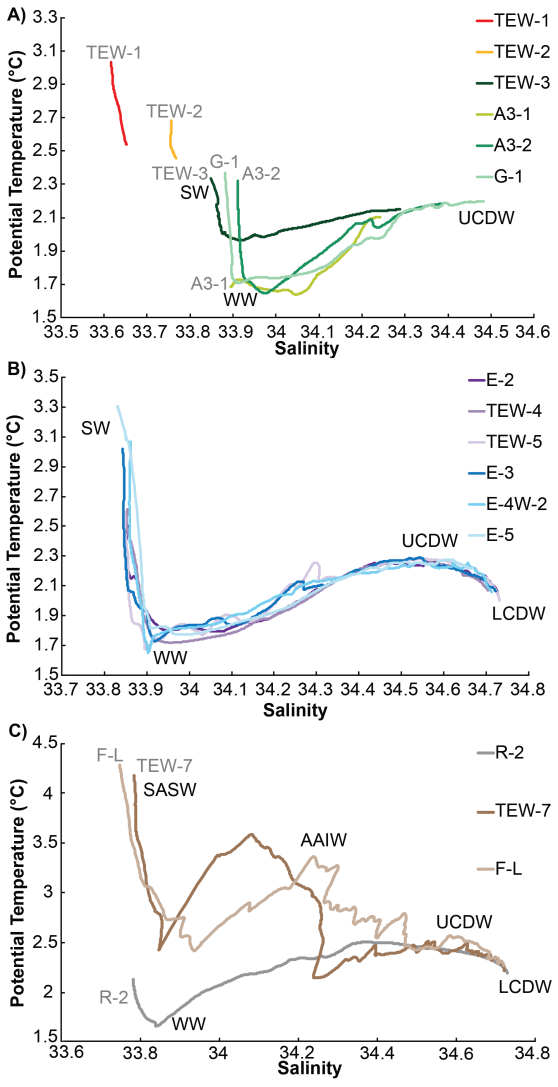

Figure 2. Potential temperature–salinity diagram for stations sampled during KEOPS2 for dissolved iron. Water masses are indicated in black, and station names in grey. The same colour code as used in Fig. 1 applies here. **(a)** Clusters 1 and 2: near-coastal (TEW-1, TEW-2) and Kerguelen Plateau (A3-1, A3-2, G-1, TEW-3) stations. Three water masses are displayed: surface water (SW), winter water (WW), Upper Circumpolar Deep Water (UCDW). **(b)** Cluster 3: the recirculation area (E-2, TEW-4, TEW-5, E-3, E-4W-2, E-5). Four water masses are displayed: surface water (SW), winter water (WW), Upper Circumpolar Deep Water (UCDW), Lower Circumpolar Deep Water (LCDW). **(c)** Clusters 4 and 5: north of the polar front (F-L, TEW-7) and the HNLC area (R-2). Five water masses are displayed: Subantarctic Surface Water (SASW), Antarctic Intermediate Water (AAIW), winter water (WW), Upper Circumpolar Deep Water (UCDW), Lower Circumpolar Deep Water (LCDW).

in the surface waters to the data set compiled by Tagliabue et al. (2012), R-2 had lower values than the mean value of the Indian Antarctic zone (0.43 ± 0.51 nmol L^{-1}), whereas the mean value in cluster 4 was higher than the mean value of the Indian subantarctic zone (0.23 ± 0.20 nmol L^{-1}). Tagliabue et al. (2012) suggested that the higher mean surface value in the Antarctic than in the subantarctic zone could be due to a lower biological activity in the former. In our study, the biological activity was much lower at station R-2 (Antarctic zone) than in cluster 4 (subantarctic zone). Indeed the highest integrated concentrations over 200 m for chlorophyll *a* (Chl *a*) were observed in cluster 4 (223–35 mg m^{-2}, Lasbleiz et al., 2014). Therefore, the lower dFe value at R-2 compared to cluster 4 might not reflect differences in biological activity but, rather, in Fe inputs (see below).

At intermediate depths, median dFe values were not significantly different among clusters 2, 3, and 5 in the WW (ANOVA, $F = 0.54$, $p = 0.5904$), suggesting that the whole area presented similar dFe concentrations at the surface during wintertime. In cluster 4, dFe in the AAIW presented relatively high values (0.46 ± 0.06 nmol L^{-1}), consistent with the high dFe values in the surface waters of the Antarctic zone (Tagliabue et al., 2012).

In the deep waters (LCDW and UCDW), stations above the plateau were enriched with Fe compared to all other clusters. When considering the clusters in offshore waters, values for stations in cluster 4 (0.57 ± 0.04 nmol L^{-1}) were significantly higher than those in cluster 3 (0.41 ± 0.09 nmol L^{-1}; Mann–Whitney, $W = 3.0$, $p = 0.0007$) and in cluster 5 (0.33 ± 0.02 nmol L^{-1}; Mann–Whitney, $W = 45.0$, $p = 0.003$). This is consistent with the compilation by Tagliabue et al. (2012), which showed that deep values were higher in the subantarctic zone than in the Antarctic zone (0.64 ± 0.31 and 0.51 ± 0.24 nmol L^{-1}, respectively). This difference was attributed to both higher ligand concentrations at depth (Thuróczy et al., 2011) and deep Fe inputs such as hydrothermal activity, with the greatest input in the Indian subantarctic region (Tagliabue et al., 2012).

3.3 Coastal area (cluster 1)

Stations TEW-1 and TEW-2 were sampled on the same day in order to provide a nearshore data set of dFe. Stations TEW-1 and TEW-2 were in shallow waters approximately 10 and 75 km away from Hillsborough Bay coast, respectively.

Median profiles of dFe, with minimum and maximum values in this cluster, are shown in Fig. 4a. At station TEW-1, dFe concentrations were high (> 1.8 nmol L^{-1}, Table 1), and increased steadily from 15 m (1.82 nmol L^{-1}) to 50 m depth (2.58 nmol L^{-1}). Close to the seafloor a sharp increase at 62 m depth (3.82 nmol L^{-1}) was measured. These are the highest values measured during this study. At TEW-2, dFe concentrations were lower than at TEW-1, increasing from 1.26 nmol L^{-1} in surface waters to 1.82 nmol L^{-1} at 62 m depth.

Several studies have already measured dFe at near-coastal stations in the Southern Ocean (Table 2). Around the Kerguelen Islands (KEOPS1), Crozet Islands (CROZEX), and South

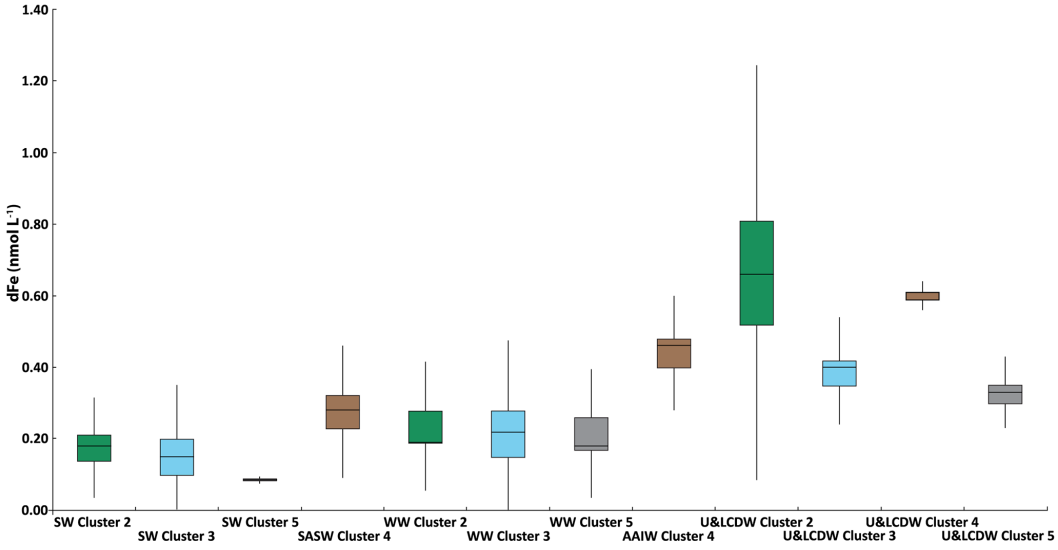

Figure 3. A box plot of the dFe concentrations in each water mass present in clusters 2 to 5: surface waters (SW and SASW), winter waters (WW), Antarctic Intermediate Water (AAIW), and Lower and Upper Circumpolar Deep Water (LCDW and UCDW). Median values are indicated by a horizontal line within the box, the box represents the interquartile range, and the whiskers extend to 5th and 95th percentile values. Data from cluster 1 are not shown to allow a clearer representation of the other clusters.

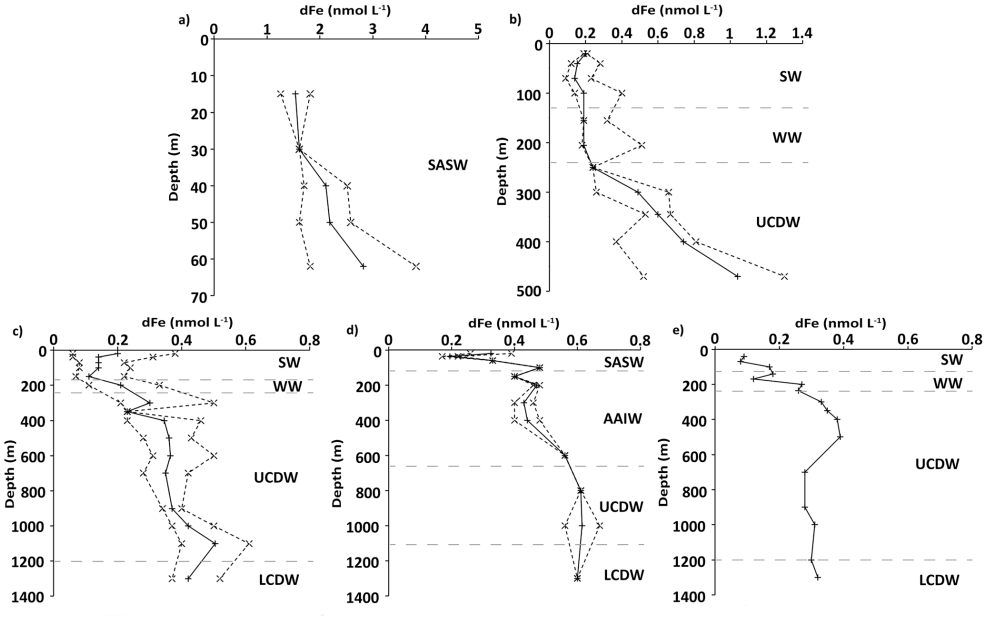

Figure 4. Vertical distribution of dFe concentrations measured in clusters 1 **(a)**, 2 **(b)**, 3 **(c)**, 4 **(d)**, and 5 **(e)** showing the median dFe (solid line with crosses). The interquartile range, defined as the range around the median containing 50 % of the data, is given between the two dotted lines.

Shetland Islands, dFe concentrations were within the same order of magnitude as the present study (~ 2–4 nmol L^{-1}; Table 2). During ANTARES3 (Kerguelen), dFe concentrations were 5- to 10-fold higher (22.6 nmol L^{-1}). This discrepancy was already discussed (Blain et al., 2008) and is likely partly due to methodological differences (0.4 µm filtration, nitric acid acidification, and 2-year storage).

The elevated dFe concentrations observed at nearshore sites are most certainly indicative of Fe sourced from the islands, a feature clearly evident during the present study and illustrated in Fig. 5. This source is most likely a combination of direct island runoff, glacial melt and resuspended sediments. High particle loads (as estimated by beam attenuation data) were encountered throughout the water col-

Table 2. Concentrations of dissolved iron (nmol L^{-1}) for various Southern Ocean regions influenced by natural iron fertilisation. Near-coastal and shelf water stations were defined as stations where the bottom depth was less than 100 m and between 100 and 600 m depth, respectively. Furthermore, near-coastal stations were less than 25 km distant from shore. The recirculation area corresponds to the polar front meander at the north-east of the Kerguelen Islands.

Location	Near-coastal	Shelf water	Recirculation	North polar front	HNLC	Sampling period	Reference
Kerguelen Islands	1.26–3.82	0.09–1.30		0.17–0.67	0.08–0.39	spring	This study
	0.78–0.81	0.05–0.71	0.08–0.17	–	0.05–0.38	summer	Blain et al. (2008)
	5.04–22.60	0.26–1.74	0.46–2.71	0.88–4.11	–	spring	Bucciarelli et al. (2001)
Crozet Islands	0.39–2.16	0.15–0.42	–	0.22–0.38	0.20–0.40	late spring	Planquette et al. (2007)
South Georgia	–	0.065–1.321	–	–	–	summer	Nielsdóttir et al. (2012)
South Orkney Islands	0.966–2.275	–	–	–	–	summer	Nielsdóttir et al. (2012)
South Shetland Islands	> 3	1.2–2.6	–	–	–	winter	Hatta et al. (2013)
	0.8–2.2	–	–	–	–	late summer	Klunder et al. (2014)

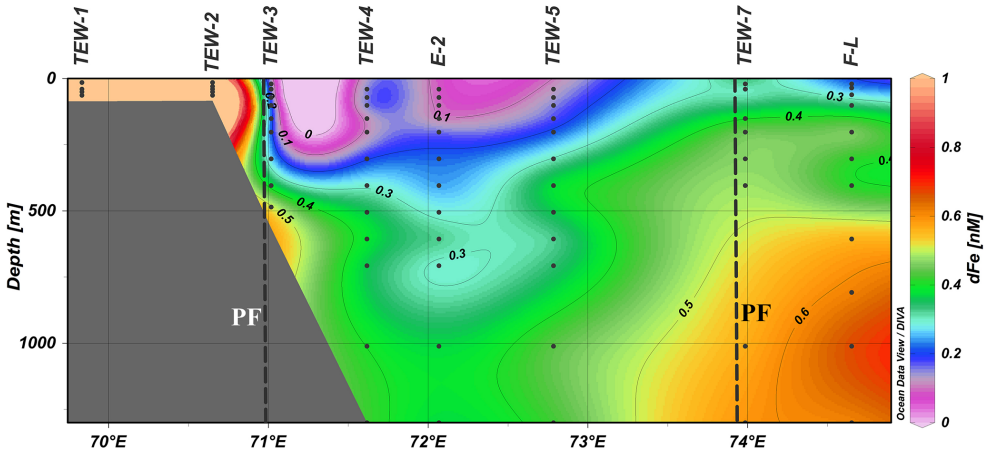

Figure 5. Concentrations of dFe (nmol L^{-1}) over the east–west transect. The PF position is indicated with black dashed lines. Stations TEW-1, TEW-2, TEW-3, TEW-4, E-2, TEW-5, TEW-7, and F-L were included in this section as they were sampled consecutively in a short time period (7 days) (Table 1).

umn of TEW-1 and TEW-2, with higher concentrations at TEW-1, especially at 10 m depth and close to the seafloor (Fig. 6). Low salinities (33.63 ± 0.01, $n = 61$) were also measured at TEW-1, which corroborates our hypothesis of direct island runoff and/or glacial melt inputs. Moreover, the Ampère Glacier, which is the largest glacier from the Cook Ice Cap (about 500 km^2), has thinned rapidly over the last decade (Berthier et al., 2009), especially towards the east of the ice cap, up to 1.5 m per year. This discharge includes small basalt-derived particles (Frenot et al., 1995) and could partially discharge in Hillsborough Bay (Y. Frenot, personal communication, 2014). Finally, TEW-1 showed the highest lithogenic silica (LSi) concentrations of the study area (1.31 ± 0.14 µmol L^{-1}; Closset et al., 2014; Lasbleiz et al., 2014) and TEW-2 showed slightly lower LSi concentrations (0.54 ± 0.02 µmol L^{-1}). Gradients in LSi and dFe are probably indicative of glacial melt inputs, Fe being leached from nanoparticulate iron (oxyhydr)oxides present in glacial rock flour (Raiswell et al., 2010; Raiswell, 2011) and LSi being weathered from silicate-rich minerals (SiO_2; Doucet et al., 2005).

Sedimentary inputs (e.g. Johnson et al., 1999; Elrod et al., 2004; Chase et al., 2005; Lam et al., 2006; Planquette et al., 2011; Homoky et al., 2013; Marsay et al., 2014) could also explain the increased dFe concentrations encountered at both stations close to the seafloor (3.82 and 1.82 nmol L^{-1} at stations TEW-1 and TEW-2, respectively). Unfortunately, particulate Fe (pFe) concentrations were not measured at these near-coastal locations to confirm sediment resuspension, but the fact that the beam attenuation increased close to the seafloor of station TEW-1 (Fig. 6) and that high dMn concentrations at TEW-1 (5.40 nmol L^{-1}) and TEW-2 (1.92 nmol L^{-1}) were also measured (Quéroué et al., unpublished data) strongly supports this hypothesis.

Dissolved Fe concentrations in the water column may reflect not only sedimentary inputs but also inputs from remineralisation processes. However, since deciphering remineralisation from sedimentary inputs at shallow stations is diffi-

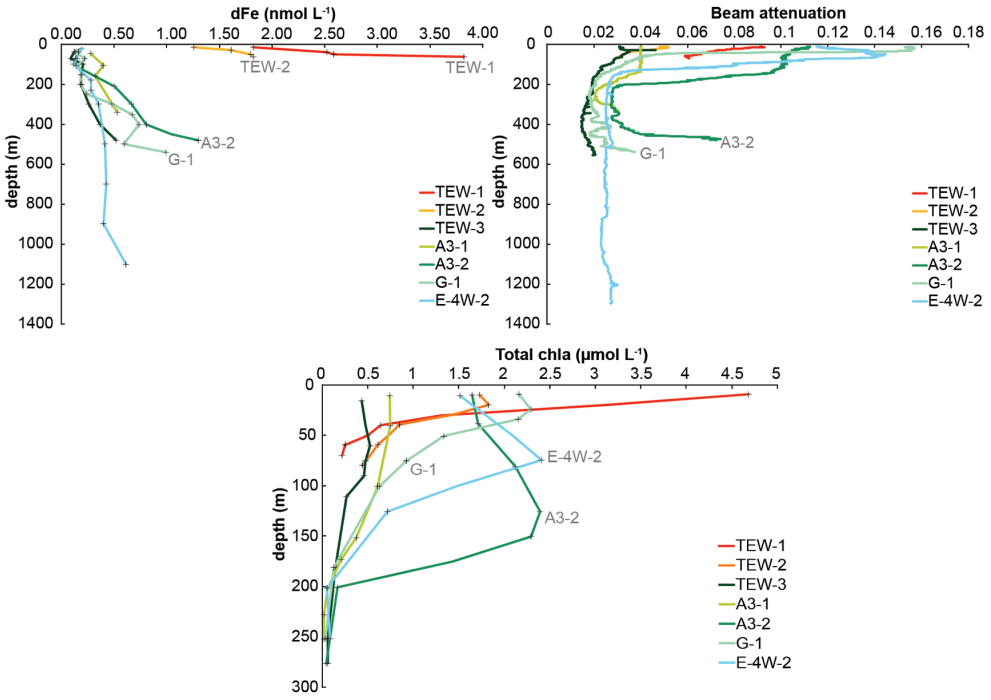

Figure 6. (a) Dissolved Fe concentrations, **(b)** beam attenuation coefficient, and **(c)** total chlorophyll *a* concentrations (from Lasbleiz et al., 2014) at near-coastal stations (cluster 1, TEW-1, and TEW-2), stations above the plateau (cluster 2, A3-1, A3-2, G-1, and TEW-3), and at E-4W-2. The same colour code as used in Fig. 1 applies here.

cult, remineralisation process will only be discussed for clusters 3, 4, and 5.

3.4 Central plateau area (cluster 2)

Similar dFe vertical profiles were observed at A3-2, G-1, and TEW-3 with low dFe concentrations at the surface ($\sim$ 0.1–0.2 nmol L^{-1}), increasing towards the bottom, up to 1.30 ± 0.01, 0.99 ± 0.01, and 0.37 ± 0.00 nmol L^{-1}, respectively (Table 1). Median profiles of dFe, with minimum and maximum values in this cluster, are shown in Fig. 4b. At station A3-1, concentrations were higher in the SML ($\sim$ 0.3–0.4 nmol L^{-1}) and then increased with depth below the SML up to 0.40 ± 0.01 nmol L^{-1} at 350 m.

Over the Kerguelen Plateau, 24 shelf stations have been investigated during several cruises (Table 2). The highest concentrations were measured during ANTARES3 ($\sim$ 6 nmol L^{-1}) in the northern part of the Kerguelen Plateau at a station located 76 km away from the shore (station K4, 40 m). The lowest concentrations were measured during KEOPS1 (0.05 nmol L^{-1}) within the top 200 m of water. Above 100 m, lower concentrations were observed during KEOPS1 compared to KEOPS2 (Table 2). This can be explained by a more advanced phytoplankton bloom during KEOPS1 (summer conditions) than KEOPS2 (spring conditions). In surface waters, dFe concentrations measured during KEOPS2 were of similar magnitude to those measured in the vicinity of the South Shetland Islands (Nielsdóttir et al., 2012; Table 2).

A deep Fe-enriched reservoir was also observed above the Kerguelen Plateau during KEOPS1 (Blain et al., 2008; Chever et al., 2010). Non-reductive dissolution of resuspended sediments is a potentially important source of dFe as observed at near-coastal stations (e.g. Homoky et al., 2013). At station A3, high LSi concentrations (1.34 ± 0.07 µmol L^{-1}; Lasbleiz et al., 2014) were observed just above the seafloor in the benthic boundary layer (BBL), also suggesting sedimentary inputs. This is corroborated by high pFe values at A3-1 and A3-2 (30 and 15 nmol L^{-1}, respectively) and pFe : pAl ratios that resemble basalt over the Kerguelen Plateau (van der Merwe et al., 2015).

The variability in the deep dFe concentrations above the plateau may be due to variability in sedimentary inputs in this highly dynamic region. All stations from this cluster except station TEW-3 had high beam attenuation values close to the seafloor, which most likely indicates the presence of resuspended particles at these depths (98 % for TEW-3 vs. 92–97 % for the other three stations, Fig. 6). Marsay et al. (2014) performed a very detailed sampling of near-bottom waters for dFe over the Ross Sea shelf and showed that dFe concentrations displayed a quasi-exponential increase with depth, with a pronounced gradient towards the seafloor. When plotting our dFe data as a function of height above the seafloor, we also observed an exponential increase with depth

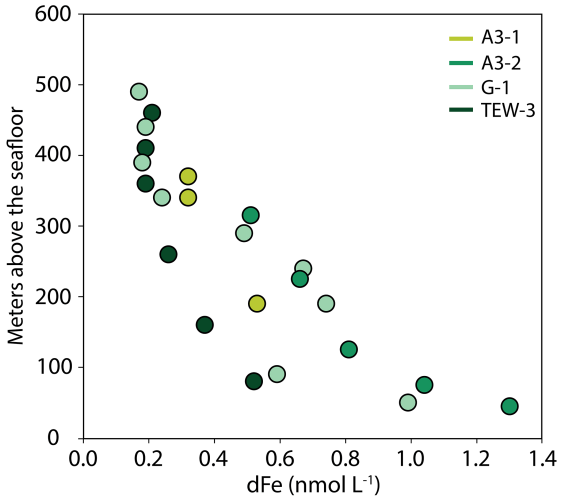

Figure 7. Dissolved Fe concentrations as a function of height above seafloor for all the stations of cluster 2. Bottom depths are taken from the CTD data. The same colour code as used in Fig. 1 applies here.

(Fig. 7). Clearly, the least pronounced gradient between dFe and height above seafloor was observed at station TEW-3.

Hydrothermal input may be an additional Fe source above the Kerguelen Plateau, more particularly in the vicinity of the Heard Island. The Mn : Al ratio at this station is much lower than at any of the other stations 0.007–0.009 (van der Merwe et al., 2015) and very similar to the Kerguelen Islands basalt mean of 0.004–0.010 (Gautier et al., 1990). This supports fresh weathering of basalt downstream of A3, which may be glacial/fluvial runoff or hydrothermal.

Diffusion from pore waters is another important possible source of Fe for the BBL (Elrod et al., 2004). When sediment receives large amount of organic carbon, it is covered by a fluff layer composed mainly of broken cells, as observed during KEOPS1 for stations above the plateau (Armand et al., 2008). Diagenesis then produces suboxic/anoxic conditions, which are key conditions to mobilise Fe because of the high solubility of the reduced Fe(II) form (Walsh et al., 1988). Anoxic conditions were observed 2 cm below the sediment surface at the A3 stations (P. Anschutz, personal communication, 2014), suggesting that, in pore waters above the plateau, Fe could be in the reduced form and diffuse into the bottom water column.

For all stations in cluster 2, dFe minima were observed in the SML, which could reflect biological uptake and/or particle scavenging. A significant decrease was observed in dFe concentrations in the SML between A3-1 (0.33 ± 0.06 nmol L^{-1}) and A3-2 (0.15 ± 0.02 nmol L^{-1}) (t test, $p < 0.05$). The first visit to site A3 (A3-1, 20 October) was characteristic of early bloom conditions, while during the second visit 28 days later (A3-2, 17 November), chlorophyll a concentrations at the sea surface increased by about 3-fold as a consequence of a large diatom bloom (Fig. 6c) (Lasbleiz et al., 2014). Moreover, based on the beam attenuation profiles, A3-2 seemed to have more particles (likely of biogenic origin) than A3-1 within the top 200 m. This is confirmed by the fact that at these depths, the Fe : Al ratio at A3-2 is higher than A3-1 and in all cases, well above the crustal ratios. This may indicate that more pFe of biogenic origin was present at A3-2 than at A3-1 (van der Merwe et al., 2015), and confirm an increased biological uptake at A3-2 compared to A3-1. Between the two visits, integrated dFe concentrations over 200 m decreased (62.6 vs. 28.1 µmol m^{-2}), while concentrations of particulate organic carbon (POC) (from 1259 to 2267 mmolC m^{-2}) increased (Lasbleiz et al., 2014). The decrease in dFe stock represents ∼ 35 % of the winter stock, defined as the dFe concentration in the WW (0.51 nmol L^{-1}) multiplied by the depth of the temperature minimum (200 m) (Blain et al., 2007). Taking into account the decrease in dFe stock and the increase in POC stock, the Fe : C ratio of the biomass that developed between the two visits at A3 can be estimated to equal 34 µmol mol^{-1}, a ratio consistent with literature values for diatoms in Fe-replete waters of the Southern Ocean (Sunda and Huntsman, 1995; Sunda, 1997; Twining et al., 2004; Sarthou et al., 2005). Although this is a rough estimate which does not take into account any additional inputs or removal processes, this result indicates that the dFe decrease between A3-1 and A3-2 could be due, at least partly, to biological uptake.

3.5 Recirculation area (cluster 3)

Median profiles of dFe, with minimum and maximum values in this cluster, are shown in Fig. 4c. A two-way ANOVA, based on depth and location (i.e. station), showed that location had a significant effect on dFe variability ($F = 24.92$, $df = 5$, $P < 0.01$). It defined five homogeneous groups from the six stations tested (E-2/E-5, E-5/TEW-4, TEW-4/TEW-5, TEW-5/E-4W-2, and E-3), showing the strong variability in vertical dFe distributions in this cluster. Stations E-2 and E-5 showed very low concentrations near the sea surface (from 0.06 to 0.10 nmol L^{-1}) and a gradual increase with depth (∼ 0.37–0.39 nmol L^{-1}, at 1300 m) (Table 1). A dFe maximum was observed at intermediate depths (500–600 m, 0.34–0.43 nmol L^{-1}). The dFe profile at station TEW-4 is homogeneous below 150 m. The dFe maximum at 600 m is 0.39 nmol L^{-1} and, at 1300 m, dFe reaches 0.42 nmol L^{-1}.

Concentrations at stations TEW-5 and E-4W-2 were close to those at stations TEW-4 in the upper 150 m (0.11–0.22 nmol L^{-1}), but these stations showed higher concentrations at intermediate depths (150–200 m, 0.21–0.30 nmol L^{-1}). Below 150–200 m, concentrations reached values of ∼ 0.4 nmol L^{-1}, except for the deepest value at station E-4W-2 (0.61 ± 0.02 nmol L^{-1}, 1100 m). This sampling depth was located less than 200 m away from the seafloor and was associated with an increase in beam attenuation (see

Fig. 6), which indicated a high number of particles and potential sedimentary inputs.

Station E-3 had high surface dFe concentrations at 40 m (0.38 ± 0.03 nmol L^{-1}) followed by a minimum at 100 m (0.22 ± 0.01 nmol L^{-1}) (Table 1). A subsurface dFe maximum was observed at intermediate depth (300 m, 0.50 ± 0.01 nmol L^{-1}), while concentrations remained homogenous at deeper depths (0.52 ± 0.01 nmol L^{-1}).

In this cluster, dFe concentrations were comparable to concentrations measured at stations off the Crozet Plateau that were not under HNLC conditions (Planquette et al., 2007). However during KEOPS2, water column dFe concentrations were lower than those observed during ANTARES 3 and in the South Shetland Islands sites, most likely due to the greater distance of the KEOPS2 stations from the shore (Table 2).

The higher sea-surface dFe concentrations at stations TEW-4, E-4W-2, and E-3, may be indicative of atmospheric inputs. However, no particulate aluminium (pAl, a proxy for atmospheric inputs) surface enrichment in the recirculation area was observed during the study (van der Merwe et al., 2015), suggesting that air masses were not carrying enough aerosols to enhance pAl surface concentrations. Moreover, Bowie et al. (2014) showed that atmospheric inputs were of the order of 50 nmol m^{-2} d^{-1}, which is insignificant compared to the lateral supply of dFe in the same area (180–2400 nmol m^{-2} d^{-1}). Significant ^{224}Ra and ^{223}Ra activities were detected in offshore waters south of the PF (Sanial et al., 2015). These observations clearly indicated that dissolved sediment-derived inputs of Ra can be rapidly transferred towards offshore waters. These Ra-enriched waters could also be enriched with dissolved sediment-derived Fe.

Within the waters characterised by an oxygen minimum, remineralisation of sinking organic matter may exert a primary control on dFe distribution. To assess this hypothesis, we looked at the relationship between dFe and the apparent oxygen utilisation (AOU), from the start of the oxycline ($\sim$ 150–200 m) to the bottom of the UCDW (700–1100 m). In these waters, the AOU indicates the amount of oxygen that has been consumed during remineralisation since the waters left the surface, whereas dFe concentration equals the preformed dFe plus any dFe released from remineralisation, minus any dFe scavenged by particles (Hatta et al., 2015). Dissolved Fe concentrations showed a significant positive correlation with the AOU for all the stations in the recirculation area (ANOVA, $p < 0.01$), meaning that remineralisation was likely a significant source of dFe at these depths. Station E-3 clearly presented a different behaviour compared to the other stations of cluster 3 (Fig. 8). Indeed, although the slopes were not significantly different (0.0016 ± 0.0003 mmol mol^{-1} for E-3 and 0.0018 ± 0.0002 mmol mol^{-1} for all stations except E-3; ANOVA, $p > 0.1$), the intercepts were different (0.26 ± 0.05 nmol L^{-1} for E-3 and 0.08 ± 0.03 nmol L^{-1} for all the other stations; ANOVA, $p < 0.01$). This suggests that a preformed dFe signal was present at E-3, which could explain the highest dFe values observed at this station. Using this slope of the dFe–AOU relationship and a modified oxygen consumption ratio of 1.6 moles of O_2 per mole of carbon remineralised (Martin et al., 1987), a net Fe : C ratio for the remineralisation process equal to 2.6–2.9 µmol mol^{-1} was estimated. This ratio is very similar to Fe : C ratios of Fe-limited diatoms from culture studies and in situ Southern Ocean data (Martin et al., 1987; Sunda, 1997; Sarthou et al., 2005).

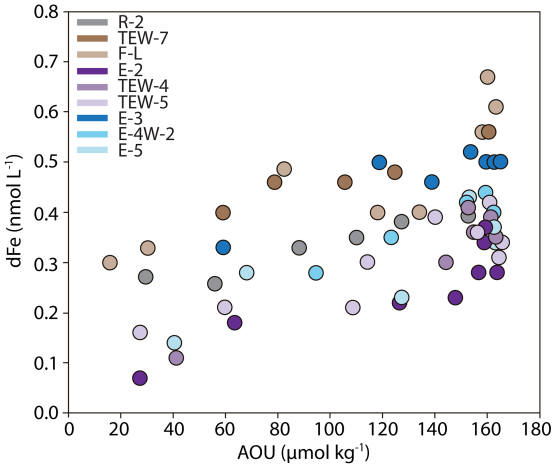

Figure 8. dFe vs. AOU in the recirculation area at stations E-2, E-5, TEW-4, TEW-5, E-4W-2, E-3, R-2, TEW-7, and F-L. The deeper dFe concentration at station E-4W-2 was not included since the observed sedimentary inputs would have masked the remineralisation signal. The same colour code as used in Fig. 1 applies here.

3.6 North polar front stations (cluster 4)

Stations TEW-7 and F-L were located north-east of the PF, approximately 270 and 313 km north-east of the Kerguelen Islands, with bottom depths of 2500 and 2700 m, respectively. These stations presented comparable vertical profiles (Fig. 4d). In the upper 50 m, dFe concentrations were depleted at 0.22 and 0.17 nmol L^{-1} (at 40 m at station TEW-7 and 35 m at station F-L, respectively) and then gradually increased within the mesopelagic zone to finally reach 0.59 nmol L^{-1} at 1300 m depth (station TEW-7) and 0.67 nmol L^{-1} at 1000 m depth (station F-L).

During ANTARES 3, station K14, which was also sampled north-east of the PF, exhibited high values at the surface (4.11 nmol L^{-1} at 40 m depth). This was interpreted as the result of a mixing between SASW and water masses coming from the west and enriched by sweeping the plateau (Bucciarelli et al., 2001), at a time when no significant sink occurred (beginning of spring, ~ 0.4 µg L^{-1} of Chl *a*).

During KEOPS2, however, the decrease in dFe concentrations within the SASW, around 35–40 m depth, can result from biological uptake. This is suggested by the high biomass reported at stations TEW-7 and F-L

(Lasbleiz et al., 2014), with the highest integrated concentrations over 200 m for Chl *a* ($>220\,\mathrm{mg\,m^{-2}}$), biogenic silica ($>300\,\mathrm{mmol\,Si\,m^{-2}}$), particulate organic carbon ($>1200\,\mathrm{mmol\,C\,m^{-2}}$), particulate organic nitrogen ($>200\,\mathrm{mmol\,N\,m^{-2}}$), and particulate organic phosphorus ($>30\,\mathrm{mmol\,P\,m^{-2}}$). This biological uptake is also reflected in the composition of suspended particles (van der Merwe et al., 2015). In surface waters, higher pFe : pAl elemental ratios were observed compared to those from the base of the SML, which is indicative of a conversion of dFe into biogenic pFe. However, compared to the less productive recirculation area (see Sect. 3.5), the surface dFe concentrations are higher by $0.1\,\mathrm{nmol\,L^{-1}}$. This could be explained by the fact that, like during ANTARES 3, a portion of the water masses found at TEW-7 and F-L likely interacted more with both the plateau and shallow coastal waters of the Kerguelen Islands than the water masses from the recirculation area. This hypothesis is supported by the general circulation in this region (Park et al., 2014) that shows that water masses are carried northwards between the island and the recirculation area and finally looped back east of the recirculation area. A Lagrangian model of Fe transport based on altimetry (d'Ovidio et al., 2015) also confirms that the waters at F-L and TEW-7 are mainly coming from the northern part of plateau. Moreover, close to the seafloor, van der Merwe et al. (2015) observed high values of pFe, pMn, and pAl, likely due to sediment resuspension.

As for the recirculation area, dFe concentrations in the mesopelagic zone may also reflect remineralisation processes. Dissolved Fe concentrations present a significant positive relationship with AOU for both stations ($\mathrm{dFe} = 0.0014 \pm 0.0003 \times \mathrm{AOU} + 0.32 \pm 0.03$, $n = 5$, $r^2 = 90\,\%$, $p < 0.05$ for station TEW-7; $\mathrm{dFe} = 0.0020 \pm 0.0005 \times \mathrm{AOU} + 0.24 \pm 0.07$, $n = 7$, $r^2 = 74\,\%$, $p < 0.05$ for station F-L). The two slopes are not significantly different (ANOVA, $p > 0.1$). When combining the two data sets (Fig. 8), the slope is also not significantly different from the slope in the recirculation area (ANOVA, $p > 0.1$), suggesting that Fe and C are remineralised at the same rates in both regions ($\mathrm{Fe : C} \sim 2\,\mu\mathrm{mol\,mol^{-1}}$). However, the intercept is significantly different from the intercept of the recirculation area (without the station E-3; see above) and from zero (ANOVA, $p < 0.01$), suggesting the presence of preformed Fe in these waters.

3.7 The HNLC station (cluster 5)

At station R-2, dFe concentrations were low within surface waters ($\sim 0.1\,\mathrm{nmol\,L^{-1}}$) and highest at 500 m depth ($0.39\,\mathrm{nmol\,L^{-1}}$) (Fig. 4e). Below 500 m, dFe concentrations decreased to a value of $\sim 0.30\,\mathrm{nmol\,L^{-1}}$.

The KEOPS, CROZEX, and South Shetland Islands studies (Planquette et al., 2007; Blain et al., 2008; Nielsdóttir et al., 2012) presented comparable ranges of dFe at open-ocean stations (Table 2). Dissolved Fe concentrations at R-2 were similar to those observed during KEOPS1 at C11 and the Kerfix station within the upper 170 m of the water column, as well as between 700 and 1300 m (Blain et al., 2008). However, dFe concentrations were up to 6.5-fold higher between 200 and 500 m at R-2 compared to C-11 and Kerfix, despite the close proximity of Kerfix and R-2.

While sea-surface lithogenic silica (LSi) concentrations (Lasbleiz et al., 2014) were low at station R-2 ($<0.042\,\mu\mathrm{mol\,L^{-1}}$), they were maximum at 500 m depth ($0.12\,\mu\mathrm{mol\,L^{-1}}$). Particulate iron, manganese, and aluminium (fraction between 1 and 55 µm) enrichments were also observed at 500 m (van der Merwe et al., 2015). Van der Merwe et al. (2015) also observed a unique particulate trace metal composition signature at this station, which could originate from the Leclaire Rise, contrasting with the basaltic signature observed above the Kerguelen Plateau (Doucet et al., 2005). The Leclaire Rise is a remarkable oceanic feature that consists of a submerged volcano with an area of $6500\,\mathrm{km^2}$, with the shallowest depth up to 100 m. It is located 75 km north-west of R-2 and could release dissolved and particulate material.

Similar to clusters 3 and 4, remineralisation may also partly explain dFe concentrations in the mesopelagic zone ($\mathrm{dFe} = 0.0012 \pm 0.0002 \times \mathrm{AOU} + 0.22 \pm 0.02$, $n = 6$, $r^2 = 91.8\,\%$, $p < 0.01$). Fe and C are also remineralised at the same rates as in clusters 3 and 4 (ANOVA, $p > 0.1$), and the intercept, significantly different from zero (ANOVA, $p < 0.01$), confirms the hypothesis of dFe sedimentary inputs at this station.

4 Conclusions

This third cruise over the Kerguelen Plateau allowed new insights into dFe sources and internal cycling. Direct runoff and glacial and sedimentary inputs can all be considered as important sources of dFe in the vicinity of the Kerguelen Islands. Remineralisation of sinking particles can explain the high concentrations of dFe in intermediate waters offshore. The strong jet of the PF was enriched with dFe from the north of the plateau as it flowed northward close to the Kerguelen Islands and later eastward to loop back into the recirculation area. This fertilised surface waters of the eastern part of the studied area. Furthermore, filaments crossing the PF allowed a more direct natural Fe fertilisation of surface water in the recirculation area. Due to variable water mass origin and variable horizontal advection mechanism (along or across the PF), the recirculation area evidenced strong dFe concentration variability. The PF is an important Southern Ocean feature that should not be neglected with regards to Southern Ocean fertilisation offshore from the Kerguelen Plateau through fast lateral Fe transport from the north of the Kerguelen Plateau.

Acknowledgements. The authors thank the crew of the R/V *Marion Dufresne* for assistance on board and Bernard Quéguiner, the chief scientist. They also greatly acknowledge Young-Hyang Park for fruitful discussions about the complex hydrography of the studied area. The authors thank the two anonymous referees for their fruitful comments. This work was supported by the French research programme of INSU-CNRS LEFE-CYBER ("Les enveloppes fluides et l'environnement" – "Cycles biogéochimiques, environnement et ressources"), the French ANR ("Agence Nationale de la Recherche", SIMI-6 programme, ANR-2010-BLAN-614 KEOPS2, and ANR-10-JCJC-606 ICOP), the French CNES programme ("Centre National d'Etudes Spatiales"), and the French Polar Institute IPEV (Institut Polaire Paul-Emile Victor). This research was supported by University of Tasmania Cross Theme (B0018994) and Rising Stars (B0019024) grants. Thanks to the Antarctic Climate and Ecosystems Cooperative Research Centre (ACE CRC) for funding participation in the KEOPS2 study through the Carbon programme. The KEOPS2 experiment was approved as a GEOTRACES process study.

Edited by: I. Obernosterer

References

Ardelan, M. V., Holm-Hansen, O., Hewes, C. D., Reiss, C. S., Silva, N. S., Dulaiova, H., Steinnes, E., and Sakshaug, E.: Natural iron enrichment around the Antarctic Peninsula in the Southern Ocean, Biogeosciences, 7, 11–25, doi:10.5194/bg-7-11-2010, 2010.

Armand, L. K., Cornet-Barthaux, V., Mosseri, J., and Quéguiner, B.: Late summer diatom biomass and community structure on and around the naturally iron-fertilised Kerguelen Plateau in the Southern Ocean, Deep-Sea Res. Pt. II, 55, 653–676, 2008.

Berthier, E., Le Bris, R., Mabileau, L., Testut, L., and Rémy, F.: Ice wastage on the Kerguelen Islands (49S, 69E) between 1963 and 2006, J. Geophys. Res.-Earth, 114, F03005, doi:10.1029/2008JF001192, 2009.

Blain, S., Quéguiner, B., Armand, L., Belviso, S., Bombled, B., Bopp, L., Bowie, A., Brunet, C., Brussaard, C., Carlotti, F., Christaki, U., Corbière, A., Durand, I., Ebersbach, F., Fuda, J.-L., Garcia, N., Gerringa, L., Griffiths, B., Guigue, C., Guillerm, C., Jacquet, S., Jeandel, C., Laan, P., Lefèvre, D., Lomonaco, C., Malits, A., Mosseri, J., Obernosterer, I., Park, Y.-H., Picheral, M., Pondaven, P., Remenyi, T., Sandroni, V., Sarthou, G., Savoye, N., Scouarnec, L., Souhaut, M., Thuiller, D., Timmermans, K., Trull, T., Uitz, J., van-Beek, P., Veldhuis, M., Vincent, D., Viollier, E., Vong, L., and Wagener, T.: Impact of natural iron fertilization on carbon sequestration in the Southern Ocean, Nature, 7139, 1070–1074, 2007.

Blain, S., Sarthou, G., and Laan, P.: Distribution of DFe during the natural iron-fertilization experiment KEOPS, Deep-Sea Res. Pt. II, 55, 594–605, doi:10.1016/j.dsr2.2007.12.028, 2008.

Bowie, A. R., Lannuzel, D., Remenyi, T. A., Wagener, T., Lam, P. J., Boyd, P. W., Guieu, C., Townsend, A. T., and Trull, T. W.: Biogeochemical iron budgets of the Southern Ocean south of Australia: Decoupling of iron and nutrient cycles in the subantarctic zone by the summertime supply, Global Biogeochem. Cy., 23, GB4034, doi:10.1029/2009GB003500, 2009.

Bowie, A. R., van der Merwe, P., Quéroué, F., Trull, T., Fourquez, M., Planchon, F., Sarthou, G., Chever, F., Townsend, A. T., Obernosterer, I., Sallée, J.-B., and Blain, S.: Iron budgets for three distinct biogeochemical sites around the Kerguelen archipelago (Southern Ocean) during the natural fertilisation experiment KEOPS-2, Biogeosciences Discuss., 11, 17861–17923, doi:10.5194/bgd-11-17861-2014, 2014.

Bucciarelli, E., Blain, S., and Tréguer, P.: Iron and manganese in the wake of the Kerguelen Islands (Southern Ocean), Mar. Chem., 73, 21–36, 2001.

Chase, Z., Johnson, K. S., Elrod, V. A., Plant, J. N., Fitzwater, S. E., Pickella, L., and Sakamotob, C. M.: Manganese and iron distributions off central California influenced by upwelling and shelf width, Mar. Chem., 95, 235–254, 2005.

Chever, F., Sarthou, G., Bucciarelli, E., Blain, S., and Bowie, A. R.: An iron budget during the natural iron fertilisation experiment KEOPS (Kerguelen Islands, Southern Ocean), Biogeosciences, 7, 455–468, doi:10.5194/bg-7-455-2010, 2010.

Closset, I., Lasbleiz, M., Leblanc, K., Quéguiner, B., Cavagna, A.-J., Elskens, M., Navez, J., and Cardinal, D.: Seasonal evolution of net and regenerated silica production around a natural Fe-fertilized area in the Southern Ocean estimated with Si isotopic approaches, Biogeosciences, 11, 5827–5846, doi:10.5194/bg-11-5827-2014, 2014.

Cutter, G., Andersson, P., Codispoti, L., Croot, P., Francois, R., Lohan, M., Obata, H., and Rutgers van der Loeff, M.: Sampling and Sample-handling Protocols for GEOTRACES Cruises, Cookbook, http://www.geotraces.org/libraries/documents/Intercalibration/Cookbook.pdf (last access: 17 July 2015), 2010.

Cutter, G. A.: Intercalibration in chemical oceanography-Getting the right number, Limnol. Oceanogr.-Meth., 11, 418–424, 2013.

d'Ovidio, F., Della Penna, A., Trull, T. W., Nencioli, F., Pujol, I., Rio, M. H., Park, Y.-H., Cotté, C., Zhou, M., and Blain, S.: The biogeochemical structuring role of horizontal stirring: Lagrangian perspectives on iron delivery downstream of the Kerguelen plateau, Biogeosciences Discuss., 12, 779–814, doi:10.5194/bgd-12-779-2015, 2015.

Doucet, S., Scoates, J. S., Weis, D., and Giret, A.: Constraining the components of the Kerguelen mantle plume: A Hf-Pb-Sr-Nd isotopic study of picrites and high-MgO basalts from the Kerguelen Archipelago, Geochem. Geophy. Geosy., 6, Q04007, doi:10.1029/2004GC000806, 2005.

Dulaiova, H., Ardelan, M. V., Henderson, P. B., and Charette, M. A.: Shelf-derived iron inputs drive biological productivity in the southern Drake Passage, Global Biogeochem. Cy., 23, GB4014, doi:10.1029/2008GB003406, 2009.

Elrod, V. A., Berelson, W. M., Coale, K. H., and Johnson, K. S.: The flux of iron from continental shelf sediments: A missing source for global budgets, Geophys. Res. Lett., 31, L12307, doi:10.1029/2004GL020216, 2004.

Frenot, Y., Van Vliet-Lanoë, B., and Gloaguen, J.-C.: Particle translocation and initial soil development n a Glacier Foreland, Kerguelen Islands, Subantarctic., Arctic Alpine Res., 27, 107–115, 1995.

Gautier, I., Weis, D., Mennessier, J.-P., Vidal, P., Giret, A., and Loubet, M.: Petrology and geochemistry of the Kerguelen Archipelago basalts (South Indian Ocean) evolution of the man-

tle sources from ridge to intraplate position, Earth Planet. Sc. Lett., 100, 59–76, 1990.

Hatta, M., Measures, C. I., Selph, K. E., Zhou, M., and Hiscock, W. T.: Iron fluxes from the shelf regions near the South Shetland Islands in the Drake Passage during the austral-winter 2006, Deep-Sea Res. Pt. II, 90, 89–101, 2013.

Hatta, M., Measures, C. I., Wu, J., Roshan, S., Fitzsimmons, J. N., Sedwick, P., and Morton, P.: An overview of dissolved Fe and Mn Distributions during the 2010–2011 U.S. GEOTRACES north Atlantic Cruises: GEOTRACES GA03, Deep-Sea Res. Pt. II, 116, 117–129, doi:10.1016/j.dsr2.2014.07.005, 2015.

Heimburger, A., Losno, R., Triquet, S., and Nguyen, E. B.: Atmospheric deposition fluxes of 26 elements over the Southern Indian Ocean: time series on Kerguelen and Crozet Islands, Global Biogeochem. Cy., 27, 440–449, doi:10.1002/gbc.20043, 2013.

Homoky, W. B., John, S. G., Conway, T. M., and Mills, R. A.: Distinct iron isotopic signatures and supply from marine sediment dissolution, Nature Communications, 4, 2143, doi:10.1038/ncomms3143, 2013.

Ibisanmi, E., Sander, S. G., Boyd, P. W., Bowie, A. R., and Hunter, K. A.: Vertical distributions of iron-(III) complexing ligands in the Southern Ocean, Deep-Sea Res. Pt. II, 58, 2113–2125, 2011.

Jickells, T. D., An, Z. S., Andersen, K. K., Baker, A. R., Bergametti, G., Brooks, N., Cao, J. J., Boyd, P. W., Duce, R. A., Hunter, K. A., Kawahata, H., Kubilay, N., La Roche, J., Liss, P. S., Mahowald, N., Prospero, J. M., Ridgwell, A. J., Tegen, I., and Torres, R.: Global Iron Connections Between Desert Dust, Ocean Biogeochemistry, and Climate, Science, 308, 67–71, 2005.

Johnson, K. S., Chavez, F. P., and Friederich, G. E.: Continental shelf sediments as a primary source of iron to coastal phytoplankton, Nature, 398, 697–700, 1999.

Johnson, K. S., Boyle, E., Bruland, K., Coale, K., Measures, C., Moffett, J., Aguilar-Islas, A., Barbeau, K., Bergquist, B., Bowie, A., Buck, K., Cai, Y., Chase, Z., Cullen, J., Doi, T., Elrod, V., Fitzwater, S., Gordon, M., King, A., Laan, P., Laglera-Baquer, L., Landing, W., Lohan, M., Mendez, J., Milne, A., Obata, H., Ossiander, L., Plant, J., Sarthou, G., Sedwick, P., Smith, G., Sohst, B., Tanner, S., Van den Berg, C. M. G., and Wu, J.: Developping standards for dissolved iron in seawater, EOS Transactions, American Geophysical Union, 88, 131–132, 2007.

Klunder, M. B., Laan, P., De Baar, H. J. W., Middag, R., Neven, I., and Van Ooijen, J.: Dissolved Fe across the Weddell Sea and Drake Passage: impact of DFe on nutrient uptake, Biogeosciences, 11, 651–669, doi:10.5194/bg-11-651-2014, 2014.

Lam, P. J., Bishop, J. K. B., Henning, C. C., Marcus, M. A., Waychunas, G. A., and Fung, I. Y.: Wintertime phytoplankton bloom in the subarctic Pacific supported by continental margin iron, Global Biogeochem. Cy., 20, GB1006, doi:10.1029/2005GB002557, 2006.

Lam, P. J. and Bishop, J. K. B.: The continental margin is a key source of iron to the HNLC North Pacific Ocean, Geophys. Res. Lett., 35, L07608, doi:10.1029/2008GL033294, 2008.

Lasbleiz, M., Leblanc, K., Blain, S., Ras, J., Cornet-Barthaux, V., Hélias Nunige, S., and Quéguiner, B.: Pigments, elemental composition (C, N, P, and Si), and stoichiometry of particulate matter in the naturally iron fertilized region of Kerguelen in the Southern Ocean, Biogeosciences, 11, 5931–5955, doi:10.5194/bg-11-5931-2014, 2014.

Marsay, C. M., Sedwick, P. N., Dinninman, M. S., Barrett, P. M., Mack, S. L., and McGillicuddy Jr., D. J.: Estimating the benthic efflux of dissolved iron on the Ross Sea continental shelf, Geophys. Res. Lett., 41, 7576–7583, doi:10.1002/2014GL061684, 2014.

Martin, J. H., Knauer, G. A., Karl, D. M., and Broenkow, W. W.: VERTEX: carbon cycling in the northeast Pacific, Deep-Sea Res. Pt. I, 34, 267–285, 1987.

Measures, C. I., Brown, M. T., Selph, K. E., Apprill, A., Zhou, M., Hatta, M., and Hiscock, W. T.: The influence of shelf processes in delivering dissolved iron to the HNLC waters of the Drake Passage, Antarctica, Deep-Sea Res. Pt. II, 90, 77–88, 2013.

Moore, J. K., Doney, S. C., Glover, D. M., and Fung, I. Y.: Iron cycling and nutrient limitation patterns in surface waters of the World Ocean, Deep-Sea Res. Pt. II, 49, 463–507, 2001.

Morris, P. J. and Charette, M. A.: A synthesis of upper ocean carbon and dissolved iron budgets for Southern Ocean natural iron fertilisation studies, Deep-Sea Res. Pt. II, 90, 147–157, 2013.

Nielsdóttir, M. C., Bibby, T. S., Moore, C. M., Hinz, D. J., Sanders, R., Whitehouse, M., Korb, R., and Achterberg, E. P.: Seasonal and spatial dynamics of iron availability in the Scotia Sea, Mar. Chem., 130–131, 62–72, 2012.

Obata, H., Karatani, H., and Nakayama, E.: Automated determination of iron in seawater by chelating resin concentration and chemiluminescence, Anal. Chem., 65, 1524–1528, 1993.

Park, Y.-H., Durand, I., Kestenare, E., Rougier, G., Zhou, M., d'Ovidio, F., Cotté, C., and Lee, J.-H.: Polar Front around the Kerguelen Islands: An up-to-date determination and associated circulation of surface/subsurface waters, J. Geophys. Res.-Oceans, 119, 6575–6592, doi:10.1002/2014JC010061, 2014.

Planquette, H., Sanders, R. R., Statham, P. J., Morris, P. J., and Fones, G. R.: Fluxes of particulate iron from the upper ocean around the Crozet Islands: A naturally iron-fertilized environment in the Southern Ocean, Global Biogeochem. Cy., 25, GB2011, doi:10.1029/2010GB003789, 2011.

Planquette, H. F., Statham, P. J., Fones, G. R., Charette, M. A., Moore, C. M., Salter, I., Nédélec, F. H., Taylor, S. L., French, M., Baker, A. R., Mahowald, N., and Jickells, T. D.: Dissolved iron in the vicinity of the Crozet Islands, Southern Ocean, Deep-Sea Res. Pt. II, 54, 1999–2019, doi:10.1016/j.dsr2.2007.07.019, 2007.

Pollard, R. T., Salter, I., Sanders, R. J., Lucas, M. I., Moore, C. M., Mills, R. A., Statham, P. J., Allen, J. T., Baker, A. R., Bakker, D. C. E., Charette, M. A., Fielding, S., Fones, G. R., French, M., Hickman, A. E., Holland, R. J., Hughes, J. A., Jickells, T. D., Lampitt, R. S., Morris, P. J., Nédélec, F. H., Nielsdottir, M., Planquette, H., Popova, E. E., Poulton, A. J., Read, J. F., Seeyave, S., Smith, T., Stinchcombe, M., Taylor, S., Thomalla, S., Venables, H. J., Williamson, R., and Zubkov, M. V.: Southern Ocean deep-water carbon export enhanced by natural iron fertilization, Nature, 457, 577–580, doi:10.1038/nature07716, 2009.

Raiswell, R., Vu, H. P., Brinza, L., and Benning, L. G.: The determination of labile Fe in ferrihydrite by ascorbic acid extraction: methodology, dissolution kinetics and loss of solubility with age and de-watering, Chem. Geol., 278, 70–79, 2010.

Raiswell, R.: Iceberg-hosted nanoparticulate Fe in the Southern Ocean: Mineralogy, origin, dissolution kinetics and source of bioavailable Fe, Deep-Sea Res. Pt. II, 58, 1364–1375, doi:10.1016/j.dsr2.2010.11.011, 2011.

Sanial, V., van Beek, P., Lansard, B., Souhaut, M., Kestenare, E., d'Ovidio, F., Zhou, M., and Blain, S.: Use of Ra isotopes to deduce rapid transfer of sediment-derived inputs off Kerguelen, Biogeosciences, 12, 1415–1430, doi:10.5194/bg-12-1415-2015, 2015.

Sarthou, G., Baker, A. R., Blain, S., Achterberg, E. P., Boye, M., Bowie, A. R., Croot, P. L., Laan, P., de Baar, H. J. W., Jickells, T. D., and Worsfold, P. J.: Atmospheric iron deposition and sea-surface dissolved iron concentrations in the eastern Atlantic Ocean, Deep-Sea Res. Pt. I, 50, 1339–1352, 2003.

Sarthou, G., Timmermans, K. R., Blain, S., and Tréguer, P.: Growth physiology and fate of diatoms in the ocean: a review, J. Sea Res., 53, 25–42, 2005.

Savoye, N., Trull, T. W., Jacquet, S. H. M., Navez, J., and Dehairs, F.: ^{234}Th-based export fluxes during a natural iron fertilization experiment in the Southern Ocean (KEOPS), Deep-Sea Res. Pt. II, 55, 841–855, 2008.

Smith Jr., W. O., Sedwick, P. N., Arrigo, K. R., Ainley, D. G., and Orsi, A. H.: The Ross Sea in a sea of change, Oceanography, 25, 44–57, 2012.

Sunda, W. G. and Huntsman, S. A.: Iron uptake and growth limitation in oceanic and coastal phytoplankton, Mar. Chem., 50, 189–206, 1995.

Sunda, W. G.: Control of dissolved iron concentrations in the world ocean: A comment, Mar. Chem., 57, 169–172, 1997.

Tagliabue, A., Bowie, A., Chever, F., Baptiste, P.-J., Dutay, J.-C., Bucciarelli, E., Lannuzel, D., Remenyi, T., Sarthou, G., Aumont, O., Gehlen, M., and Bopp, L.: On the importance of hydrothermalism to the oceanic dissolved iron inventory, Nat. Geosci., 3, 252–256, doi:10.1038/NGEO818, 2010.

Tagliabue, A., Mtshali, T., Aumont, O., Bowie, A. R., Klunder, M. B., Roychoudhury, A. N., and Swart, S.: A global compilation of dissolved iron measurements: focus on distributions and processes in the Southern Ocean, Biogeosciences, 9, 2333–2349, doi:10.5194/bg-9-2333-2012, 2012.

Thuróczy, C.-E., Gerringa, L. J. A., Klunder, M. B., Laan, P., and de Baar, H. J. W.: Observation of consistent trends in the organic complexation of dissolved iron in the Atlantic Sector of the Southern Ocean, Deep-Sea Res. Pt. II, 58, 2695–2706, 2011.

Twining, B. S., Baines, S. B., and Fisher, N. S.: Element stoichiometries of individual plankton cells collected during the Southern Ocean Iron Experiment (SOFeX), Limnol. Oceanogr., 49, 2115–2128, 2004.

van der Merwe, P., Bowie, A. R., Quéroué, F., Armand, L., Blain, S., Chever, F., Davies, D., Dehairs, F., Planchon, F., Sarthou, G., Townsend, A. T., and Trull, T. W.: Sourcing the iron in the naturally fertilised bloom around the Kerguelen Plateau: particulate trace metal dynamics, Biogeosciences, 12, 739–755, doi:10.5194/bg-12-739-2015, 2015.

Wagener, T., Guieu, C., Losno, R., Bonnet, S., and Mahowald, N.: Revisiting atmospheric dust export to the Southern Hemisphere ocean: Biogeochemical implications, Global Biogeochem. Cy., 22, GB2006, doi:10.1029/2007GB002984, 2008.

Walsh, I., Fischer, K., Murray, D., and Dymond, J.: Evidence for resuspension of rebound particles from near-bottom sediment traps, Deep-Sea Res. Pt. I, 35, 59–70, 1988.

Chapter V

Distribution of dissolved trace metals (Mn, Co, Ni, Cu, Cd, Pb) in the Kerguelen Plateau region*

F. Quéroué[1,2,3,4], P. van der Merwe[2], A. Townsend[5], D. Lannuzel[1,2], E. Bucciarelli[4], H. Planquette[4], S. Blain[6,7], G. Sarthou[4], and A. Bowie[1,2]

[1] Institute for Marine and Antarctic Studies, University of Tasmania, Hobart, Tas 7001, Australia

[2] Antarctic Climate & Ecosystems Cooperative Research Centre, University of Tasmania, Hobart, Tas 7001, Australia

[3] Université de Bretagne Occidentale, Brest, 29200, France

[4] LEMAR-UMR 6539, CNRS-UBO-IRD-IFREMER, Place Nicolas Copernic, 29280 Plouzané, France

[5] Central Science Laboratory, University of Tasmania, Hobart, Tas 7001, Australia

[6] Sorbonne Universités, UPMC Univ Paris 06, UMR7621, Laboratoire d'Océanographie Microbienne, Observatoire Océanologique, 66650 Banyuls/mer, France

[7] CNRS, UMR7621, Laboratoire d'Océanographie Microbienne, Observatoire Océanologique, 66650 Banyuls/mer, France

Correspondence to: F. Quéroué (fabien.queroue@univ-brest.fr)

* Manuscript to be submitted to special issue of *Biogeosciences* on the KEOPS2 project

1 Introduction

The Southern Ocean is the largest high nutrient low chlorophyll (HNLC) area, where iron (Fe) has been shown to limit primary productivity and may therefore be linked to the regulation of the Earth's climate over geological timescales through the control of the biological pump of carbon (Martin, 1990). Adding Fe in this region enhances primary production, whether artificially during mesoscale Fe fertilisation experiments (de Baar et al., 2005; Boyd et al., 2007) or naturally via Fe inputs to the photic zone (Hopkinson et al., 2007; Pollard et al., 2007b; Blain et al., 2008a). Other trace metals such as manganese (Mn), cobalt (Co), nickel (Ni), copper (Cu) and cadmium (Cd) are also involved in phytoplankton

metabolic processes and can (co)-limit oceanic primary productivity (Price and Morel, 1991; Morel and Price, 2003; Peers and Price, 2004; Peers et al., 2005; Ho, 2013; Twining and Baines, 2013). Lead (Pb) is a toxic element, which is the primary metal used to trace anthropogenic sources of trace metals to the ocean (Boyle, 2001; Bruland and Lohan, 2003; Boyle et al., 2014). The first Fe and Mn study in a naturally Fe-fertilized area in the Southern Ocean showed the importance of riverine discharges, soil leaching by rain water, aeolian deposition and sediment resuspension inputs over the North-East Kerguelen Plateau (Bucciarelli et al., 2001). Cobalt was later studied in the South East Kerguelen Plateau by Bown et al. (2012), showing the importance of basaltic sedimentary source from Heard Island and Kerguelen Plateau in supplying iron to fuel phytoplankton blooms. Castrillejo et al. (2013) analyzed Ni, zinc (Zn), Co, Cd, Pb, aluminium (Al) and Mn around the naturally Fe-fertilized Crozet Islands during the CROZEX experiment. This study suggested a significant biological removal of Ni and Cd and low atmospheric inputs of Pb and Mn in surface waters. Dissolved Co distributions were controlled by biological uptake and scavenging.

Prompted by the international program GEOTRACES which aims to develop and refine analytical methods for, as well as to characterise the biogeochemical cycle of trace metals in the ocean (Anderson et al., 2007; Henderson et al., 2007; Measures et al., 2008), new approaches have recently been developed allowing the analysis of multiple elements simultaneously using a single instrument (Milne et al., 2010; Biller and Bruland, 2012; Lagerstrom et al., 2013; O'Sullivan et al., 2013; Quéroué et al., 2014; Minami et al., 2015) leading to unprecedented high spatial resolution and elemental profiling of sections in the major ocean basins (Ellwood, 2008; Boyé et al., 2012; Biller and Bruland, 2013; Butler et al., 2013). While dissolved Fe (dFe) distributions have been discussed in a companion paper which focuses on Fe sources around Kerguelen Island during the KEOPS2 project (Quéroué et al., 2015), this study is the first to report the analysis of a suite of trace metals in this area. The potential origin of these trace metals, namely atmospheric inputs, freshwater inputs, sediment resuspension and anthropogenic sources, are considered. The impact of biological uptake and remineralization on the vertical distribution of dissolved Mn (dMn), Co (dCo), Ni (dNi), Cu (dCu), Cd (dCd) and Pb (dPb) is also discussed.

2 Materials and Methods

2.1 Study area and hydrography

The KEOPS2 (Kerguelen Ocean Plateau compared Study 2) oceanographic research cruise took place in the vicinity of Kerguelen Island in the Southern Ocean (48°20'S - 50°40'S and 66°40'E-74°50'E) during the austral spring (7/10/2011 - 30/11/2011). Seawater samples were collected from 17 stations over 5 oceanographically distinct areas, totalling 185 individual samples (Fig. V.1). The presentation and discussion of results are organised by clusters, which were defined considering the hydrography and the complex regional circulation. Waters masses were identified using Θ-S diagrams (Fig. V.1). Definition of clusters has been detailed in Quéroué et al. (2015).

Firstly, in cluster 1 (near-coastal area), TEW-1 and TEW-2 were characterised by shallow bathymetry (< 65 m) and low salinities (33.62 < S < 33.77). At these stations, below the surface mixed layer (SML), subsurface (shelf) waters were sampled

Secondly, in cluster 2 (Kerguelen Plateau area), three stations (A3, TEW-3 and G-1) were studied, characterised by shallow bathymetry (~500 m). Station A3 was visited twice, 28 days apart, the first visit (A3-1, 20 October) being characteristic of early bloom conditions, while during the second visit (A3-2, 17 November), chlorophyll-a concentrations at the sea-surface increased by about three-fold as a consequence of a large diatom bloom (Lasbleiz et al., 2014). Accordingly, a time-series study can thus be considered. At these stations, below the SML, Winter Water (WW) was encountered followed by Upper Circumpolar Deep Water (UCDW).

Thirdly, the cluster 3 (recirculation area), was within a stationary meander of the PF and was sampled 8 times (E-1, E-2, E-3, E-4E, E-4W-2, E-5, TEW-4 and TEW-5). In this area, 3 stations (E-1, E-3, E-5) were considered as pseudo-lagrangian stations allowing a time-series study to be carried out (d'Ovidio et al., 2015). In this area, below the SML, WW and UCDW were sampled. Below this, Lower Circumpolar Deep Water (LCDW) was encountered.

Fourthly, in cluster 4 (North Polar Front area), two stations were sampled (TEW-7 and F-L), characterised by warmer Sub-Antarctic Surface Water (SASW). Below the SASW, Antarctic Intermediate Water (AAIW) was encountered followed by UCDW and LCDW.

Finally, station R-2 was sampled south-west of the Island and south of the Polar Front (PF) in the high nutrient low chlorophyll (HNLC) area (cluster 5). At this station, below the SML, WW, UCDW and LCDW were sampled.

Comprehensive descriptions of the physical, biological and biogeochemical features of the studied area are described in Park et al. (2014), Sackett et al. (2014) and Lasbleiz et al. (2014), respectively.

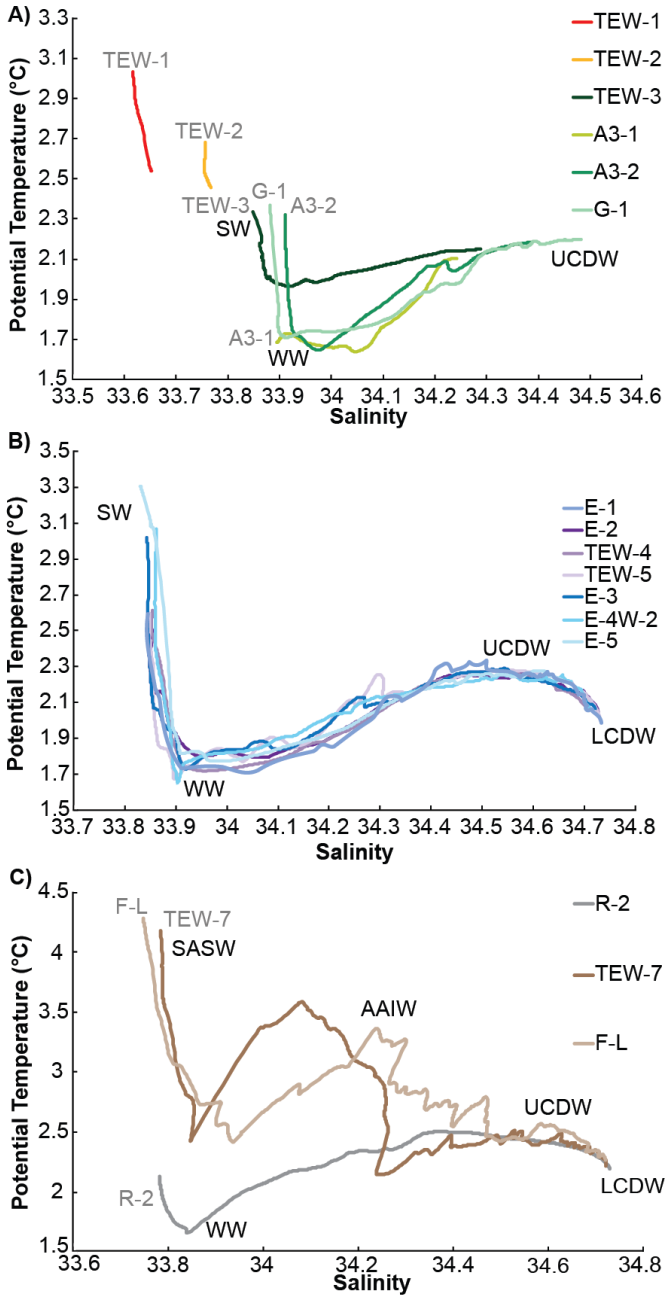

Figure V.1 Temperature–Salinity diagram for stations sampled during KEOPS2 for dissolved trace metals. Water masses are indicated in black, and station names in grey. (a) Clusters 1 and 2: near-coastal (TEW-1, TEW-2) and Kerguelen Plateau (A3-1, A3-2, G-1, TEW-3) stations. Three water masses are displayed: surface water (SW), winter water (WW) and upper circumpolar deep water (UCDW). (b) Cluster 3: the recirculation area (E-1, E-2, TEW-4, TEW-5, E-3, E-4W-2, E-2, E-5). Four water masses are displayed: SW, WW, UCDW,

lower circumpolar deep water (LCDW). (c) Clusters 4 and 5: north of the polar front (F-L, TEW-7) and the HNLC area (R2). Five water masses are displayed: subantarctic surface water (SASW), antarctic intermediate water (AAIW), WW, UCDW, LCDW.

2.2 Sampling and analytical methods

The sampling and analytical methods used in this paper are described in Quéroué et al. (2014); Quéroué et al. (2015). Briefly, cleaning, sampling, handling and processing of the samples was conducted using stringent trace metal clean protocols as recommended by the GEOTRACES program (Cutter et al., 2010; Cutter, 2013). Samples were collected using a trace metal clean rosette (TMR, model 1018, General Oceanics) equipped with specially modified externally-closing Niskin-X bottles (Queroue et al., 2015), before sub-sampling for dissolved trace metals via a Teflon tap connected to acid cleaned 0.2 µm filter cartridges (Pall Acropak and Sartorius SARTOBRAN 300). Samples were acidified to a pH of 1.8 using concentrated ultrapure hydrochloric acid (0.2 %, Seastar Baseline, HCl), and the bottles were double bagged and stored at ambient temperature in the dark until analysis at the home laboratory. The shallowest sample was collected at 15 m depth to avoid contamination from the research vessel. Samples collected off plateau were collected to a maximum depth of 1300 m, which was limited by the length of the clean Kevlar wire.

Dissolved trace metals were analysed one year after sample collection by solid phase trace metal extraction onto Nobias-Chelate PA1 resin (Hitachi High-Technologies) followed by Sector Field Inductively Coupled Plasma Mass Spectrometry (ICP-MS) analysis (Quéroué et al., 2014). Before extraction, samples were UV-irradiated for one hour to break down organic ligand complexes which has been shown to be particularly important when measuring Co and Cu (Vega and van den Berg, 1997; Achterberg et al., 2001). For all metals, blanks were low in comparison to the measured concentrations (Table V.1) and were therefore deemed suitable for open ocean seawater analysis. The North Pacific SAFe Surface (SAFe S) and GEOTRACES Deep (D2) measured values were in excellent agreement with the consensus values except for the dCu SAFe S, which was lower than the consensus value possibly due to reformation of Cu complexes competing with the extraction resin after UV-irradiation (Table V.1; Johnson et al., 2007).

Samples for particulate organic phosphorus (POP) were analysed on a 3-SEAL autoanalyser after filtration of 0.5 L of seawater sample on precombusted Whatman GF/F filters. Methods and results are presented by (Lasbleiz et al., 2014). Nitrate, phophate and

silicate concentrations were measured on an autoanalyser following Aminot and Kérouel (2007) at the Microbial Oceanography Laboratory (LOMIC).

Table V.1 Blanks, detection limits (3 times the blanks standard deviation), SAFe and GEOTRACES reference seawater measured and consensus values (n=8)

	Blanks (n=40)	Detection limit (n=8)	SAFe S (n=8)		GEOTRACES D (n=8)	
			Measured	Consensus	Measured	Consensus
dMn [nmol L^{-1}]	0.008	0.003	0.89±0.06	0.81±0.06	0.25±0.01	0.22±0.03
dCo [pmol L^{-1}]	5	1	4±1	2.8±0.7	67±5	67±1
dNi [nmol L^{-1}]	0.02	0.01	2.32±0.10	2.33±0.09	3.98±0.14	4.10±0.10
dCu [nmol L^{-1}]	0.06	0.03	0.36±0.02	0.50±0.04	1.55±0.08	1.66±0.07
dCd [pmol L^{-1}]	1	2	1±1	1.1±0.3	266±13	277±6
dPb [pmol L^{-1}]	0.7	0.7	49±2	49±2	43±2	44±2

3 Results and discussions

Sampling locations are detailed in Fig. V.2 and Table V.2 while the measured dMn, dCo, dNi, dCu, dCd and dPb concentrations range during the KEOPS2 cruise are presented in Table V.3.

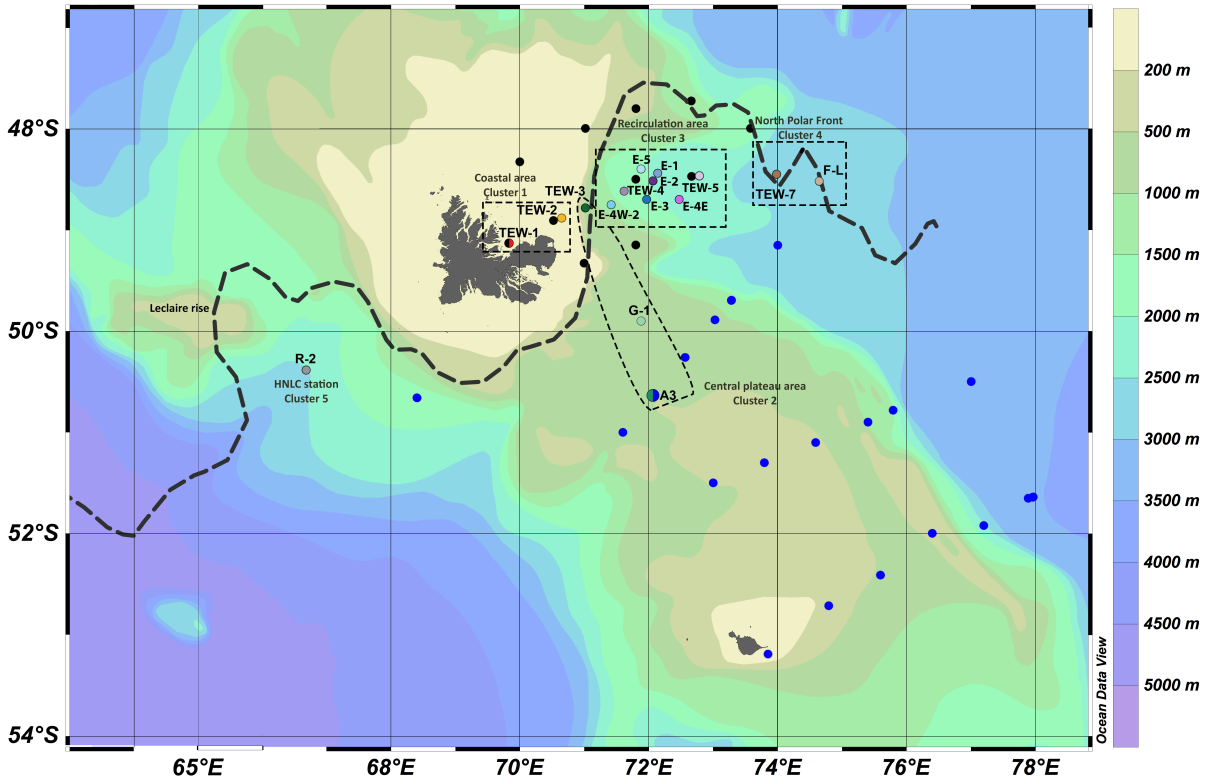

Figure V.2 Map showing the bathymetry of the area and the stations visited during ANTARES 3 (black dots), KEOPS1 (Blue dots) and KEOPS2 (coloured circled dots). The dashed line represented the approximate location of the Polar Front (200 m) (Park et al., 2014).

Table V.2 Cluster, station name, longitude, latitude, sampling date, mixed layer depth (MLD), station bottom depth, during KEOPS2. Cluster 3 is splitted in two groups to dissociate the stations included in pseudo lagrangian study from the other stations within the recirculation area.

Cluster	Station	Long [degree -east]	Lat [degree -south]	Date	MLD [m]	Bot depth [m]
Cluster 1: coastal area (close to Kerguelen island and bottom depth < 65 m)	TEW-1	69.83	49.13	31/10/11	32-42	86
	TEW-2	70.65	48.88	31/10/11	40-70	85
Cluster 2: Kerguelen Plateau area (over the Kerguelen shelf)	A3-1	72.06	50.62	20/10/11	165	530
	TEW-3	71.02	48.78	31/10/11	16-94	560
	G-1	71.88	49.90	9/11/11	60-68	560
	A3-2	72.05	50.62	16/11/11	123	525
Cluster 3: recirculation area pseudo-lagrangian study (within a stationary meander of the polar front)	E-1	72.18	48.45	30/10/11	64	2000
	E-3	71.97	48.70	3/11/11	32	1900
	E-5	71.88	48.40	19/11/11	36-41	1920
Cluster 3: recirculation area (within a stationary meander of the Polar Front)	TEW-4	71.62	48.62	1/11/11	20-33	1600
	E-2	72.07	48.52	1/11/11	42	2000
	TEW-5	72.78	48.47	1/11/11	22-56	2250
	E-4E	72.55	48.70	13/11/11	80	2200
	E-4W-2	71.42	48.75	18/11/11	26-35	1390
Cluster 4: North polar front area	TEW-7	73.98	48.45	2/11/11	22	2500
	F-L	74.65	48.52	7/11/11	47	2700
Cluster 5: HNLC area west of the Kerguelen Plateau	R-2	66.68	50.38	26/10/11	76	2500

Table V.3 Trace metal concentration ranges found in selected Southern Ocean regions (adapted from Castrillejo et al., 2013).

Location	Study	dMn [nmol L^{-1}]	dCo [nmol L^{-1}]	dNi [nmol L^{-1}]	dCu [nmol L^{-1}]	dCd [nmol L^{-1}]	dPb [nmol L^{-1}]
Vicinity of Kerguelen Islands	This study (n = 177)	0.06-5.46	0.028-0.284	5.36-7.52	1.07-2.59	0.23-0.96	0.003-0.018
	Bown et al. (2012)		0.019-0.375				
	Bucciarelli et al. (2001)	0.68-8.54					
Crozet Island	Castrillejo et al. (2013)	0.07-0.64	0.024-0.049	4.64-6.31		0.135-0.673	0.006-0.022
Zero meridian transect from South Africa to Antarctica	Baars et al. (2014)					0.004-0.865	
	Boyé et al. (2012)	0.2-1.3			0.58-2.33	0.004-0.895	0.007-0.055
	Bown et al. (2011)		0.005-0.074				
	Middag et al. (2011a)	0.05-3.20					
	Abouchami et al. (2011)					0.036-0.620	
	Ellwood et al. (2005)		0.015-0.045				
Drake passage	Middag et al. (2012)	0.08-2.64					
	Measures et al. (2013)	0.04-6.13					
	Hatta et al. (2013)	0.06-4.68					
Australian sector of the Southern Ocean	Butler et al. (2013)		0.005-0.043	2.51-7.31	0.22-1.79	0.004-0.900	
	Ellwood (2008)		0.010-0.050	3.00-7.00	0.40-1.50	0.020-0.650	0.012-0.033
	Lai et al. (2008)			2.15-7.91	0.50-3.40		0.006-0.170

3.1 Dissolved Manganese

Dissolved Mn (dMn) concentrations ranged from 0.06 nmol L^{-1} at 25 m at G-1 (cluster 2) to 5.40 nmol L^{-1} at 10 m at TEW-1 (cluster 1) (Fig. V.3a). A higher concentration range was observed by Bucciarelli et al. (2001) and Measures et al. (2013) during the ANTARES3 study around Kerguelen Island and in the Drake Passage, respectively (Table V.3). Results here exhibit a wider range than observed by Middag et al. (2011a), Middag et al. (2012), Hatta et al. (2013), Boyé et al. (2012) and Castrillejo et al. (2013) in the Atlantic sector of the Southern Ocean, in the Drake Passage, across the Southern Ocean along the zero meridian, and around the Crozet Islands, respectively (Table V.3). The lowest KEOPS2 concentrations are consistent with the lowest observations in the Southern Ocean during previous studies (Middag et al., 2011a; Middag et al., 2012; Castrillejo et al., 2013; Hatta et al., 2013; Measures et al., 2013).

Atmospheric dust deposition is known to be a source of Mn to the ocean in addition to aluminium (Al) and Fe (Statham et al., 1998; Middag et al., 2011a; Wuttig et al., 2013). Previous studies considering Kerguelen Islands estimated Mn daily deposition fluxes at least 1 order of magnitude higher than the other trace metals of our study (Heimburger et al., 2013). Despite the vicinity of the Kerguelen Islands and the downwind location of our stations, no important dMn surface maximum was observed during this study, indicating that atmospheric inputs are not a major source of dMn in the study area or that photo reduction after atmospheric deposition is not sufficient to increase the local dMn concentrations in the deep water column (Hatta et al., 2014).

The highest dMn concentrations were observed at the coastal stations. TEW-1 and TEW-2 showed enhanced dMn concentrations over the whole water column with concentrations up to 5.40 nmol L^{-1} at TEW-1 surface waters, decreasing rapidly at TEW-2 (1.92 nmol L^{-1}) (Fig. V.3a). Manganese is the only metal along with Fe showing enhanced dissolved concentrations at TEW-1 compared to TEW-2. The relatively high dMn concentrations (up to 5.40 nmol L^{-1}) and low salinity (33.62) at station TEW-1 could be indicative of Mn-rich freshwater inputs from Kerguelen Island into Hillsborough Bay as also suggested for dFe (Quéroué et al., 2015). Higher LSi concentrations were observed at TEW-1 compared to TEW-2, which could again be due to fluvial inputs (Lasbleiz et al., 2014). Freshwater inputs containing dMn were previously observed in the Arctic Ocean by Middag et al. (2011b) revealing dMn seawater

concentrations up to 6 nmol L^{-1}, attributed to fluvial runoff and melting sea-ice. At TEW-1, the highest LSi was observed in surface waters coincident with the lowest salinity indicating supply of LSi by fluvial melt water while at TEW-2; the highest LSi was observed at depth, likely due to sediment resuspension. It has been shown that elevated surface concentrations of dMn may be the result of photo reduction that reduces insoluble Mn oxides back to soluble phase (Sunda et al., 1983; Sunda and Huntsman, 1988; Sunda and Huntsman, 1994). Furthermore this process is favoured by light exposure, so in shallow water column, even if Mn is sourced from the seafloor, the dMn maximum may be observed in surface water, coincident with the maximum the solar radiation such as at station TEW-1. In cluster 1, the combination of sediment resuspension and fluvial input may be responsible for the elevated dMn concentrations.

The lowest dMn concentration was observed over the Kerguelen Plateau (cluster 2) in surface waters due to biological uptake (lower than 0.10 nmol L^{-1} within the first 40 m at G-1) (Fig. V.3b) (discussed in section V.3.7). Relatively homogeneous concentrations over the water column were measured at the first visit to A3 (A3-1, 0.50 nmol L^{-1}), while depleted surface concentrations were observed (0.31 nmol L^{-1}) at the second visit to A3 (A3-2). Station A3-2 presented the highest dMn concentrations at sites sampled over the plateau close to the bottom (1.12 nmol L^{-1} at 480 m) (Fig. V.3b) and therefore showed a nutrient like profile strongly influenced by deep water inputs. At this station, the highest dFe concentration was observed and attributed to sediment resuspension and associated pore water release (Quéroué et al., 2015). At stations G-1, from 250 m to 500m, and at the deepest sampled location at TEW-3, 480 m, despite higher dMn concentrations compared to other cluster at the same depth, the dMn enhancement was not of the same scale than at A3-2 despite comparable bottom depth. This may be attributed to the more intense sediment resuspension observed at A3 or to different pore water concentration compared to the other stations (Quéroué et al., 2015). In addition, different sediment compositions could also explain this discrepancy but unfortunately sedimentary composition was studied only at site A3 in this cluster. Very similar trends were observed for dMn and dFe close to the bottom and furthermore dMn and dFe showed a significant relationship using samples with higher dMn concentration at cluster 2 only compared to cluster 3, 4 and 5 ($dMn = 0.83\ dFe + 0.03$, $R^2 = 0.93$, $P < 0.01$). This indicates a potential common source for dMn and dFe at depth which may be sediment resuspension and / or pore water diffusion (Quéroué et al., 2015).

In the recirculation area (cluster 3) dMn profiles showed at the most productive stations i.e. TEW-4 (Integrated Chla over 200 m (intChla) = 187 µg m^{-3}), E-5 (intChla = 126 µg m^{-3}) and E-4W-2 (intChla = 249 µg m^{-3}), a (sub)surface minimum followed by a maximum between 150 and 200 m depth, likely due to biological uptake (section V.3.7). The other cluster's stations showed relatively homogenous concentrations in the first 200 m. Below 200 m, a slow decrease was observed likely due to scavenging (Fig. V.3c and Fig. V.3d). A profile combining nutrient like vertical distribution in surface water (as examplified at the most productive stations), followed by scavenged-like vertical distribution at depth is also called a hybrid profile. Although dissolved Mn had the highest concentrations in cluster 1, no significant surface water enhancement was observed in cluster 3 even if it has been observed for dFe (Quéroué et al., 2015). Lateral advection of seawater brought by the PF via cluster 4 or across the PF might be a mechanism of dMn transport at these stations (Quéroué et al., 2015). Drifter data and radium isotopes studies have shown that water masses from cluster 1 were transported to cluster 3 after crossing the PF or flowing along it, heading north east, and then south east again to join cluster 3 (Sanial et al., 2014). Increases in lithogenic particulate Fe (PFe) and lithogenic Si concentrations at E stations also suggest lateral transport of enriched waters from the plateau (Lasbleiz et al., 2014; van der Merwe et al., 2015). The lack of dMn surface enhancement most likely arises due to scavenging and redox transformations (Landing and Bruland, 1980; Noble et al., 2012), or biological uptake (section V.3.7) during water mass advection.

In the North Polar Front area (cluster 4) surface dMn depletion was observed at both stations (0.23 nmol L^{-1}) followed by a rapid increase to a maximum (0.53 nmol L^{-1}) at 40 m and 100 m at TEW-7 and F-L respectively likely due to biological uptake (Fig. V.3e) (section V.3.7). Below those depths, concentrations rapidly decreased followed by a local maximum around 400 m and 600 m at TEW-7 and F-L respectively. Below, similar to the dMn trend observed at cluster 3 below 200 m, relatively low dMn concentrations were observed (0.25 ± 0.04 nmol L^{-1}) with decreasing concentrations with depth due to scavenging.

At R-2, dMn concentrations were relatively homogeneous in the upper 400 m (0.31 ± 0.04 nmol L^{-1}) and decreased with depth to an average value of 0.23 ± 0.03 nmol L^{-1}, similar to cluster 3 and 4 (Fig. V.3e). A local maximum was observed at intermediate depth similar to dFe (300 m to 400 m for dMn versus 500 m for dFe). Located only 75 km north west from R-2, a submerged volcano, The Leclaire Rise, may be a source of dissolved and particulate material as discussed by Quéroué et al. (2015). Indeed, this small and shallow plateau of

about 6500 km^2 (based on the 500 m isobath), with the shallowest bathymetry of about 100 m is partially located South of the PF allowing water masses to interact with the plateau and its slopes, enhancing the dissolved and particulate phases before to be transported to R-2.

To summarize, this study shows that dMn profiles were impacted both by biological activity (and scavenging) and external sources. In surface water, the most productive stations showed depleted dMn concentrations followed by a maximum at intermediate depth. Cluster 1 was strongly influenced by fluvial and/or sediment resuspension. Cluster 2 and cluster 5 showed maxima due to sediment resuspension and/or associated pore water release. Below 200 m, when profiles were not influenced by external sources, slightly decreasing dMn concentrations with depth were observed with an average value of 0.26 ± 0.05 nmol L^{-1} (n = 57).

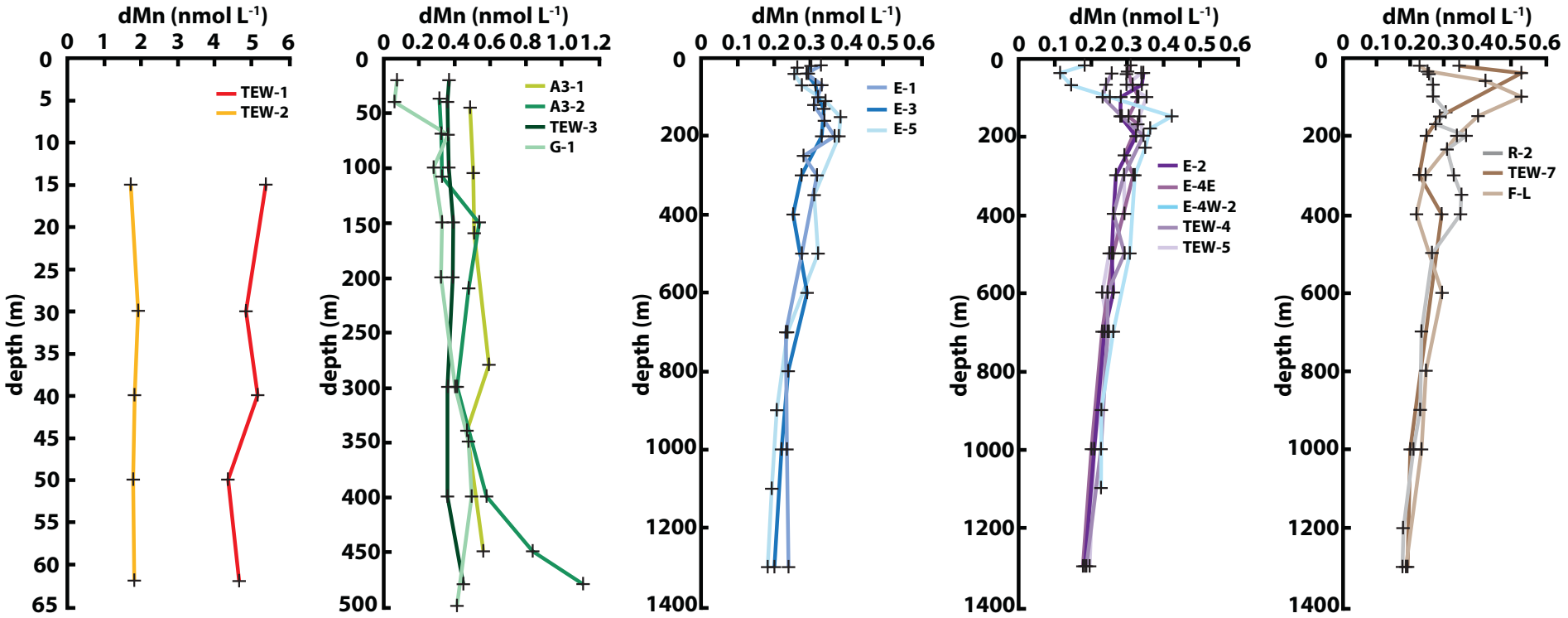

Figure V.3 dMn vertical profiles. Different scales are used due to the wide range of dMn observed in the different clusters.

3.2 Dissolved Cobalt

Dissolved Co (dCo) concentrations (Fig. V.4) ranged from 28 pmol L^{-1} at G-1 (Fig. V.4b) to 284 pmol L^{-1} at TEW-2 (Fig. V.4a). A similar dCo range was observed during KEOPS1 over the southern part of the Kerguelen Plateau (0.019-0.375 nmol L^{-1}, Bown et al., 2012) (Table V.3). The highest values observed in this study are almost 4 times higher than in other studies in the Southern Ocean (Ellwood, 2008; Bown et al., 2011; Castrillejo et al., 2013).

Bown et al. (2012) showed that atmospheric inputs of dCo would increase surface dCo concentrations by 0.03 pmol L^{-1} to 0.06 pmol L^{-1}. This input was found to be negligible during the KEOPS1 study (Bown et al., 2012) due to the observed surface concentration being at least 3 orders of magnitude higher. In the present study, similar surface dCo concentration enhancements to KEOPS1 were observed in the recirculation area at E-3, E-4-E and TEW-4, suggesting that other sources of Co enhance the dCo surface concentrations cluster 3.

In cluster 1, enhanced dCo concentrations were observed at TEW-1 and TEW-2 showing wide range of concentrations from 62 pmol L^{-1} to 284 pmol L^{-1} (Fig. V.4a). Unlike dMn and dFe (Quéroué et al., 2015), no dCo trend was observed between TEW-1 and TEW-2, despite TEW-2 being significantly further away from the coastline of Kerguelen Island. This may be due to the lower impact of the fluvial input on dCo profile in the bay such as observed in the South Atlantic Ocean (Noble et al., 2012). The high dCo concentrations might be due to sedimentary inputs. Indeed, high dCo concentrations were observed during KEOPS1 due to lateral advection of lithogenic material (discussed below).

In cluster 2, dCo concentrations remained below 100 pmol L^{-1} except at 60 m at station A3-1 and 450 m at station A3-2 (109 and 114 pmol L^{-1} respectively, Fig. V.4b). Over the plateau, no significant high dCo deep water concentration were observed, in contrast to dFe (Quéroué et al., 2015) and dMn, indicating that this part of the Kerguelen Plateau is not a major source of dCo for this cluster. By contrast with KEOPS1, no significantly high dCo concentrations were observed in surface waters at A3, which may indicate that the sampled water mass had not mixed with the shallow water column influenced by Heard Island (Bown et al., 2012).

In cluster 3, strong surface Co enrichments were observed at stations E-3 (150-160 pmol L^{-1}, Fig. V.4c), E-4-E (201 pmol L^{-1}, Fig. V.4d) and TEW-4 (210 pmol L^{-1}, Fig. V.4d). Lateral advection of seawater brought by the PF via the North Polar Front area or across the

PF may be a mechanism of dCo transport at these stations (Quéroué et al., 2015). Drifter data and radium isotopes studies have showed that water masses from the coastal area can be transported to the recirculation area after crossing it or flowing with it doing a loop to join the recirculation area (Sanial et al., 2014). Increased lithogenic particulate Fe (PFe) and lithogenic Si concentrations at E stations also suggested lateral transport of enriched waters from the plateau (Lasbleiz et al., 2014; van der Merwe et al., 2015).

In the North Polar Front area, the highest dCo concentration was measured at F-L at 35 m (127 pmol L^{-1}) (Fig. V.4e). At F-L, subsurface minimum was observed at 100 m (37 pmol L^{-1}) and concentrations remained relatively homogeneous between 200 m and 800 m. At deeper depths, higher dCo concentrations were observed possibly due to lateral advection of lithogenic material as dNi concentrations were also enhanced (section V.3.3). TEW-7 concentrations were generally lower than found at F-L, and were relatively homogeneous throughout the water column (range 40 pmol L^{-1} to 56 pmol L^{-1}).

At R-2, in the HNLC cluster, relatively low and homogeneous surface dCo were observed (0.042 ± 0.005 nmol L^{-1} first 200 m). Homogenous dCo concentrations were observed below 500 m (0.052 ± 0.004 nmol L^{-1}) (Fig. V.4e). The measured dCo concentrations in this area are in agreement with concentrations observed in the HNLC waters Atlantic sector of the Southern Ocean by Bown et al. (2011) and also in good agreement with the concentrations observed at the HNLC station A11 during KEOPS1 (Bown et al., 2012).

The results of this study suggest that the dCo vertical profiles seem to be more impacted by external sources, such as lateral advection of seawater which interacted with the North of the Kerguelen plateau, than by uptake and remineralization. By contrast to KEOPS1, the water masses sampled over the plateau did not show high dCo concentration. The sampled water masses cluster 2 may not have interacted with the shallow plateau in the vicinity of Heard Island.

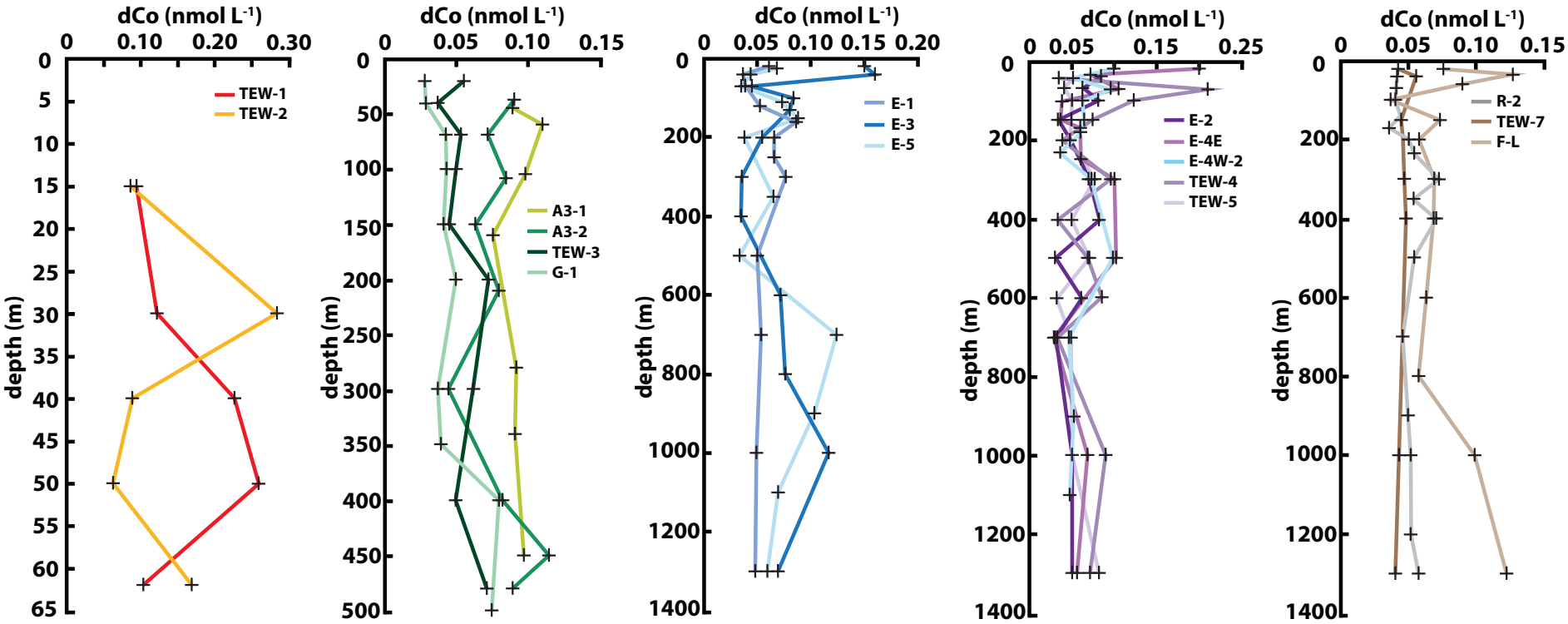

Figure V.4 dCo vertical profiles. Different scales are used due to the wide range of dCo observed in the different clusters.

3.3 Dissolved Nickel

Dissolved Ni (dNi) concentrations (Fig. V.5) varied between 5.4 nmol L^{-1} at TEW-2 (Fig. V.5e) and 7.5 nmol L^{-1} at G-1 (Fig. V.5b), which is similar to other Southern Ocean studies in the Australian sector of the Southern Ocean and around Crozet Island (Ellwood, 2008; Lai et al., 2008; Butler et al., 2013; Castrillejo et al., 2013) (Table V.3).

Over Kerguelen Island, Ni atmospheric deposition fluxes of the same order of magnitude as Co were observed (Heimburger et al., 2013). Furthermore, Co and Ni aerosols and rain water solubilities are similar for Co and Ni (Guieu et al., 1997; Hsu et al., 2010) so Co and Ni atmospheric inputs of the same order of magnitude should occur. Recalling that dCo atmospheric inputs should increase surface water concentration by 0.03 pmol L^{-1} to 0.06 pmol L^{-1}, a dNi atmospheric input of the same order of magnitude can be considered negligible with regards to dNi nanomolar concentrations.

In cluster 1, dNi presented heterogeneous profiles and a wide range of concentrations from 5.45 nmol L^{-1} to 7.23 nmol L^{-1}. Similarly to dCo, the observed dNi concentration ranges were similar at TEW-1 and TEW-2, which may be due to low fluvial input. Locally enhanced dNi concentrations were also observed at TEW-1 and TEW-2 and may be due to lateral advection of lithogenic material (similar to dCo) (section V.3.2).

In cluster 2 (Fig. V.5b), dNi concentrations increased with depth and reached a maximum near the seafloor except at G-1, which showed a dNi maximum at intermediate waters at 300 m. On the contrary to dMn and dFe, no significant dNi maximum was observed close to the seafloor, showing that local sediment resuspension was not a source of dNi for the water column above.

In cluster 3, nutrient-like dNi vertical profiles were observed with local sea surface maximum at E-1, E-3 (Fig. V.5c) TEW-4, E-4-E and E-4W-2 (Fig. V.5d). E-5 presented the lowest surface concentration compared to E-1 and E-3 stations. Similarly to dCo, high surface dNi concentrations were observed at E-3, TEW-4 and E-4E (Fig. V.5c, V.5d). In a similar process that delivers dFe and dCo, lateral advection of seawater across the PF might be a mechanism of dNi transport at these stations (Quéroué et al., 2015) (see section V.3.2).

In cluster 4 and 5, nutrient-like vertical profiles were observed (Fig. V.5e). Below 300 m, relatively homogenous concentrations were observed at both clusters except at F-L, where higher concentration were observed at 1000 and 1200 m. Higher dCo concentrations were

also observed, which may indicate that the sampled water mass interacted with the plateau (section V.3.2).

Similar to Co, Ni vertical profiles appear to be primarily influenced by lateral advection of seawater, which interacted with the Kerguelen plateau, than by biological uptake and remineralization.

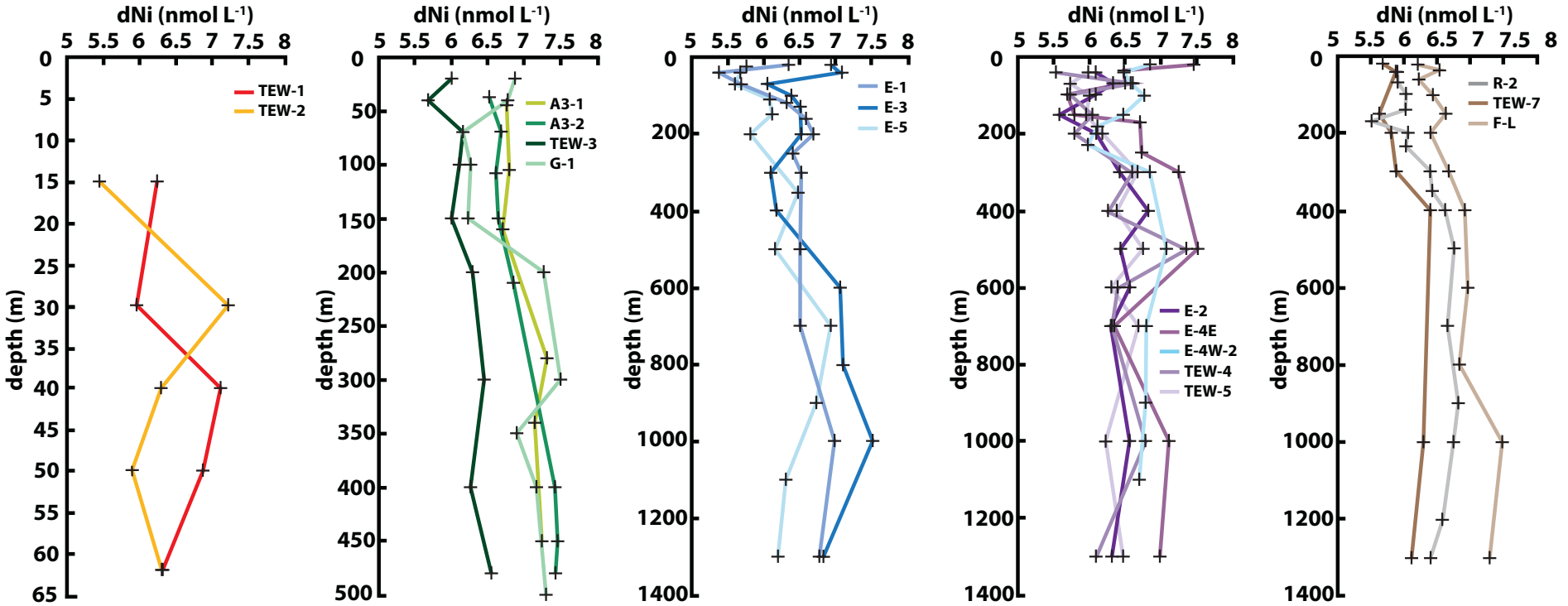

Figure V.5 dNi vertical profiles.

3.4 Dissolved Copper

Dissolved Cu (dCu) concentrations (Fig. V.6) varied between 1.1 and 2.6 nmol L^{-1}. The lowest concentration was observed at F-L (Fig. V.6e) and the highest at E-3 (Fig. V.6c). Dissolved Cu concentrations are consistent with observed values in other Southern Ocean sites reported by Boyé et al. (2012) and Lai et al. (2008) (Table V.3). However, our maximum values are higher than those reported by Ellwood (2008) and Butler et al. (2013) at 1.59 and 1.79 nmol L^{-1}, in the Southern Ocean. A clear meridional gradient with a northward decrease of dCu concentrations was observed in previous studies in the Southern Ocean due to biological uptake (Ellwood, 2008; Boyé et al., 2012; Butler et al., 2013). The more southern location considered here, as well as the UV irradiation of our samples prior to extraction (known to release Cu from organic ligands) may have resulted in higher dCu concentrations compared to Ellwood (2008) and Butler et al. (2013), who did not use UV irradiation.

Over Kerguelen Island, Cu deposition fluxes of the same order of magnitude as Co and Ni were observed (Heimburger et al., 2013). Furthermore, Co, Ni and Cu aerosol and rain water solubilities are of the same order of magnitude (Guieu et al., 1997; Hsu et al., 2010) so dissolved Co, Ni and Cu atmospheric inputs of the same order of magnitude should occur. These inputs can be considered negligible with regards to dCu nanomolar concentrations and could explain the non-occurrence of significant dCu surface maxima.

In cluster 1, similar and homogeneous concentrations (range from 1.55 to 1.75 nmol L^{-1}) were observed, except close to the bottom at TEW-1 where concentration decreased below 50 m (1.37 nmol L^{-1}) (Fig V.6a). Similar to dCo, dNi and dCd (section V.3.5) but in contrast to dMn and dFe (Quéroué et al., 2015), the observed dCu concentration range was similar at TEW-1 and TEW-2. Furthermore the observed surface dCu concentrations in this cluster were significantly higher than observed in other clusters surface water (t-test, $p<0.05$, $n = 10$), which could be due to freshwater inputs, sediment resuspension and/or lower biological uptake. The latter might be the most influencing process, as no differences between TEW-1 and TEW-2 (t test, $p > 0.05$) and no deep water dCu enhancement in the coastal area were observed respectively. Indeed in Fe deficient waters, cellular Cu demands increased by 2 to 3 fold (Annett et al., 2008) suggesting that the higher dCu concentrations observed in the coastal area is likely due to lower Cu uptake due to higher Fe concentrations.

In cluster 2, dCu concentrations generally increased with depth and showed nutrient like profiles. The lowest sea-surface dCu concentrations were observed at G-1, as observed for

dMn, dCd and dCo, which could also be due to biological uptake, as G-1 was the most productive station of this cluster (section V.3.7).

In cluster 3, 4 and 5 dCu concentrations also showed dCu nutrient like profiles with a regular increase with depth (range from 1.08 to 2.59 nmol L^{-1}). E-5 showed lower dCu surface concentrations compared to E-1 and E-3 (Fig. V.6c), which may be due to biological uptake as E-5 is the most productive time series station (section V.3.7). As observed for dMn, these clusters showed homogenous concentrations below 500 m (2.1 ± 0.2 nmol L^{-1}) (Fig. V.6c, Fig. V.6d and Fig. V.6e).

Overall, dCu vertical profiles seem to be impacted by uptake in surface water while the relatively homogenous dCu concentrations at depth show that remineralization does not seem to be a major influence. The low number of significant relationship with nutrients in surface waters or at depth tends to indicate that the dCu distributions in less influenced by internal processes than by external sources.

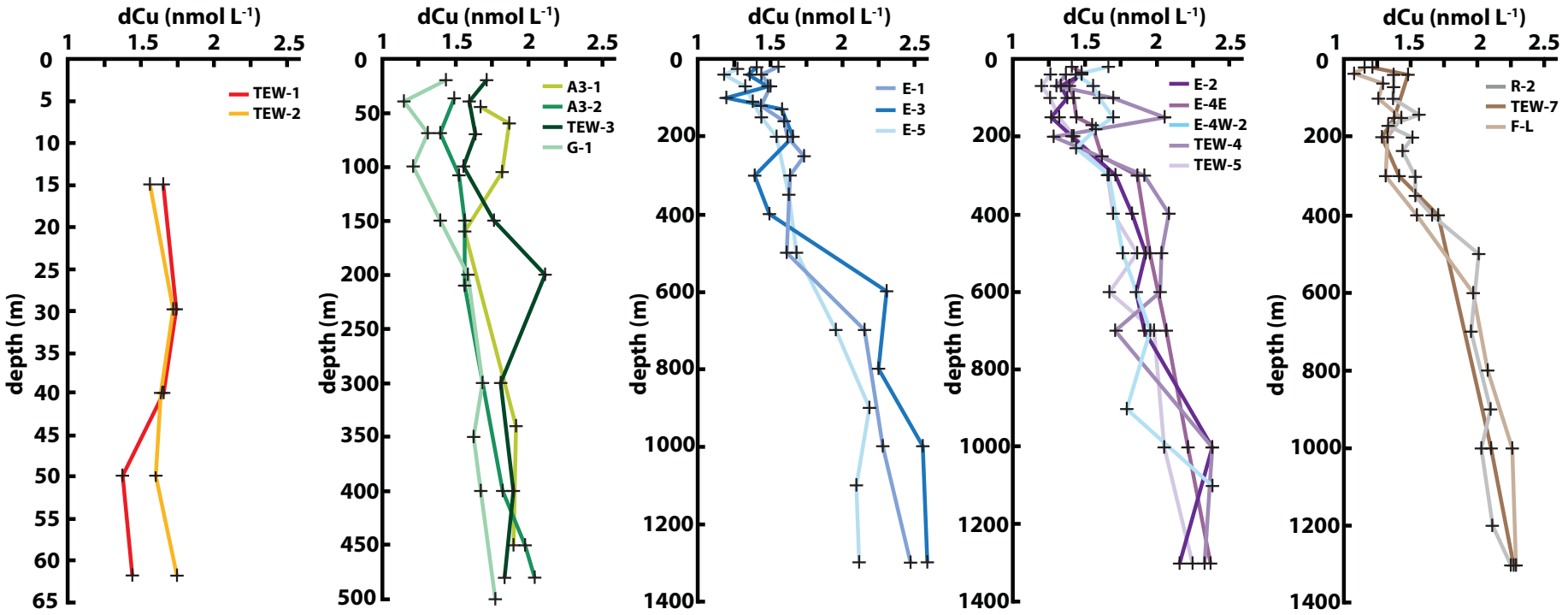

Figure V.6 dCu vertical profiles.

3.5 Dissolved Cadmium

The lowest dissolved cadmium (dCd) concentrations (Fig. V.7) were observed at the sea surface in the North Polar Front area at station F-L (0.23 nmol L^{-1}) (Fig. V.7e) and the highest within the recirculation area at TEW-5 (0.96 nmol L^{-1}, Fig. V.7d). Observed concentration ranges were consistent with previous Southern Ocean studies (Boyé et al., 2012; Butler et al., 2013; Baars et al., 2014), however lower dCd concentrations have been observed in Ellwood (2008); Abouchami et al. (2011); Castrillejo et al. (2013) (Table V.3). A clear meridional gradient with a northward decrease of dCd concentrations was observed in previous studies in the Southern Ocean due to biological uptake (Ellwood, 2008; Boyé et al., 2012; Butler et al., 2013). The northern location of the study sites selected by Ellwood (2008) and Castrillejo et al. (2013) likely explains the lower dCd range measured while the late summer measurement by Abouchami et al. (2011) could also induce lower dCd concentration along the meridional transect over the Southern Ocean due to biological uptake.

In cluster 1, TEW-1 and TEW-2, presented the highest dCd surface concentrations (0.75 nmol L^{-1}, 15 m, Fig. V.7a). The higher dCd concentration may be due to lower biological uptake, due to lower dCd requirement due to the highest dFe concentrations observed in this cluster (section V.3.7). Indeed, Cullen et al. (2003) and Lane et al. (2009) showed that under Fe-limitation, the relative Cd quota to P quota increases. At both stations, vertical profiles are very similar despite TEW-2 being further from the coastline of Kerguelen Island. The profiles were homogeneous below 0.58 - 0.65 nmol L^{-1}. This may be due to the low impact of fluvial and sedimentary inputs on dCd profile in the bay.

In cluster 2, G-1 presented the lowest dCd surface concentrations likely due to biological uptake as G-1 is the most productive station of this cluster (Fig. V.7b) (section V.3.7). Nutrient like profiles were observed with depleted surface concentrations followed by subsurface maximum at 300-500 m at all stations, except A3-1.

In cluster 3 and 5, all the profiles were similar and were nutrient like. The lowest dCd was observed in surface waters at E-4W-2 may be due to biological uptake as E-4W-2 is the most productive station of this cluster (Fig. V.7d) (section V.3.7). The lowest concentrations were observed in surface waters increasing up to a maximum at intermediate waters between 300 m and 500 m before decreasing with depth. E-4W-2 showed higher concentrations at depth (below 500 m) in comparison with other stations of the cluster 3, which is likely due to strong

remineralization inputs at depth due to high biological productivity and uptake in surface waters (section V.3.7).

In cluster 4, the lowest sea-surface dCd concentrations were observed compared to the other stations of this study (Fig. V.7e). The lower dCd concentrations measured at TEW-7 and F-L compared with samples from cluster 2, 3 and 5 may be explained by the meridional gradient observed in previous studies in the Southern Ocean due to biological uptake (Ellwood, 2008; Boyé et al., 2012; Butler et al., 2013).

With the exception of the clusters 1 and 2, the overall distribution of dCd is similar and showed a nutrient-like vertical profile. At clusters, 3, 4 and 5, relatively homogenous concentrations were observed below 500 m (0.84 ± 0.04 nmol L^{-1}) (Fig. V.7c, Fig. V.7d and Fig. V.7e).

Similarly to dCu, dCd is not influenced by lithogenic inputs from riverine or sediment resuspension associated with pore water release as seen in cluster 1 and 2. Biological uptake and remineralization seem to be the dominant controlling factors of the dCd profiles (section V.3.7)

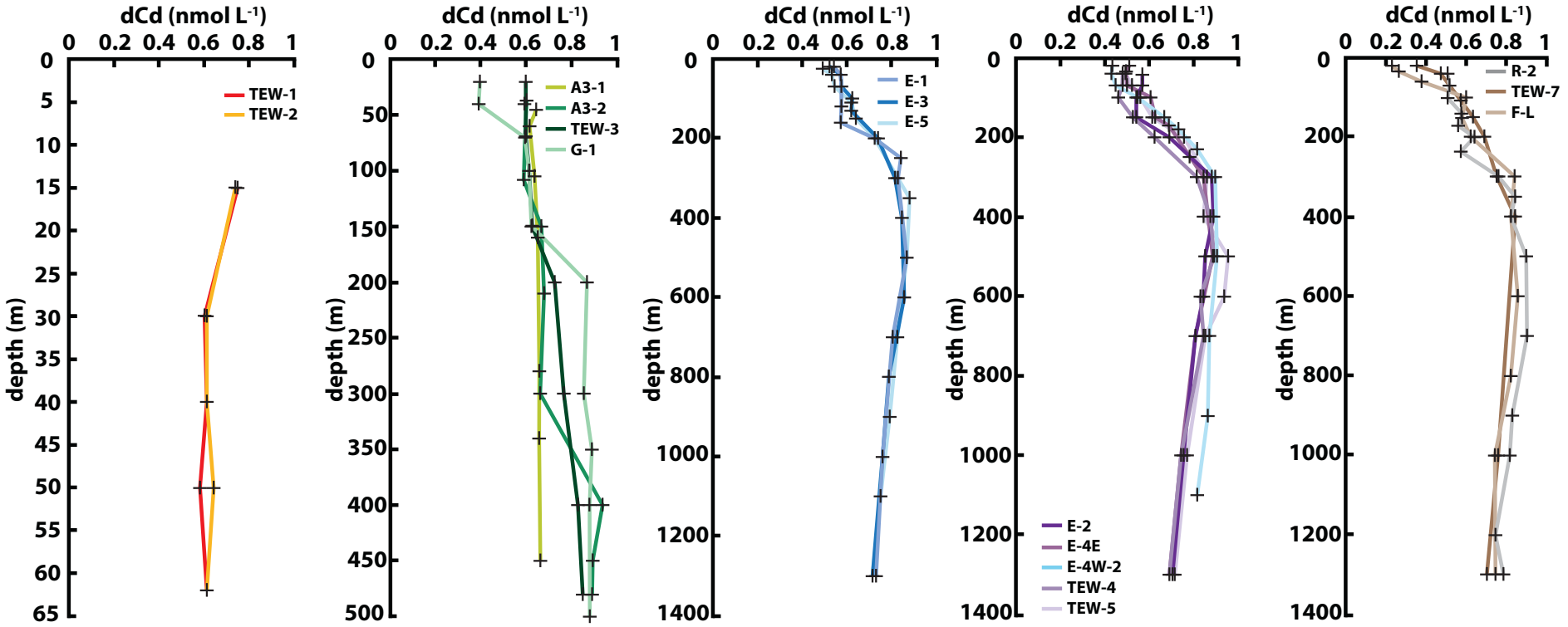

Figure V.7 dCd vertical profiles.

3.6 Dissolved Lead

Dissolved Pb (dPb) concentrations found in this study (Fig. V.8) varied between 3 pmol L^{-1} and 18 pmol L^{-1}, which is within the ranges observed by Castrillejo et al. (2013), Boyé et al. (2012), Lai et al. (2008) and Ellwood (2008) (Table V.3). During our study, every cluster showed low dPb concentrations (Fig. V.8), homogeneously distributed throughout the water column similarly to Ellwood (2008). Boyé et al. (2012) and Castrillejo et al. (2013) observed enhanced surface concentrations possibly due to atmospheric deposition or advection followed by decreases in dPb with depth due to scavenging. Furthermore high surface water dPb concentrations where observed by Lai et al. (2008) presumably due to atmospheric or sea-ice inputs in the Southern Ocean. In other basins such as the Atlantic and the Pacific Oceans, it has been suggested that surface dPb concentrations are enhanced by atmospheric wet and dry deposition (Duce et al., 1991; Aparicio-González et al., 2012), which leads to surface maximums and then scavenged type vertical profiles. Lead has been recognized as a good tracer of anthropogenic inputs by atmospheric deposition to surface waters (Boyle, 2001; Bruland and Lohan, 2003; Boyle et al., 2014). Lead anthropogenic inputs via atmospheric dust were observed only during austral winter over Kerguelen Island by Heimburger et al. (2013). Therefore, the low dust flux may explain the homogeneously low dPb concentrations during this austral summer study. Furthermore, no evidence of anthropogenic Pb was observed; even close to the island where human impact associated with research stations may be expected. Low dPb concentrations were measured in the vicinity of Kerguelen Island due to the low Pb emission of the Kerguelen base because of its small size and the use of unleaded fuel. This was combined with the lack of other pollution sources due to the remoteness of the study sites.

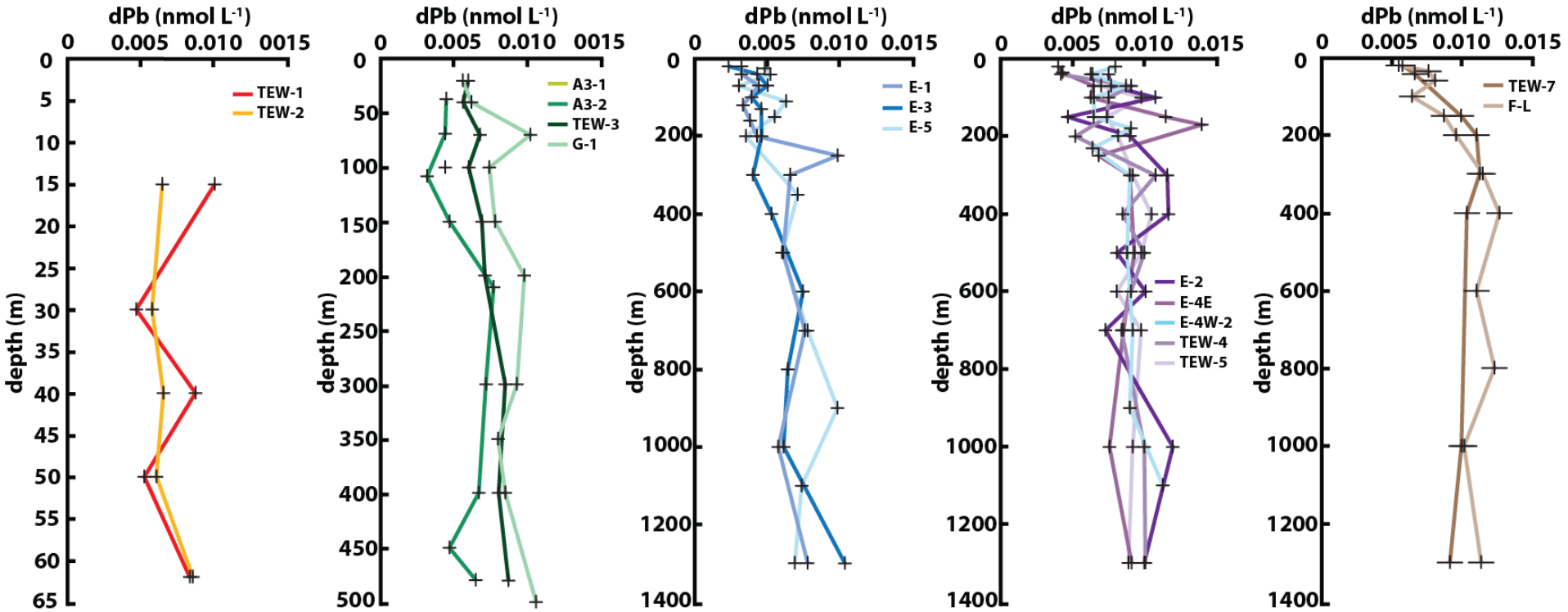

Figure V.8 dPb vertical profiles.

3.7 Biological uptake and associated remineralisation

At the time series A3 and the Lagrangian stations E, an estimate of metal uptake in the surface mixed layer was made, using the decrease in integrated trace metal concentrations over the increase in integrated biomass (as particulate organic phosphorus (POP)) measured between two consecutive visits at these sites (Tables V.4 and V.5). These ratios were compared with metal quotas calculated by Twining and Baines (2013), using data from diatom cultures, settling particles, Synchrotron X-ray fluorescence (SXRF) and dissolved profiles, and with metal quotas from replete cultures determined by Ho et al. (2003).

Integrated dMn in the mixed layer decreased by 60 % during the A-3 time series and 20 % at the E time series (Tables V.4 and V.5). During both time series, Mn quotas determined here span the whole range of values found by Twining and Baines (2013) and Ho et al. (2003) (from 0.2 to 7.7 mmol mol^{-1}), which suggests that at least part of the surface depleted concentrations of dMn in our study area can be explained by biological uptake. However, as Mn is prone to scavenging and redox transformations (Landing and Bruland, 1980; Noble et al., 2012), the imprint of biological uptake (and remineralization at depth) on vertical profiles can be difficult to detect (Twining and Baines, 2013), especially in oceanic regions like the Kerguelen Plateau where external sources of Mn are strong. That are the reasons why dMn showed hybrid like vertical profile, cluster 2, 3, 4 and 5.

Dissolved Cd uptake represents only 2 % and 11 % of the dCd stock over 27 days at A3 station and 20 days at E station, respectively (Tables V.4 and V.5). This is sufficient to strongly imprint vertical profiles. The Cd deficit:POP increase ratios (Table V.4) are within the range calculated by Twining and Baines (2013) (from 0.01 to 2 mmol mol^{-1}) and Ho et al. (2003) (from 0.007 to 0.73 mmol mol^{-1}). This consistency shows the importance of uptake on the distributions of Cd in the water column, even in an oceanic region strongly impacted by external sources. At depth, these two time series exhibited high dCd concentrations compared to the other stations of their respective cluster, which is notably due to remineralization (discussed below).

Dissolved Mn and Cd showed surface depletion followed by a maximum in subsurface waters at stations from cluster 2 and 3. Such a surface nutrient like characteristic was particularly significant at A3-2, G-1 (plateau area), E-5, E-4W-2, TEW-4 (recirculation area). Such a profile indicated the potential influence of biological uptake on dMn and dCd concentrations. At these locations, in surface waters above the WW, dCd showed significant

correlations with phosphate, nitrate, silicate and fluorescence (p value < 0.01) and dMn showed significant correlations with phosphate, nitrate, silicate and inverse correlation with fluorescence (p value < 0.01) (Fig. V.9 and 10). With regards to dMn, such correlations have already been observed by Middag et al. (2011a) and (Boyé et al., 2012) in the Atlantic sector of the Southern Ocean highlighting the role of Mn as a micronutrient. Over the whole water column, dCd was significantly correlated with phosphate (Fig. V.11, p < 0.01). Such relationship has already been observed in the Southern Ocean and is typical of this ocean (de Baar et al., 1994; Cullen et al., 2003; Ellwood, 2008; Boyé et al., 2012; Castrillejo et al., 2013; Cullen and Maldonado, 2013; Abouchami et al., 2014; Baars et al., 2014). A similar slope of the dCd:PO_4 relationship was also observed during these studies. For surface mixed layer samples collected at A3-2, G-1, E-5, E-4W-2 and TEW-4, dCd/PO_4 ratios (0.29 ± 0.03, n=11) where in the top of the range observed by Baars et al. (2014) and Boyé et al. (2012) in the ACC. This can be explained by the lower dCd requirement by phytoplankton in Fe replete conditions (Cullen et al., 2003; Lane et al., 2009). This may explain the higher dissolved ratio observed in the surface water of the naturally fertilized area (Cullen, 2006). The highest dCd/PO_4 spot ratios (>0.40) where observed in the coastal area which might be due to highest dFe concentration and the subsequent lower requirement of dCd. Biological uptake could therefore explain the lowest dMn and dCd surface concentrations found over the plateau and recirculation areas observed at both of the most productive stations of their respective cluster, G-1 and E-4W-2, respectively.

Dissolved Co uptake represents only 10 % of the dCo stock over 27 days at A3 station (Tables V.4 and V.5). The estimates of Co elemental ratios at A-3 are in the lower limit of estimates by Twining and Baines (2013) (from 0.01 to 2 mmol mol^{-1}) and also in the lower limit of measurement of replete phytoplankton cultures (Ho et al., 2003) (from 0.01 to 0.46 mmol mol^{-1}) showing that the dCo surface water decrease at A3 may be due to biological uptake. The stock decrease has not been studied at E time series as high dCo concentrations have been observed at E-3 due to lateral advection of water masses particularly enriched in dCo while the concentration of the other studied elements was not significantly influenced.

The low variability in the dNi vertical profiles generally indicates the biological requirement for dNi compared to surface dissolved Ni concentrations (decrease of 3% of the dNi stock during the A-3 time series, Tables V.4 and V.5). Low biological demand at this early stage of the bloom could also explain the relatively low (16 %) decrease of the mixed layer dCu stocks at both time series (Tables V.4 and V.5) in addition to strong external

sources. Estimates of Ni and Cu quotas at A-3 were in the higher range of those of Twining and Baines (2013) (Ni: from 0.25 to 1,8 mmol mol^{-1}, Cu: from 0.25 to 2 mmol mol^{-1}). Similar to dCo, dNi stock decrease has not been studied at E time series. Estimates of Cu quotas at E sites were in the range of those of Twining and Baines (2013) (Cu: from 0.25 to 2 mmol mol^{-1}) (Table V.5). The estimates of dNi and dCu quotas seem to indicate that the biological uptake may be responsible for the low surface layer concentration decrease. However, at G-1, where a phytoplankton bloom was underway, the dNi and dCu vertical profile did not show particularly depleted surface concentrations, which is in contrast to some other micronutrients such as Cd, Co and Mn showing that biological uptake is not a major influence on dNi and dCu vertical profiles.

For bioactive trace metals, linear relationships between dissolved metal concentrations versus dissolved macronutrients found below the mixed layer, can estimate remineralization if external sources of metals (and macronutrients) in the deep waters are minimal. Such remineralization ratios reflect phytoplankton metal stoichiometries in surface layers. We calculated the ratio of each bioactive trace metal (Mn, Ni, Cu, Co, Cd) over phosphate at R-2, TEW-4, TEW-5, TEW-7, E-2, E-3, E4-E, E-5, F-L and A3-2 when the correlation was significant.

However, in the wake of Kerguelen Islands, dMn and dCo did not show any significant relationship with phosphate below the mixed layer, irrespective of the station considered. The absence of any correlation suggests that remineralization is not the main process controlling these trace metal distributions at depth in the vicinity of Kerguelen Islands (e.g., due to external sources of these metals at depth, or scavenging and redox processes) and explain the hybrid like profile observed for these metals.

In cluster 5, in deep waters bellow 200 m, dCd, dNi, and dCu exhibited significant ($p < 0.05$) correlation versus phosphate. The ratios of the dissolved metal:phosphate were 0.48 ($R^2 = 0.97$), 1.32 ($R^2 = 0.80$) and 0.84 ($R^2 = 0.48$) mmol:mol^{-1} for Cd, Ni and Cu, respectively. These values are within the ranges of metal quota ratios calculated by Twining and Baines (2013), confirming that their distributions at this open ocean station was likely driven by biological uptake with deeper remineralization. With regards to dNi and dCu, R-2 was the only station where such significant relationship has been observed. This unique regression suggests that remineralization is not the main process controlling dNi and dCu distributions at depth cluster 2, 3 and 4 (e.g., due to external sources of these metals at depth, or redox processes) and/or that these metals and phosphate are not remineralized at the same rate.

Only dCd was significantly correlated to phosphate at other stations of this study. At TEW-4 (0.64 mmol mol^{-1}, $R^2 = 0.96$), TEW-5 (0.70 mmol mol^{-1}, $R^2 = 0.85$), E-3 (0.36 mmol mol^{-1}, $R^2 = 0.85$) and E-5 (0.35 mmol mol^{-1}, $R^2 = 0.88$). These values that are similar to the ratio calculated at R-2 and to the metal quotas calculated by Twining and Baines (2013) and measured in replete cultures by Ho et al. (2003) show the importance of uptake and remineralization on the distributions of Cd in the water column, even in an oceanic region strongly impacted by external sources.

Over the whole water column, dCu was significantly correlated with silicic acid (Fig. V.12, $p < 0.01$). Such relationship has already been observed in the Southern Ocean (Löscher, 1999; Boyé et al., 2012). In the whole water column, similar and relatively low Cu/Si slope has been observed by Löscher (1999), in the Polar Front area characterized by a developing diatom spring bloom. In surface water, decreasing Cu/Si ratio with depth has been observed up to 200 m, which may result from the preferential Si uptake in surface water and preferential Si release during the diatom's frustule dissolution (Löscher, 1999). This would also explain the highest dCu/Si ratio observed in surface water at the most productive stations such as G-1 (0.13 10^{-3}), E-4W-2 (0.18 10^{-3}), TEW-1 (0.15 10^{-3}) and F-L (0.20 10^{-3}). Furthermore, bellow 200 m, the Cu/Si ratio is homogenous (0.030 10^{-3} ± 0.005 10^{-3}, n=53) and similar to the deep ratio observed by Löscher (1999). This showed that the Cu/Si remineralization rate is constant bellow 200 m. These results suggest that the dCu nutrient like profiles is likely influenced in surface water by biological uptake followed by remineralization at depth.

These estimates of trace metal quotas, and the relationship of TM with phosphate in deep waters associated with evaluation of external sources, identify 3 groups of trace metals: 1) Cd, whose vertical profiles are mainly impacted by uptake and remineralization, with seemingly little impact of external sources except at the most coastal stations, 2) Mn which is impacted both by biological activity (and scavenging) and external sources, and 3) Cu, Ni and Co whose vertical profiles seem to be more impacted by external sources than by uptake and remineralization.

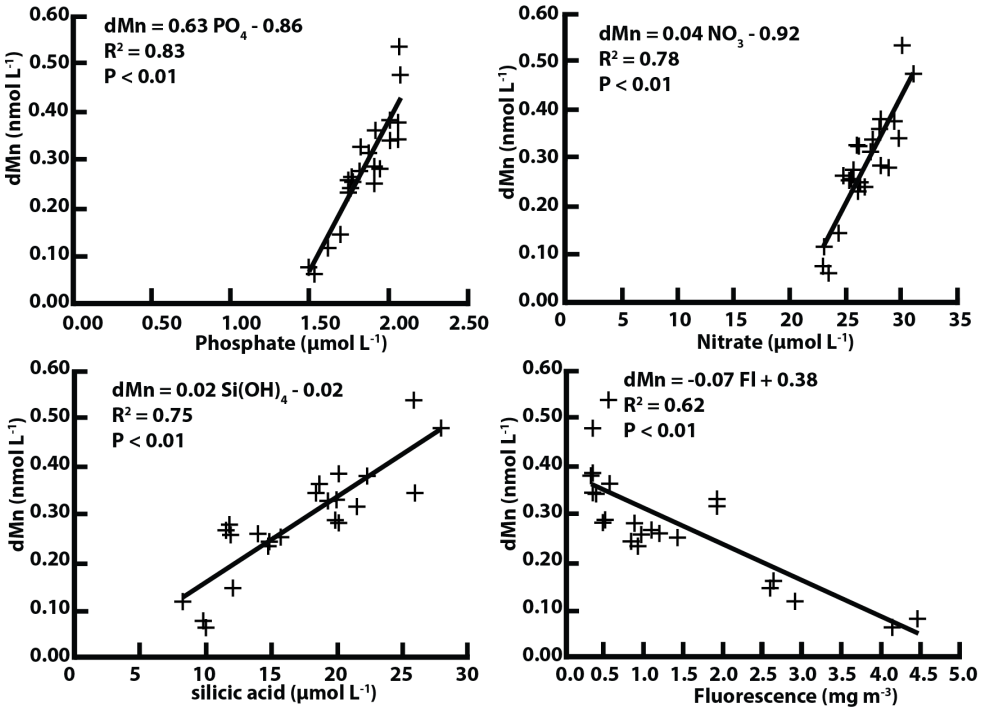

Figure V.9 Concentrations of dMn versus concentrations of nutrients and fluorescence at the most productive station south of the PF, cluster 2 and 3 A3-2, G-1 (cluster 2), E-3, E-5, E-4W-2, TEW-4 (cluster 3)

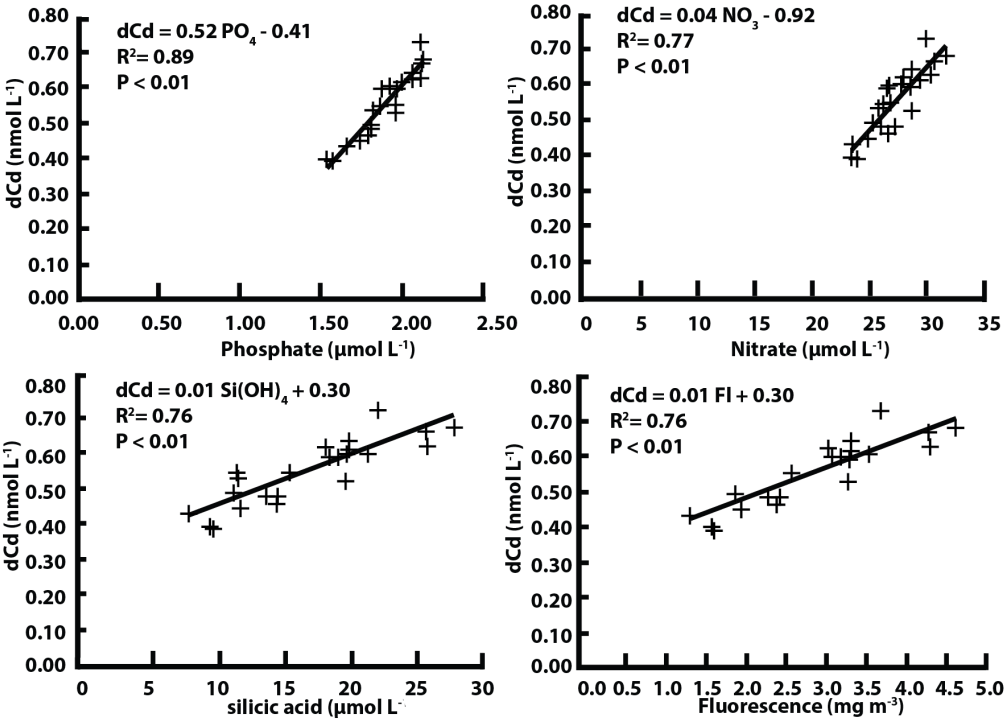

Figure V.10 Concentrations of dCd versus concentrations of nutrients and fluorescence at the most productive station south of the PF, A3-2, G-1 (cluster 2), E-3, E-5, E-4W-2, TEW-4 (cluster 3).

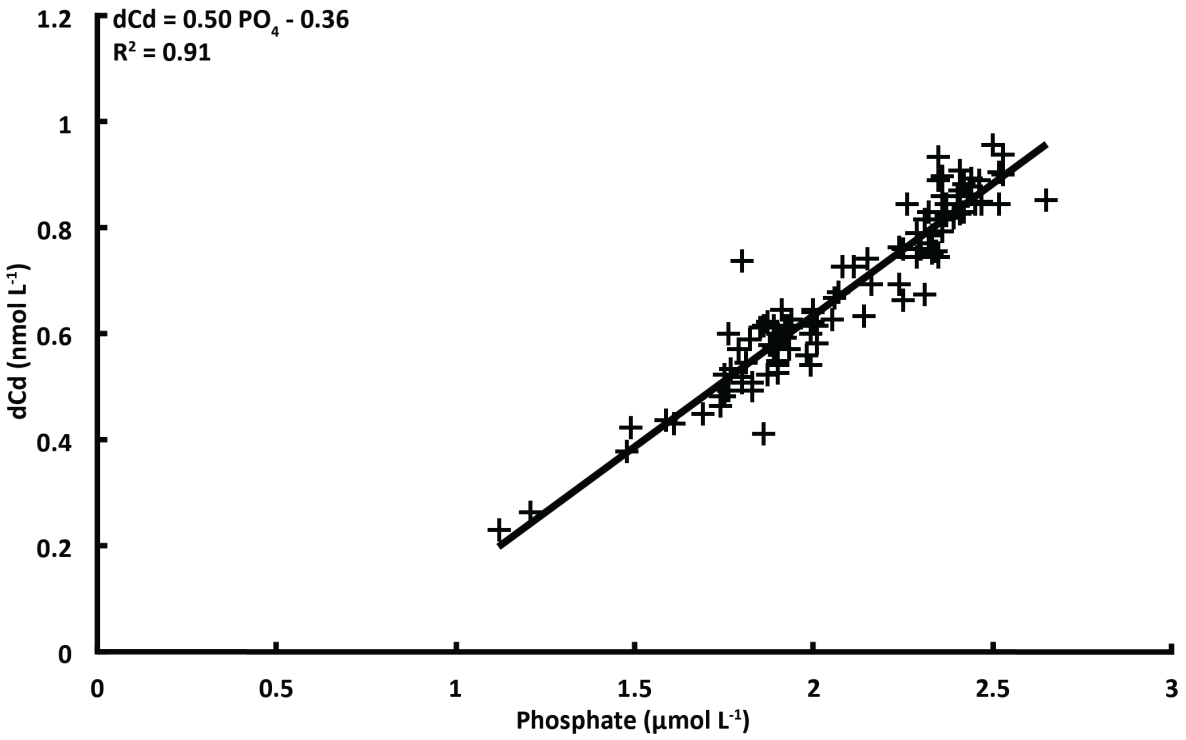

Figure V.11 Concentrations of dCd versus phosphate over the whole water column at all the sampled stations.

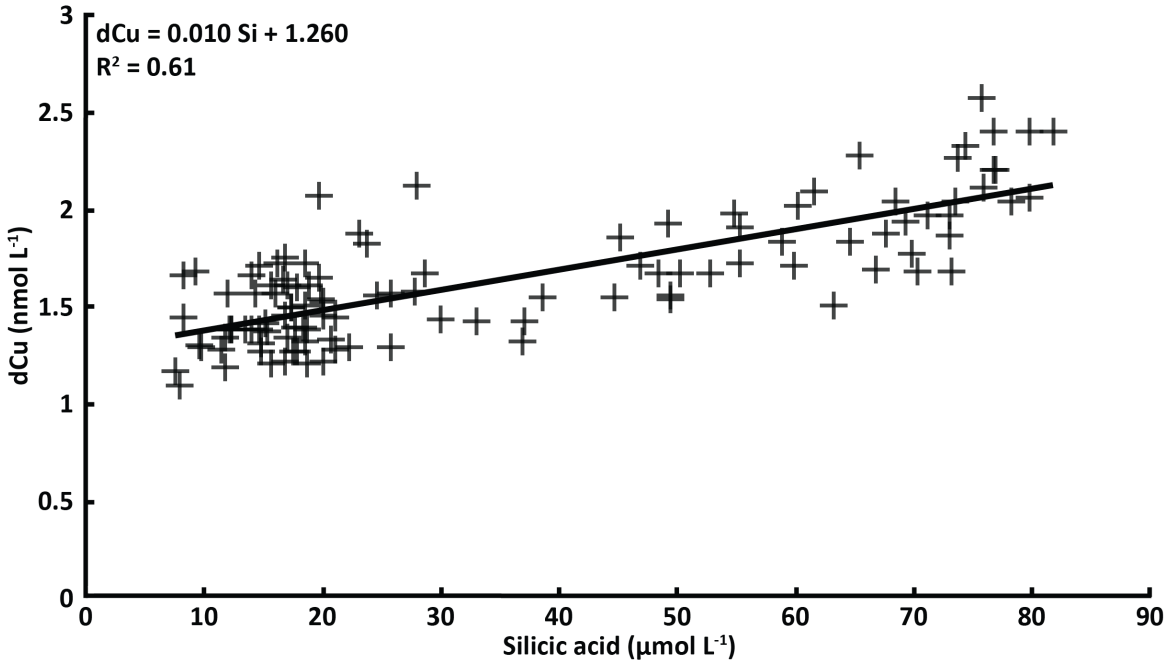

Figure V.12 Concentrations of dCu versus silicic acid over the whole water column at all the sampled stations.

Table V.4 Integrated dissolved trace elements and POP values at stations where time-series could be carried out. See text for more detail.

	Integration depth	ΣdMn µmol m^{-2}	ΣdCo µmol m^{-2}	ΣdNi µmol m^{-2}	ΣdCu µmol m^{-2}	ΣdCd µmol m^{-2}	ΣdPOP mmol m^{-2}
A3-1	150	130	14.1	1024	271	94	9.9
A3-2	150	53.5	12.6	989	227	92	28.4
E-1	40	13.2	2.4	254	62.3	21.7	0.9
E-3	40	12.1	6	277	56	20.9	5.5
E-5	40	10.7	3.1	231	52	19.2	8.4

Table V.5 Integrated dissolved trace elements and POP values at the two A3 stations and E-1, E-3 and E-5. Some ratios are bracketed due to potential external source intrusion between E-1 and E-3. The integration depth was deeper at A3 compared to E stations, as the mixed layer depth encountered at A3 was deeper than at E sites (see Table 1 in Bowie et al. (2014))

	Integration depth	ΔMn/ΔPOP mmol mol^{-1}	ΔCo/ΔPOP mmol mol^{-1}	ΔNi/ΔPOP mmol mol^{-1}	ΔCu/ΔPOP mmol mol^{-1}	ΔCd/ΔPOP mmol mol^{-1}
A3-1 - A3-2	150	4.14	0.08	1.89	2.38	0.11
E-1 - E-3	40	0.24	(-0.78)	(-5)	1.37	0.17
E-3 - E-5	40	0.48	1	15.9	1.38	0.59

4 Conclusion

The KEOPS 2 cruise over the Kerguelen Plateau allowed, for the first time, observations on the distribution of Ni, Cu, Cd and Pb in a naturally iron fertilized area. It was only the second study of Mn and Co in this sector of the Southern Ocean. Dissolved Mn concentrations were impacted by biological activity with external sources strongly affecting dMn vertical profiles. Sedimentary input of dMn was identified at site A3-2. Kerguelen Island was identified as a likely source of dMn, particularly to the Hillsborough Bay area. No dMn surface concentration enhancements were observed indicating that atmospheric inputs of trace metals were insignificant in this study. The bioactive trace metals, Ni, Cu and Co were not strongly influenced by uptake and remineralization and their vertical profiles were mainly controlled by external sources. In the coastal areas, dCo concentrations were enhanced. However it was not possible to distinguish between freshwater and sediment resuspension inputs due to a lack of data concerning Kerguelen Island rivers concentrations. However these coastal enhanced concentrations allowed the use of dCo, in combination with dNi, to indicate lateral advection sources of trace metals. Estimates of metal quotas and linear regressions of

dissolved metals vs phosphate at depth indicate that dCd concentrations were mainly controlled by uptake and remineralization, with no strong impact by external sources. At all stations, dPb displayed a homogenous profile. The small pollution emissions from the Kerguelen base along with the remoteness of the study sites considered, explain the low Pb concentration measured and the clear absence of anthropogenic source of trace metals.

Acknowledgements

The authors thank the crew of the R/V Marion-Dufresne for assistance on board, Bernard Quéguiner as chief scientists. Thanks to M.Lasbleiz for the analysis of POP and thanks to J.Caparros, A.Guénneuguès and L.Oriol, from the Microbial Oceanography Laboratory (LOMIC) for the analysis of the nutrients. Thanks to the Antarctic Climate and Ecosystems Cooperative Research Centres (ACE CRC) for funding through the Carbon program. This work was supported by the French Research program of INSU-CNRS LEFE−CYBER (‘Les enveloppes fluides et l'environnement’ – ‘Cycles biogéochimiques, environnement et ressources’), the French ANR (‘Agence Nationale de la Recherche’, SIMI-6 program, ANR-2010-BLAN-614 KEOPS2 and, ANR-10-JCJC-606 ICOP), the French CNES program (‘Centre National d’Etudes Spatiales’) and the French Polar Institute IPEV (Institut Polaire Paul−Emile Victor). Support from the University of Tasmania Cross Theme (B0018994) and Rising Stars (B0019024) grants is acknowledged. Access to ICP-MS instrumentation was funded through ARC LIEF LE0989539.

Table V.6 Station name, depth, dissolved manganese concentrations (dMn), dissolved cobalt concentrations (dCo), dissolved nickel concentrations (dNi), dissolved copper concentrations (dCu), dissolved cadmium concentrations (dCd), dissolved lead concentrations (dPb) during KEOPS2 (DNS = data not shown as contamination is suspected.)

Station	Depth [m]	dMn [nmol L^{-1}]	dCo [nmol L^{-1}]	dNi [nmol L^{-1}]	dCu [nmol L^{-1}]	dCd [nmol L^{-1}]	dPb [pmol L^{-1}]
A3-1	45	0.49	0.089	6.76	1.67	0.644	8.5
	60	DNS	0.110	DNS	1.86	0.614	DNS
	105	0.50	0.098	6.79	1.82	0.638	14.6
	160	0.51	0.076	6.71	1.56	0.651	18.5
	280	0.59	0.091	7.31	2.64	0.659	57.9
	340	0.47	0.091	7.14	1.91	0.656	31.7
	450	0.56	0.097	7.24	1.89	0.664	29.7
R-2	40	0.26	0.042	5.89	1.37	0.508	7.5
	70	0.27	0.042	5.90	1.37	0.518	10.4
	100	0.27	0.040	6.02	1.37	0.507	9.8
	140	0.31	0.044	6.01	1.56	0.577	8.9
	170	0.28	0.036	5.49	1.33	0.561	15.6
	200	0.37	0.051	6.05	1.51	0.647	8.8
	235	0.31	0.054	6.02	1.44	0.573	12.7
	300	0.33	0.073	6.39	1.53	0.762	10.0
	350	0.35	0.054	6.43	1.53	0.846	11.5
	400	0.35	0.071	6.62	1.66	0.829	15.1
	500	0.27	0.055	6.75	2.01	0.900	17.9
	700	0.23	0.046	6.66	1.95	0.905	13.1
	900	0.23	0.050	6.82	2.10	0.832	21.8
	1000	0.21	0.052	6.74	2.03	0.819	12.9
	1200	0.18	0.052	6.58	2.11	0.748	28.2
	1300	0.18	0.058	6.40	2.25	0.788	16.4
E-1	20	0.33	0.061	6.35	1.56	0.542	6.3
	40	0.29	0.037	5.37	1.44	0.574	6.3
	70	0.33	0.039	5.69	1.50	0.576	7.5
	120	0.31	0.052	6.32	1.43	0.577	6.4
	160	0.34	0.087	6.59	1.60	0.574	6.9
	200	0.37	0.066	6.70	1.62	0.725	7.4
	250	0.28	0.066	6.39	1.73	0.845	13.0
	300	0.32	0.077	6.52	1.64	0.828	9.7
	500	0.28	0.051	6.50	1.61	0.868	9.2
	700	0.23	0.054	6.51	2.16	0.807	10.7
	1000	0.22	0.049	6.99	2.28	0.760	8.9
	1300	0.20	0.048	6.77	2.48	0.732	10.9

Station	Depth [m]	dMn [nmol L^{-1}]	dCo [nmol L^{-1}]	dNi [nmol L^{-1}]	dCu [nmol L^{-1}]	dCd [nmol L^{-1}]	dPb [pmol L^{-1}]
TEW-1	15	5.40	0.093	6.25	1.64	0.751	10.1
	30	4.86	0.121	5.96	1.73	0.599	4.7
	40	5.16	0.226	7.12	1.65	0.614	8.8
	50	4.36	0.259	6.88	1.37	0.578	5.3
	62	4.67	0.103	6.32	1.44	0.617	8.4
TEW-2	15	1.73	0.085	5.45	1.55	0.739	6.5
	30	1.92	0.284	7.23	1.71	0.617	5.8
	40	1.83	0.088	6.30	1.63	0.614	6.6
	50	1.79	0.062	5.90	1.60	0.645	6.1
	62	1.82	0.169	6.31	1.74	0.614	8.6
TEW-3	20	0.37	0.055	6.01	1.71	0.599	6.0
	40	0.36	0.037	5.69	1.59	0.593	5.6
	70	0.36	0.053	6.17	1.64	0.593	6.8
	100	0.36	0.050	6.11	1.55	0.619	6.0
	150	0.39	0.045	6.00	1.76	0.626	6.9
	200	0.39	0.072	6.29	2.11	0.726	7.1
	300	0.36	0.062	6.45	1.80	0.766	8.5
	400	0.36	0.049	6.27	1.89	0.827	8.0
	480	0.45	0.071	6.55	1.83	0.849	8.7
TEW-4	40	0.26	0.035	5.53	1.37	0.483	4.2
	70	0.24	0.211	6.61	1.30	0.482	9.1
	100	0.23	0.123	5.72	1.70	0.462	7.5
	150	0.29	0.073	6.04	2.05	0.528	7.4
	200	0.34	0.038	5.79	1.28	0.627	5.2
	300	0.29	0.097	6.59	1.92	0.816	10.8
	400	0.26	0.034	6.26	2.08	0.877	8.5
	500	0.29	0.069	7.35	2.03	0.893	10.0
	600	0.25	0.085	6.40	2.02	0.832	9.1
	700	0.25	0.033	6.31	1.71	0.846	8.4
	1000	0.23	0.089	6.77	2.39	0.746	10.0
	1300	0.19	0.071	6.09	2.33	0.692	10.1

Station	Depth [m]	dMn [nmol L^{-1}]	dCo [nmol L^{-1}]	dNi [nmol L^{-1}]	dCu [nmol L^{-1}]	dCd [nmol L^{-1}]	dPb [pmol L^{-1}]
E-2	40	0.34	0.084	6.08	1.48	0.570	7.5
	70	0.34	0.062	6.33	1.33	0.571	7.7
	100	0.28	0.080	6.09	1.38	0.543	10.8
	150	0.28	0.034	5.58	1.26	0.542	4.7
	200	0.32	0.048	6.09	1.41	0.693	9.0
	300	0.27	0.070	6.41	1.71	0.883	11.6
	400	0.26	0.082	6.82	1.82	0.890	11.7
	500	0.26	0.032	6.42	1.92	0.854	8.1
	600	0.26	0.060	6.56	1.86	0.845	10.1
	700	0.24	0.031	6.30	1.91	0.812	7.3
	1000	0.21	0.051	6.56	2.38	0.754	12.0
	1300	0.18	0.050	6.30	2.16	0.706	10.0
TEW-5	40	0.34	0.052	5.98	1.26	0.495	6.4
	70	0.30	0.041	5.72	1.20	0.523	7.0
	100	0.35	0.050	6.00	1.26	0.562	9.8
	150	0.33	0.049	5.95	1.32	0.615	7.4
	200	0.34	0.048	6.17	1.42	0.759	8.2
	300	0.29	0.077	6.67	1.66	0.861	9.2
	400	0.29	0.049	6.38	1.70	0.846	10.5
	500	0.25	0.070	6.74	1.86	0.957	9.8
	600	0.23	0.032	6.31	1.67	0.939	8.1
	700	0.25	0.048	6.68	1.98	0.852	9.8
	1000	0.21	0.051	6.22	2.05	0.771	9.2
	1300	0.20	0.082	6.47	2.25	0.715	8.9
TEW-7	20	0.35	0.043	5.67	1.21	0.353	5.8
	40	0.53	0.056	5.86	1.48	0.476	6.7
	150	0.29	0.045	5.60	1.37	0.635	10.1
	200	0.25	0.046	5.80	1.28	0.692	11.2
	300	0.23	0.048	5.87	1.41	0.755	11.5
	400	0.29	0.049	6.38	1.70	0.846	10.5
	1000	0.20	0.043	6.28	2.10	0.760	10.1
	1300	0.19	0.040	6.10	2.28	0.703	9.3

Station	Depth [m]	dMn [nmol L^{-1}]	dCo [nmol L^{-1}]	dNi [nmol L^{-1}]	dCu [nmol L^{-1}]	dCd [nmol L^{-1}]	dPb [pmol L^{-1}]
E-3	20	0.30	0.150	6.94	1.41	0.523	5.4
	40	0.29	0.160	7.08	1.36	0.571	7.4
	70	0.31	0.045	6.05	1.48	0.580	8.1
	100	0.32	0.084	6.39	1.19	0.625	7.0
	130	0.34	0.080	6.51	1.58	0.622	7.7
	200	0.33	0.055	6.52	1.66	0.742	7.7
	300	0.28	0.036	6.09	1.39	0.819	7.1
	400	0.25	0.035	6.17	1.50	0.850	8.4
	600	0.29	0.072	7.06	2.31	0.860	10.6
	800	0.24	0.076	7.10	2.25	0.790	9.5
	1000	0.24	0.117	7.52	2.56	0.765	9.2
	1300	0.24	0.069	6.83	2.59	0.715	13.5
F-L	20	0.23	0.076	6.19	1.15	0.230	5.5
	35	0.25	0.127	6.52	1.08	0.263	7.7
	60	0.42	0.090	6.21	1.29	0.377	8.2
	100	0.53	0.037	6.42	1.26	0.600	6.5
	150	0.40	0.074	6.62	1.43	0.581	8.8
	200	0.34	0.058	6.40	1.32	0.626	9.8
	300	0.25	0.069	6.67	1.31	0.845	11.5
	400	0.22	0.069	6.91	1.55	0.825	12.9
	600	0.30	0.064	6.96	1.97	0.859	11.2
	800	0.25	0.058	6.83	2.08	0.823	12.6
	1000	0.24	0.099	7.48	2.26	0.745	10.3
	1300	0.19	0.123	7.30	2.29	0.746	11.5
G-1	20	0.08	0.028	6.87	1.43	0.397	5.6
	40	0.06	0.029	6.77	1.15	0.392	6.2
	70	0.36	0.043	6.16	1.31	0.595	10.2
	100	0.28	0.043	6.27	1.21	0.613	7.4
	150	0.33	0.042	6.24	1.40	0.622	7.8
	200	0.32	0.050	7.26	1.58	0.868	9.8
	300	0.40	0.038	7.50	1.68	0.853	9.3
	350	0.48	0.040	6.90	1.62	0.888	8.0
	400	0.50	0.080	7.17	1.67	0.878	8.5
	500	0.41	0.074	7.30	1.77	0.880	10.6

Station	Depth [m]	dMn [nmol L^{-1}]	dCo [nmol L^{-1}]	dNi [nmol L^{-1}]	dCu [nmol L^{-1}]	dCd [nmol L^{-1}]	dPb [pmol L^{-1}]
E4-E	20	0.31	0.201	7.46	1.41	0.511	4.0
	35	0.30	0.072	6.48	1.48	0.498	4.3
	70	0.31	0.104	6.49	1.39	0.500	6.5
	100	0.33	0.038	5.69	1.42	0.607	6.3
	150	0.30	0.036	5.78	1.44	0.628	11.5
	170	0.33	0.059	6.71	1.55	0.691	14.0
	250	0.29	0.061	6.72	1.62	0.783	6.8
	300	0.32	0.101	7.24	1.87	0.846	9.0
	500	0.26	0.103	7.51	1.96	0.888	9.3
	700	0.23	0.030	6.35	2.07	0.809	8.5
	1000	0.20	0.068	7.10	2.22	0.744	7.6
	1300	0.18	0.054	6.98	2.38	0.706	9.1
E-4W-2	20	0.18	0.100	6.84	1.66	0.437	8.0
	40	0.12	0.051	6.48	1.43	0.432	6.3
	70	0.15	0.096	6.58	1.56	0.450	8.7
	100	0.25	0.063	6.76	1.60	0.549	6.5
	150	0.42	0.065	6.47	1.70	0.669	6.5
	180	0.36	0.060	6.11	1.57	0.733	9.1
	230	0.35	0.036	5.97	1.44	0.818	6.4
	300	0.32	0.074	6.84	1.66	0.898	9.0
	500	0.31	0.098	7.07	1.76	0.907	8.8
	700	0.26	0.046	6.78	1.96	0.872	9.2
	900	0.23	0.052	6.78	1.79	0.866	9.0
	1100	0.23	0.048	6.69	2.39	0.817	11.3
A3-2	37	0.31	0.090	6.52	1.49	0.602	4.5
	69	0.33	0.072	6.68	1.39	0.597	4.4
	108	0.33	0.084	6.61	1.52	0.589	3.2
	150	0.54	0.064	6.65	1.56	0.666	4.7
	210	0.48	0.080	6.85	1.56	0.679	7.7
	300	0.41	0.044	DNS	DNS	0.663	7.2
	400	0.58	0.082	7.42	1.82	0.936	6.7
	450	0.84	0.114	7.46	1.97	0.892	4.7
	480	1.12	0.089	7.43	2.04	0.890	6.5

Station	Depth [m]	dMn [nmol L^{-1}]	dCo [nmol L^{-1}]	dNi [nmol L^{-1}]	dCu [nmol L^{-1}]	dCd [nmol L^{-1}]	dPb [pmol L^{-1}]
E-5	25	0.26	0.068	5.75	1.27	0.493	7.9
	40	0.26	0.043	5.67	1.18	0.534	8.3
	70	0.28	0.035	5.59	1.33	0.546	6.1
	110	0.34	0.073	6.08	1.38	0.621	9.4
	150	0.38	0.088	6.12	1.44	0.642	8.6
	200	0.38	0.038	5.81	1.54	0.728	6.6
	350	0.31	0.065	6.47	1.63	0.884	10.2
	500	0.32	0.034	6.15	1.68	0.871	9.1
	700	0.24	0.124	6.94	1.95	0.828	10.9
	900	0.21	0.103	6.73	2.19	0.795	13.0
	1100	0.19	0.069	6.30	2.10	0.753	10.5
	1300	0.18	0.059	6.19	2.12	0.716	10.0

Chapter VI

Conclusions and future work

1 Implementation of a new analytical method for the measurement of dissolved metals in the ocean

The GEOTRACES program highlights the central role of TMs in marine biogeochemistry, so the implementation of fast and precise analytical methods has quickly become a priority. Indeed, the wide range of TMs of interest and the development of new seawater sampling techniques (de Baar et al., 2008b; Cutter and Bruland, 2012) has led to a lag in the analytical capabilities available to efficiently handle the very large amount of samples collected and archived in laboratories worldwide, hence a pressing demand for fast and low cost methods to analyse multiple TMs in one sample.

In the framework of the GEOTRACES program, and in line with the need to study several trace metals in the Kerguelen Plateau area, this study developed an automated manifold to extract dissolved fraction of Mn, Co, Ni, Cu, Cd, Pb from seawater, using a Nobias-chelate PA1 chelating resin (Hitachi High-Technologies). This system allowed the saline matrix to be separated while simultaneously pre-concentrating the analytes of interest. The aliquots of concentrated analyte were then analysed off-line by SF-ICP-MS (Sector Field-Inductively Coupled Plasma-Mass Spectrometry). We chose to develop an off-line extraction manifold as a means to build a relatively simple device and reduce the running time and costs associated with SF-ICP-MS analysis. The extraction manifold was built with valves, peristaltic pumps, tubing and electronics, which are all commercially available, easy to connect, and controlled using a user-friendly computer program. This method allows the extraction of 12 samples in one automated sequence, a number, which can be upgraded with further modification/adaption. In a working day, 3 to 4 automated sequences can be processed, leading to the extraction of 2 to 3 oceanographic stations consisting of samples collected from 12 depths. The cost of the manifold does not exceed 10,000 euros (14,000 AUD), which is comparatively low for specialised scientific equipment. Our system can be adapted for use at sea to extract seawater directly after sampling, with subsequent ICP-MS analysis upon return to shore. We successfully measured Mn, Co, Ni, Cu, Cd and Pb concentrations in 176

samples for the KEOPS2 study in 3 weeks. We achieved good consistency with reference seawater samples, which were measured daily to assess the accuracy of the measurement, while in-house seawater aliquots were used to assess the precision of the analysis typically < 5 % for all the studied elements, except Co (8 %). With regards to Fe determination, using this method, standard addition calibrations were not reliable and the analysis of reference material showed that measurements were precise but not accurate. The loss of accuracy was probably due to Fe organic complexation during the calibration.

2 Trace metal concentrations around Kerguelen Islands

In the framework of the KEOPS2 project, dissolved Fe concentrations were measured in the vicinity of the Kerguelen Islands using flow injection analysis. Concentrations ranged from 0.06 nmol L^{-1} in offshore, Southern Ocean waters, to values as high as 3.82 nmol L^{-1} within Hillsborough Bay, on the north-eastern coast of Kerguelen Island. The new analytical method that was developed during this PhD work allowed us to measure the concentrations of other trace metals (Mn, Co, Ni, Cu, Cd, Pb) in the same samples, in order to better constrain the trace metal sources in this complex area. Only dFe, dCo and dMn have previously been studied in the Kerguelen area: Fe during ANTARES3 (October-November 1995) and KEOPS1 (January-February 2005) (Bucciarelli et al., 2001; Blain et al., 2008b), Mn during ANTARES3 (Bucciarelli et al., 2001). and Co during KEOPS1 (Bown et al., 2012). In the Southern Ocean, other areas potentially influenced by the island mass effect were studied. Around the Crozet Island during CROZEX, dFe (Planquette et al., 2007) and dMn, dCo, dNi, dCd, dPb (Castrillejo et al., 2013) were all studied. In the vicinity of the South Shetlands islands, dFe (Ardelan et al., 2010; Nielsdóttir et al., 2012; Hatta et al., 2013; Measures et al., 2013) and dMn (Hatta et al., 2013; Measures et al., 2013) were studied. During KEOPS2, dFe ranges in the different cluster were in agreement with the ranges observed previously in the Kerguelen, Crozet or South Shetland areas, except during ANTARES3. Indeed during ANTARES3 higher dFe concentrations were observed potentially due to methodological differences (Blain et al., 2008b). During this study, the same dCo range was observed as found during KEOPS1 (Bown et al., 2012) while around Crozet Island the observed concentrations were significantly lower due to the lack of island inputs off shore (Castrillejo et al., 2013). Similar to dFe, lower dMn ranges were observed compared to ANTARES3 (Bucciarelli et al., 2001). On the contrary, the observed dMn ranges during this study was

higher than previously observed in the Southern Ocean (Middag et al., 2011a; Boyé et al., 2012; Middag et al., 2012; Castrillejo et al., 2013; Hatta et al., 2013) due to the high dMn concentrations observed in the coastal area, however, the lowest dMn concentrations was in agreement with the previously published studies in the Southern Ocean (Middag et al., 2011a; Middag et al., 2012; Castrillejo et al., 2013; Hatta et al., 2013; Measures et al., 2013).

Around Kerguelen island, the same dCd, dNi and dPb range has been observed as measured around Crozet Island previously (Castrillejo et al., 2013).

3 Trace metal sources around Kerguelen Islands

3.1 Atmospheric inputs

While Bucciarelli et al. (2001) and Heimburger et al. (2012) revealed that atmospheric deposition could be an important source of Fe, Blain et al. (2008b) and Wagener et al. (2008) showed that during KEOPS1 atmospheric inputs were not significant. In the present study, surface dFe maximum were observed in the recirculation and North Polar Front areas. At some sampling stations, computed air mass trajectories indicated a plausible impact of the island on the air mass composition above the sampling site (Quéroué et al., 2015). However, the lack of surface pAl maximum (van der Merwe et al., 2014) and the low dMn surface concentrations found in samples collected in this study, proxies of atmospheric inputs, indicated that the dFe maximum could not be linked to atmospheric inputs. Atmospheric deposition was not considered to be a significant source of Fe for fertilizing the spring phytoplankton bloom. This might be due to the frequent rain event that occurred on the island before and during the cruise, which humidified the island soil and decrease the amount of soil particles released in the atmosphere.

3.2 KEOPS2 meltwater inputs and subsequent lateral advection

As suggested by Bucciarelli et al. (2001), the surface dFe maximum observed in the recirculation and the North Polar Front areas could be due to lateral advection of enriched water from the northern Kerguelen Plateau. In this study, the combination of direct island run-off, melting of seasonal ice and sediment resuspension were all sources of dFe and dMn to the northern plateau. The gradient of LSi and dFe concentrations from TEW-1 to TEW-2 in addition to the gradient of salinity suggested freshwater inputs from the Cook Glacier. This large glacier, of approximately 500 km^2, on Kerguelen Island, discharges part of its meltwaters into Hillsborough Bay, subsequently enhancing dFe concentrations in the nearby

ocean. The combination of high LSi, high dFe and high dMn concentrations suggested also potential inputs from sediment resuspension. In addition, the highest dNi and dCo concentrations were observed locally. Furthermore, out of the Kerguelen Plateau and the coastal area, surface dFe, dCo and dNi maxima were observed. Atmospheric inputs were shown to be negligible so lateral advection of water masses from the coastal area was likely a source of dissolved TM out of the plateau. The analysis of drifter trajectories released west of the Kerguelen Island (Zhou et al., 2014) showed that water masses were flowing north of the island, eventually reaching the polar front (PF). Moreover, short half-life Ra isotope studies (Sanial et al., 2014) have revealed that water masses can be transported across the PF. van der Merwe et al. (2014) also showed that above the mixed layer, lateral advection of small particles from glacial flour from either Kerguelen Island or Heard Island can remain suspended in surface water for up to more than 800 days, enough to be transported and mixed into the PF. Even if the PF can rapidly dilute dTM inputs, these inputs from the coastal area may remain important locally where water masses cross the PF.

3.3 Sediment inputs

Over the Kerguelen Plateau and in the coastal area, sediment resuspension is also a possible source of dFe and dMn. During KEOPS2 high dFe and dMn concentrations were observed close to the seafloor, as was noted during ANTARES3 (dFe and dMn) (Bucciarelli et al., 2001) and KEOPS1 (dFe)(Blain et al., 2008b). The observed dFe concentrations over the plateau were higher during KEOPS2 than KEOPS1 showing that the input of dFe estimated during KEOPS1 may have been underestimated or that this input is temporally variable. In addition, the 3 stations sampled over the plateau showed different dFe and dMn concentrations in samples collected close to the seafloor. The highest concentrations were observed at the station showing evidence of more intense sediment resuspension (A3-2), as shown by higher beam attenuation coefficient at A3 than at the other stations from the plateau. This clearly shows that sediment resuspension is not homogenous over the Kerguelen Plateau, therefore leading to large standard deviations on the Fe flux estimated for this source (Bowie et al., 2014). Variability might be due to different processes within the sediment, as at A3, reductive dissolution has been observed (P. Anschutz, personal communication, 2014) but no observation has been made at other plateau stations. The composition of the sediment may also be different. At R-2, open ocean station, high LSi, pAl, pFe and pMn has been observed at the same depth as the high dFe and dMn concentration, which seems to indicate a

potential source from sediment input. Indeed, The Leclaire Rise, a submerged volcano, may be a source of dissolved and particulate material as it is located only 75 km north west from R-2. This small and shallow plateau of about 6500 km^2 showed a shallowest bathymetry of about 100 m and is partially located South of the PF allowing water masses to interact with the plateau and its slopes, enhancing the TM dissolved and particulate phases before to be transported to R-2.

3.4 Remineralization

The remineralization of sinking particles has been showed to be a source of TM. The lack of relationships of dMn and dCo with phosphate in deep water showed that these two TM distributions in deep water was more influenced by external sources than by remineralization. At R-2, in the mesopelagic zone, dFe, dNi, dCu and dCd showed increasing concentrations with depth. At R-2, where the highest remineralization rate has been observed Twining and Baines (2013), the significant relationship of dFe with AOU showed that remineralization may explain the dFe increase to depths up to 500 m, and confirms that sedimentary inputs may also enhance the dFe concentrations at this station. The ratios of the dissolved metal:phosphate were within the ranges of the ratios of metal quotas calculated by (Jacquet et al., 2014), confirming that this station was not impacted by external sources for these trace metals and that their distributions at this open ocean station was mainly driven by biological uptake and remineralization in this cluster. Dissolved Fe showed also significant relationships with AOU in the recirculation and the North Polar Front areas showing that remineralization was controlling the dFe distribution at depth. Amongst the other studied trace metal of this study, only dCd showed significant relationship with phosphate at station from a different cluster than R-2 and notably in the recirculation area, showing that dCd vertical profiles are mainly impacted by uptake and remineralization. Jacquet et al. (2014) showed that during KEOPS2, the POC remineralization rate was significant but variable which might explain the variable dFe, dNi, dCu and dCd profiles in the mesopelagic zone.

4 Directions for Future Research

4.1 Methodological advances

Recently an extraction system utilising the same resin as considered in this study and able to be set up in-line with ICP-MS instrumentation has become commercially available (seaFAST S2, Elemental Scientific) (Lagerstrom et al., 2013). This commercially available

instrument is more expensive (3 to 4 fold) and when used in-line requires more ICP-MS operational time. However, this system offers a number of advantages including the use of lower sample volumes, it automatically adjusts the pH for extraction it uses syringe pumps for more precise mixing of the reagents for better control in the delivery of buffer, samples and reagents (and hence in-line pH adjustments), it reduces sample handling, and provides samples with a higher concentration factor. The technological advances developed in both of these systems represent the next step to automation of micronutrients analysers and is a great tool to achieve the GEOTRACES goals.

The method developed here allows the analysis of multiple TMs of interest in a short period of time. Today, the commercially available system allows for the same output. However in both systems, the amount of buffer added to the sample needs to be verified and adjusted manually. In the future, it would be beneficial to have pH microelectrodes incorporated to record the sample pH deviation occurring with time and able to adjust the added buffer automatically, to provide a fully automated extraction system. In addition, before sample extraction, the manifold could be modified to add an online UV-digestion step. This step would require a fine setup of the timing parameters to allow the complete release of trace metal from organic matter and cooling of the sample before extraction.

The core of the developed analytical method is the extraction column. Most of the studied TMs except Cu and Fe can be extracted at seawater pH so the sample extraction could be achieved directly on the sampling device. The column could be rinsed after extraction, stored and later plugged to the analytical device for elution of the TMs from the column and analysis by multi-element techniques such as SF-ICP-MS. If storage within a column is possible, an autonomous in situ seawater sampler could be developed in order to increase the spatial and temporal resolution of the TM studies.

4.2 TM cycles

This study focused on Fe, Mn, Co, Ni, Cu, Cd and Pb concentrations in the dissolved phase. The developed analytical technologies can be used to further study the physical speciation of TMs using this method to study the soluble fraction obtained after filtration on 0.02 µm filter. Such observation is particularly relevant as the soluble fraction is supposed to be the more bioavailable fraction due to its nutrient like profiles notably for Fe (Chen and Wang, 2001; Wu et al., 2001; Bergquist et al., 2007; Chever et al., 2010a). The determination of the repartition of TMs within the different phases of the physical speciation spectrum is

critical to understand the pathways between the different phases and fully understand the influence of the TMs sources and sinks on the TMs bioavailability.

Sediment resuspension, meltwater inputs, atmospheric dust deposition or other particle sources (e.g. whale faeces (Ratnarajah et al., 2014)) enhance dissolved TM concentrations in seawater directly and/or after dissolution/extraction, which occurs at different rate and magnitude. This suggests that the bioactive TM distributions in surface water are influenced by the TM concentrations in the source media. It would be beneficial for phytoplankton culture experiments to be conducted according to observed field concentrations and/or simulating new sources of TMs, either directly dissolved in seawater or as particles. Such experiments could determine the solubility of these particles in the ocean and their potential impact on dissolved TMs concentration over time in presence of biological activity. The impact of the phytoplankton on the solubility, organic speciation and bioavailability of TMs could be assessed. This is particularly relevant as Fourquez et al. (2014) showed that at the onset of the bloom heterotrophic bacteria Fe uptake was 1-2 % to total Fe uptake due to competition with small size phytoplankton cells while at the late stage of the bloom, when phytoplankton cell shifted to larger sizes (Quéguiner, 2013), it represented 17-27 % of the total Fe uptake (Sarthou et al., 2008).

It is also important to model the possible impact of climate change on the delivery and abundance of TMs from Southern Ocean landmasses such as the Kerguelen Plateau. Indeed in the case of warming of the Kerguelen Plateau area and glacial retreat, the meltwater source of TMs might decrease, which will decrease the horizontal input of dFe out of the plume and could rapidly decrease the magnitude of the Kerguelen phytoplankton bloom. However this ice retreat will show more ice free soil to the prevailing Westerlies, which might increase the atmospheric dust inputs. Antarctica could be an important source of meltwaters in the case of global warming, which might lead to important Southern Ocean fertilisation due to the seasonal continental ice melt such as observed around Kerguelen Island.

To better assess the biogeochemical cycles of TMs and their impact on primary production in the World's ocean, this PhD work will be followed and built upon by the postdoctoral studies of three other biogeochemically different regions of the World's oceans. Firstly, the GEOTRACES GP13 section along an east-to-west transect from Australia to New Zealand will allow us to examine the possible continental source of TMs from the Australian deserts. This transect also crossed the Kermadec Trench, which might reveal potential deep water TMs enhancement via hydrothermal sources. Furthermore the Pandora study of the

different veins of current flowing in and out of the Solomon Sea will help to determine the Equatorial Pacific fertilization mechanisms. Indeed water masses entering the Solomon Sea interact with land masses formed by the Papua New Guinea coastline and the Solomon Islands and might be a significant source of dissolved and particulate TMs for the Equatorial Pacific, a HNLC area by lateral advection via the Equatorial Undercurrent (Slemons et al., 2009; Radic et al., 2011). Finally, the GEOVIDE study will focus on the distribution of TMs in the North Atlantic, an area where sources are expected to be widely contrasting. The North Atlantic is a key region for Earth climate and oceanic circulation, being a major area of the Meridional Overturning Circulation, which characteristics and variability have been studied since 2002. GEOVIDE aims to better constrain (i) the uncertainties on water and heat fluxes, notably by adding new tracers and information on export and circulation of deep waters, and (ii) the biogeochemical fluxes and processes impacting TMs in this region to better determine their impact on the primary production in this ocean. These studies will be part of the GEOTRACES program. One of the forthcoming GEOTRACES process study, Shelf Sea Biogeochemistry, will focus on TM cycles in shelf environment within the next two years with 3 legs in the Celtic sea. This program will help to better understand the processes involved in the TM cycles and their impact on open ocean TM cycles. The aims are to understand the effect of coastal and shelf seas sediment and pore-water advection effects have on nutrient fluxes to the overlying water and any subsequent impact on water chemistry and thus primary production using in situ fieldwork, laboratory work and modelling. The results of this project will be particularly interesting for areas subject to coastal or shelf influences such as the Kerguelen plateau.

References

Abouchami, W., Galer, S. J. G., de Baar, H. J. W., Alderkamp, A. C., Middag, R., Laan, P., Feldmann, H., and Andreae, M. O.: Modulation of the Southern Ocean cadmium isotope signature by ocean circulation and primary productivity, Earth and Planetary Science Letters, 305, 83-91, http://dx.doi.org/10.1016/j.epsl.2011.02.044, 2011.

Abouchami, W., Galer, S. J. G., de Baar, H. J. W., Middag, R., Vance, D., Zhao, Y., Klunder, M., Mezger, K., Feldmann, H., and Andreae, M. O.: Biogeochemical cycling of cadmium isotopes in the Southern Ocean along the Zero Meridian, Geochimica et Cosmochimica Acta, 127, 348-367, http://dx.doi.org/10.1016/j.gca.2013.10.022, 2014.

Achterberg, E. P., Braungardt, C. B., Sandford, R. C., and Worsfold, P. J.: UV digestion of seawater samples prior to the determination of copper using flow injection with chemiluminescence detection, Analytica Chimica Acta, 440, 27-36, 2001.

Aguilar-Islas, A. M., and Bruland, K. W.: Dissolved manganese and silicic acid in the Columbia River plume: A major source to the California current and coastal waters off Washington and Oregon, Marine Chemistry, 101, 233-247, 2006.

Alderkamp, A.-C., Mills, M. M., van Dijken, G. L., Laan, P., Thuróczy, C.-E., Gerringa, L. J. A., de Baar, H. J. W., Payne, C. D., Visser, R. J. W., Buma, A. G. J., and Arrigo, K. R.: Iron from melting glaciers fuels phytoplankton blooms in the Amundsen Sea (Southern Ocean): Phytoplankton characteristics and productivity, Deep Sea Research Part II: Topical Studies in Oceanography, 71–76, 32-48, http://dx.doi.org/10.1016/j.dsr2.2012.03.005, 2012.

Aminot, A., and Kérouel, R.: Dosage automatique des nutriments dans les eaux marines: méthodes en flux continu, Editions Quae, 2007.

Anderson, R. F., Henderson, G. M., Adkins, J., Andersson, P., Eisenhauer, A., Frank, M., and Oschlies, A.: GEOTRACES-An international study of the global marine biogeochemical cycles of trace elements and their isotopes, Chemie der Erde-Geochemistry, 67, 85-131, 2007.

Annett, A. L., Lapi, S., Ruth, T. J., and Maldonado, M. T.: The effects of Cu and Fe availability on the growth and Cu:C ratios of marine diatoms, Limnology and Oceanography, 53, 2451-2461, 10.4319/lo.2008.53.6.2451, 2008.

Aparicio-González, A., Duarte, C. M., and Tovar-Sánchez, A.: Trace metals in deep ocean waters: A review, Journal of Marine Systems, 100–101, 26-33, http://dx.doi.org/10.1016/j.jmarsys.2012.03.008, 2012.

Ardelan, M. V., Holm-Hansen, O., Hewes, C. D., Reiss, C. S., Silva, N. S., Dulaiova, H., Steinnes, E., and Sakshaug, E.: Natural iron enrichment around the Antarctic Peninsula in the Southern Ocean, Biogeosciences, 7, 11-25, 10.5194/bg-7-11-2010, 2010.

Armand, L. K., Cornet-Barthaux, V., Mosseri, J., and Quéguiner, B.: Late summer diatom biomass and community structure on and around the naturally iron-fertilised Kerguelen

Plateau in the Southern Ocean, Deep Sea Research Part II: Topical Studies in Oceanography, 55, 653-676, 2008.

Baars, O., and Croot, P. L.: Comparison of Alternate Reactants for pM Level Cobalt Analysis in Seawater by the Use of Catalytic Voltammetry, Electroanalysis, 23, 1663-1670, 2011.

Baars, O., Abouchami, W., Galer, S. J. G., Boye, M., and Croot, P. L.: Dissolved cadmium in the Southern Ocean: Distribution, speciation, and relation to phosphate, Limnol. Oceanogr, 59, 385-399, 2014.

Baker, A. R., and Jickells, T. D.: Mineral particle size as a control on aerosol iron solubility, Geophysical Research Letters, 33, L17608-L17608, 2006.

Baker, A. R., Jickells, T. D., Witt, M., and Linge, K. L.: Trends in the solubility of iron, aluminium, manganese and phosphorus in aerosol collected over the Atlantic Ocean, Marine Chemistry, 98, 43-58, 2006.

Barbeau, K., Moffet, J. W., Caron, D. A., Croot, P. L., and Erdner, D. L.: Role of protozoan grazing in relieving iron limitation of phytoplankton, Nature, 380, 61-64, 1996.

Barbeau, K., Kujawinski, E. B., and Moffett, J. W.: Remineralization and recycling of iron, thorium and organic carbon by heterotrophic marine protists in culture, Aquatic Microbial Ecology, 24, 69-81, 2001.

Beard, B. L., Johnson, C. M., Von Damm, K. L., and Poulson, R. L.: Iron isotope constraints on Fe cycling and mass balance in oxygenated Earth oceans, Geology, 31, 629-632, 2003.

Bennett, S. A., Achterberg, E. P., Connelly, D. P., Statham, P. J., Fones, G. R., and German, C. R.: The distribution and stabilisation of dissolved Fe in deep-sea hydrothermal plumes, Earth and Planetary Science Letters, 270, 157-167, 2008.

Bergquist, B. A., Wu, J., and Boyle, E. A.: Variability in oceanic dissolved iron is dominated by the colloidal fraction, Geochimica et Cosmochimica Acta, 71, 2960-2974, http://dx.doi.org/10.1016/j.gca.2007.03.013, 2007.

Bertrand, E. M., Saito, M. A., Rose, J. M., Riesselman, C. R., Lohan, M. C., Noble, A. E., Lee, P. A., and DiTullio, G. R.: Vitamin B-12 and iron colimitation of phytoplankton growth in the Ross Sea, Limnology And Oceanography, 52, 1079-1093, 2007.

Bhatia, M. P., Kujawinski, E. B., Das, S. B., Breier, C. F., Henderson, P. B., and Charette, M. A.: Greenland meltwater as a significant and potentially bioavailable source of iron to the ocean, Nature Geoscience, 6, 274-278, 2013.

Biller, D. V., and Bruland, K. W.: Analysis of Mn, Fe, Co, Ni, Cu, Zn, Cd, and Pb in seawater using the Nobias-chelate PA1 resin and magnetic sector inductively coupled plasma mass spectrometry (ICP-MS), Marine Chemistry, 130-131, 12-20, 2012.

Biller, D. V., and Bruland, K. W.: Sources and distributions of Mn, Fe, Co, Ni, Cu, Zn, and Cd relative to macronutrients along the central California coast during the spring and summer upwelling season, Marine Chemistry, 155, 50-70, http://dx.doi.org/10.1016/j.marchem.2013.06.003, 2013.

Blain, S., Quéguiner, B., Armand, L., Belviso, S., Bombled, B., Bopp, L., Bowie, A., Brunet, C., Brussaard, C., Carlotti, F., Christaki, U., Corbière, A., Durand, I., Ebersbach, F., Fuda, J.-L., Garcia, N., Gerringa, L., Griffiths, B., Guigue, C., Guillerm, C., Jacquet, S., Jeandel, C., Laan, P., Lefèvre, D., Lomonaco, C., Malits, A., Mosseri, J., Obernosterer, I., Park, Y.-H., Picheral, M., Pondaven, P., Remenyi, T., Sandroni, V., Sarthou, G., Savoye, N., Scouarnec, L., Souhaut, M., Thuiller, D., Timmermans, K., Trull, T., Uitz, J., van Beek, P., Veldhuis, M., Vincent, D., Viollier, E., Vong, L., and Wagener, T.: Effect of natural iron fertilisation on carbon sequestration in the Southern Ocean, Nature, 446, 1070-1075, 2007.

Blain, S., Quéguiner, B., and Trull, T.: The natural iron fertilization experiment KEOPS (KErguelen Ocean and Plateau compared Study): An overview, Deep Sea Research Part II: Topical Studies in Oceanography, 55, 559-565, http://dx.doi.org/10.1016/j.dsr2.2008.01.002, 2008a.

Blain, S., Sarthou, G., and Laan, P.: Distribution of dissolved iron during the natural iron-fertilization experiment KEOPS (Kerguelen Plateau, Southern Ocean), Deep Sea Research Part II: Topical Studies in Oceanography, 55, 594-605, http://dx.doi.org/10.1016/j.dsr2.2007.12.028, 2008b.

Blain, S., Trull, T., and d'Ovidio, F.: KEOPS2 study overview, Biogeosciences Discuss., in prep.

Bonnet, S., and Guieu, C.: Dissolution of atmospheric iron in seawater, Geophysical Research Letters, 31, doi:10.1029/2003GL018423, 2004.

Bowie, A. R., Achterberg, E. P., Mantoura, R. F. C., and Worsfold, P. J.: Determination of sub-nanomolar levels of iron in seawater using flow injection with chemiluminescence detection, Analytica Chimica Acta, 361, 189-200, 1998.

Bowie, A. R., Achterberg, E. P., Ussher, S., and Worsfold, P. J.: Design of an automated flow injection-chemiluminescence instrument incorporating a miniature photomultiplier tube for monitoring picomolar concentrations of iron in seawater, Journal Of Automated Methods And Management In Chemistry, 37-43, 2005.

Bowie, A. R., Lannuzel, D., Remenyi, T. A., Wagener, T., Lam, P. J., Boyd, P. W., Guieu, C., Townsend, A. T., and Trull, T. W.: Biogeochemical iron budgets of the Southern Ocean south of Australia: Decoupling of iron and nutrient cycles in the subantarctic zone by the summertime supply, Global Biogeochemical Cycles, 23, 10.1029/2009GB003500, 2009.

Bowie, A. R., van der Merwe, P., Quéroué, F., Trull, T., Fourquez, M., Planchon, F., Sarthou, G., Chever, F., Townsend, A. T., and Obernosterer, I.: Iron budgets for three distinct biogeochemical sites around the Kerguelen archipelago (Southern Ocean) during the natural fertilisation experiment KEOPS-2, Biogeosciences Discussions, 11, 17861-17923, 2014.

Bown, J., Boye, M., Baker, A., Duvieilbourg, E., Lacan, F., Le Moigne, F., Planchon, F., Speich, S., and Nelson, D. M.: The biogeochemical cycle of dissolved cobalt in the Atlantic and the Southern Ocean south off the coast of South Africa, Marine Chemistry, 126, 193-206, http://dx.doi.org/10.1016/j.marchem.2011.03.008, 2011.

Bown, J., Boye, M., Laan, P., Bowie, A. R., Park, Y. H., Jeandel, C., and Nelson, D. M.: Imprint of a dissolved cobalt basaltic source on the Kerguelen Plateau, Biogeosciences, 9, 2012.

Boyd, P. W., Jickells, T., Law, C. S., Blain, S., Boyle, E. A., Buesseler, K. O., Coale, K. H., Cullen, J. J., de Baar, H. J. W., Follows, M., Harvey, M., Lancelot, C., Levasseur, M., Owens, N. P. J., Pollard, R., Rivkin, R. B., Sarmiento, J., Schoemann, V., Smetacek, V., Takeda, S., Tsuda, A., Turner, S., and Watson, A. J.: Mesoscale iron enrichment experiments 1993-2005: Synthesis and future directions, Science, 315, 612-617, 2007.

Boyd, P. W., and Ellwood, M. J.: The biogeochemical cycle of iron in the ocean, Nature Geoscience, 3, 675-682, 2010.

Boyd, P. W., Mackie, D. S., and Hunter, K. A.: Aerosol iron deposition to the surface ocean — Modes of iron supply and biological responses, Marine Chemistry, 120, 128-143, http://dx.doi.org/10.1016/j.marchem.2009.01.008, 2010.

Boyé, M., Wake, B. D., Garcia, P. L., Bown, J., Baker, A. R., and Achterberg, E. P.: Distributions of dissolved trace metals (Cd, Cu, Mn, Pb, Ag) in the southeastern Atlantic and the Southern Ocean, Biogeosciences, 9, 3231-3246, 2012.

Boyle, E. A., Sherrell, R. M., and Bacon, M. P.: Lead Variability in the Western North-Atlantic Ocean and Central Greenland Ice - Implications for the Search for Decadal Trends in Anthropogenic Emissions, Geochimica Et Cosmochimica Acta, 58, 3227-3238, 1994.

Boyle, E. A.: Anthropogenic trace elements in the ocean, Marine Ecological Processes: A derivative of the Encyclopedia of Ocean Sciences, 162-169, 2001.

Boyle, E. A., Bergquist, B. A., Kayser, R. A., and Mahowald, N.: Iron, manganese, and lead at Hawaii Ocean Time-series station ALOHA: Temporal variability and an intermediate water hydrothermal plume, Geochimica Et Cosmochimica Acta, 69, 933-952, 2005.

Boyle, E. A., Lee, J.-M., Echegoyen, Y., Noble, A., Moos, S., Carrasco, G., Zhao, N., Kayser, R., Zhang, J., and Gamo, T.: Anthropogenic Lead Emissions in the Ocean, Oceanography, 69, 2014.

Brand, L. E., Sunda, W. G., and Guillard, R. R. L.: Reduction of Marine-Phytoplankton Reproduction Rates by Copper and Cadmium, Journal of Experimental Marine Biology and Ecology, 96, 225-250, 1986.

Brown, M. T., and Bruland, K. W.: An improved flow-injection analysis method for the determination of dissolved aluminum in seawater, Limnology and Oceanography-Methods, 6, 87-95, 2008.

Bruland, K. W., Franks, R. P., Knauer, G. A., and Martin, J. H.: Sampling and analytical methods for the determination of copper, cadmium, zinc, and nickel at the nanogram per liter level in sea water, Analytica Chimica Acta, 105, 233-245, 1979.

Bruland, K. W., and Lohan, M. C.: Controls of Trace Metals in Seawater, in: Treatise on Geochemistry, edited by: Elderfield, H., Elsevier Ltd., 23-47, 2003.

Bucciarelli, E., Blain, S., and Treguer, P.: Iron and manganese in the wake of the Kerguelen Islands (Southern Ocean), Marine Chemistry, 73, 21-36, 2001.

Butler, E. C. V., O'Sullivan, J. E., Watson, R. J., Bowie, A. R., Remenyi, T. A., and Lannuzel, D.: Trace metals Cd, Co, Cu, Ni, and Zn in waters of the subantarctic and Polar Frontal Zones south of Tasmania during the 'SAZ-Sense' project, Marine Chemistry, 148, 63-76, http://dx.doi.org/10.1016/j.marchem.2012.10.005, 2013.

Byrne, R. H., Kump, L. R., and Cantrell, K. J.: The influence of temperature and pH on trace metal speciation in seawater, Marine Chemistry, 25, 163-181, 1988.

Byrne, R. H.: Inorganic speciation of dissolved elements in seawater: the influence of pH on concentration ratios, Geochemical Transactions, 2, 11, 2002.

Cameron, V., and Vance, D.: Heavy nickel isotope compositions in rivers and the oceans, Geochimica et Cosmochimica Acta, 128, 195-211, http://dx.doi.org/10.1016/j.gca.2013.12.007, 2014.

Capodaglio, G., Coale, K. H., and Bruland, K. W.: Lead Speciation in Surface Waters of the Eastern North Pacific, Marine Chemistry, 29, 221-233, 1990.

Castrillejo, M., Statham, P. J., Fones, G. R., Planquette, H., Idrus, F., and Roberts, K.: Dissolved trace metals (Ni, Zn, Co, Cd, Pb, Al, and Mn) around the Crozet Islands, Southern Ocean, Journal of Geophysical Research: Oceans, 118, 5188-5201, 10.1002/jgrc.20359, 2013.

Chase, Z., and Price, N. M.: Metabolic consequences of iron deficiency in heterotrophic marine protozoa, Limnology and Oceanography, 42, 1673-1684, 1997.

Chen, M., and Wang, W.-X.: Bioavailability of natural colloid-bound iron to marine plankton: Influences of colloidal size and aging, Limnology and Oceanography, 46, 1956-1967, 2001.

Chester, R.: Marine Geochemistry, Academic Division of Unwin Hyman Ltd, London, 1990.

Chester, R.: Marine geochemistry, John Wiley & Sons, 2009.

Chever, F., Bucciarelli, E., Sarthou, G., Speich, S., Arhan, M., Penven, P., and Tagliabue, A.: Physical speciation of iron in the Atlantic sector of the Southern Ocean along a transect from the subtropical domain to the Weddell Sea Gyre, Journal Of Geophysical Research-Oceans, 115, C10059-C10059, 2010a.

Chever, F., Sarthou, G., Bucciarelli, E., Blain, S., and Bowie, A. R.: An iron budget during the natural iron fertilisation experiment KEOPS (Kerguelen Islands, Southern Ocean), Biogeosciences, 7, 455-468, 2010b.

Chisholm, S. W.: Stirring times in the Southern Ocean, Nature, 407, 685-687, 2000.

Coale, K. H., Johnson, K. S., Fitzwater, S. E., Blain, S. P. G., Stanton, T. P., and Coley, T. L.: IronEx-I, an in situ iron-enrichment experiment: Experimental design, implementation and results, Deep-Sea Research Part II-topical Studies In Oceanography, 45, 919-945, 1998.

Conway, T. M., and John, S. G.: Quantification of dissolved iron sources to the North Atlantic Ocean, Nature, 511, 212-215, 2014.

Conway, T. M., and John, S. G.: Biogeochemical cycling of cadmium isotopes along a high-resolution section through the North Atlantic Ocean, Geochimica et Cosmochimica Acta, 148, 269-283, http://dx.doi.org/10.1016/j.gca.2014.09.032, 2015.

Ćosović, B., Degobbis, D., Bilinski, H., and Branica, M.: Inorganic cobalt species in seawater, Geochimica et Cosmochimica Acta, 46, 151-158, http://dx.doi.org/10.1016/0016-7037(82)90242-3, 1982.

Croft, M. T., Lawrence, A. D., Raux-Deery, E., Warren, M. J., and Smith, A. G.: Algae acquire vitamin B12 through a symbiotic relationship with bacteria, Nature, 438, 90-93, 2005.

Croot, P. L.: Rapid Determination of Picomolar Titanium in Seawater with Catalytic Cathodic Stripping Voltammetry, Analytical Chemistry, 83, 6395-6400, 2011.

Cullen, J. T., Chase, Z., Coale, K. H., Fitzwater, S. E., and Sherrell, R. M.: Effect of iron limitation on the cadmium to phosphorus ratio of natural phytoplankton assemblages from the Southern Ocean, Limnology And Oceanography, 48, 1079-1087, 2003.

Cullen, J. T.: On the nonlinear relationship between dissolved cadmium and phosphate in the modern global ocean: Could chronic iron limitation of phytoplankton growth cause the kink?, Limnology And Oceanography, 51, 1369-1380, 2006.

Cullen, J. T., and Maldonado, M. T.: Biogeochemistry of cadmium and its release to the environment, in: Cadmium: From Toxicity to Essentiality, Springer, 31-62, 2013.

Cutter, G., Anderson, P., Codispoti, L., Croot, P., Francois, R., Lohan, M., Obata, H., and Rutgers van der Loeff, M.: Sampling and Sample-handling Protocols for GEOTRACES Cruises, 2010.

Cutter, G. A., and Bruland, K. W.: Rapid and noncontaminating sampling system for trace elements in global ocean surveys, Limnology And Oceanography-Methods, 10, 425-436, 2012.

Cutter, G. A.: Intercalibration in chemical oceanography-Getting the right number, Limnol. Oceanogr.: Methods, 11, 418-424, 2013.

d'Ovidio, F., Della Penna, A., Trull, T. W., Nencioli, F., Pujol, I., Rio, M. H., Park, Y. H., Cotté, C., Zhou, M., and Blain, S.: The biogeochemical structuring role of horizontal stirring: Lagrangian perspectives on iron delivery downstream of the Kerguelen plateau, Biogeosciences Discussions, 12, 779-814, 2015.

de Baar, H. J. W., Saager, P. M., Nolting, R. F., and van der Meer, J.: Cadmium versus phosphate in the world ocean, Marine Chemistry, 46, 261-281, http://dx.doi.org/10.1016/0304-4203(94)90082-5, 1994.

de Baar, H. J. W., de Jong, J. T. M., Bakker, D. C. E., Löscher, B. M., Veth, C., Bathmann, U., and Smetacek, V.: Importance of iron for plankton blooms and carbon dioxide drawdown in the Southern Ocean, Nature, 373, 412-415, 1995.

de Baar, H. J. W., and de Jong, J. T. M.: Distributions, sources and sinks of iron in seawater, in: The biogeochemistry of iron in seawater, edited by: Turner, D. R., and Hunter, K. A., SCOR-IUPAC, Baltimore, 123-253, 2001.

de Baar, H. J. W., Boyd, P. W., Coale, K. H., Landry, M. R., Tsuda, A., Assmy, P., Bakker, D. C. E., Bozec, Y., Barber, R. T., Brzezinski, M. A., Buesseler, K. O., Boye, M., Croot, P. L., Gervais, F., Gorbunov, M. Y., Harrison, P. J., Hiscock, W. T., Laan, P., Lancelot, C., Law, C. S., Levasseur, M., Marchetti, A., Millero, F. J., Nishioka, J., Nojiri, Y., van Oijen, T., Riebesell, U., Rijkenberg, M. J. A., Saito, H., Takeda, S., Timmermans, K. R., Veldhuis, M. J. W., Waite, A. M., and Wong, C. S.: Synthesis of iron fertilization experiments: From the iron age in the age of enlightenment, Journal Of Geophysical Research-Oceans, 110, C09S16-C09S16, 2005.

de Baar, H. J. W., Gerringa, L. J. A., Laan, P., and Timmermans, K. R.: Efficiency of carbon removal per added iron in ocean iron fertilization, Marine Ecology-progress Series, 364, 269-282, 2008a.

de Baar, H. J. W., Timmermans, K. R., Laan, P., De Porto, H. H., Ober, S., Blom, J. J., Bakker, M. C., Schilling, J., Sarthou, G., Smit, M. G., and Klunder, M.: Titan: A new facility for ultraclean sampling of trace elements and isotopes in the deep oceans in the international Geotraces program, Marine Chemistry, 111, 4-21, 2008b.

de Jong, J., Schoemann, V., Maricq, N., Mattielli, N., Langhorne, P., Haskell, T., and Tison, J.-L.: Iron in land-fast sea ice of McMurdo Sound derived from sediment resuspension and wind-blown dust attributes to primary productivity in the Ross Sea, Antarctica, Marine Chemistry, 157, 24-40, http://dx.doi.org/10.1016/j.marchem.2013.07.001, 2013.

Degens, E. T., Kempe, S., and Richey, J. E.: SCOPE 42: Biogeochemistry of major world rivers, UK: Wiley, 1991.

Desboeufs, K. V., Losno, R., and Colin, J. L.: Factors influencing aerosol solubility during cloud processes, Atmospheric Environment, 35, 3529-3537, http://dx.doi.org/10.1016/S1352-2310(00)00472-6, 2001.

Desboeufs, K. V., Sofikitis, A., Losno, R., Colin, J. L., and Ausset, P.: Dissolution and solubility of trace metals from natural and anthropogenic aerosol particulate matter, Chemosphere, 58, 195-203, 2005.

Donat, J., and Dryden, C.: Transition metals and heavy metal speciation, Encyclopedia of Ocean Sciences, 2, 3027-3035, 2001.

Donat, J. R., Lao, K. A., and Bruland, K. W.: Speciation of Dissolved Copper and Nickel in South San-Francisco Bay - a Multimethod Approach, Analytica Chimica Acta, 284, 547-571, 1994.

Duce, R. A., Liss, P. S., Merrill, J. T., Atlas, E. L., Buat-Menard, P., Hicks, B. B., Miller, J. M., Prospero, J. M., Arimoto, R., Church, T. M., Ellis, W., Galloway, J. N., Hansen, L., Jickells, T. D., Knap, A. H., Reinhardt, K. H., Schneider, B., Soudine, A., Tokos, J. J., Tsunogai, S., Wollast, R., and Zhou, M.: The atmospheric input of trace species to the world ocean, Global Biogeochemical Cycles, 5, 193-259, 10.1029/91GB01778, 1991.

Duce, R. A., and Tindale, N. W.: Atmospheric Transport of Iron and Its Deposition In the Ocean, Limnology And Oceanography, 36, 1715-1726, 1991.

Duckworth, O., Bargar, J., and Sposito, G.: Coupled biogeochemical cycling of iron and manganese as mediated by microbial siderophores, BioMetals, 22, 605-613, 10.1007/s10534-009-9220-9, 2009.

Dulaiova, H., Ardelan, M. V., Henderson, P. B., and Charette, M. A.: Shelf-derived iron inputs drive biological productivity in the southern Drake Passage, Global Biogeochemical Cycles, 23, GB4014, 10.1029/2008GB003406, 2009.

Dulaquais, G., Boye, M., Rijkenberg, M. J. A., and Carton, X. J.: Physical and remineralization processes govern the cobalt distribution in the deep western Atlantic Ocean, Biogeosciences, 11, 1561-1580, 2014.

Durand, A., Chase, Z., Remenyi, T., and Quéroué, F.: Microplate-reader method for the rapid analysis of copper in natural waters with chemiluminescence detection, Frontiers in Microbiology, 3, DOI:10.3389/fmicb.2012.00437-DOI:00410.03389/fmicb.02012.00437, 2012.

Echegoyen, Y., Boyle, E. A., Lee, J.-M., Gamo, T., Obata, H., and Norisuye, K.: Recent distribution of lead in the Indian Ocean reflects the impact of regional emissions, Proceedings of the National Academy of Sciences, 111, 15328-15331, 2014.

Ellwood, M. J., and van den Berg, C. M. G.: Determination of organic complexation of cobalt in seawater by cathodic stripping voltammetry, Marine Chemistry, 75, 33-47, 2001.

Ellwood, M. J., van den Berg, C. M. G., Boye, M., Veldhuis, M., de Jong, J. T. M., de Baar, H. J. W., Croot, P. L., and Kattner, G.: Organic complexation of cobalt across the Antarctic Polar Front in the Southern Ocean, Marine & Freshwater Research, 56, 1069-1075, 2005.

Ellwood, M. J.: Wintertime trace metal (Zn, Cu, Ni, Cd, Pb and Co) and nutrient distributions in the Subantarctic Zone between 40–52°S; 155–160°E, Marine Chemistry, 112, 107-117, http://dx.doi.org/10.1016/j.marchem.2008.07.008, 2008.

Elrod, V. A., Berelson, W. M., Coale, K. H., and Johnson, K. S.: The flux of iron from continental shelf sediments: A missing source for global budgets, Geophysical Research Letters, 31, L12307-L12307, 2004.

Falkowski, P. G.: The ocean's invisible forest - Marine phytoplankton play a critical role in regulating the earth's climate. Could they also be used to combat global warming, Scientific American, 287, 54-61, 2002.

Fan, S.-M., Moxim, W. J., and Levy II, H.: Aeolian input of bioavailable iron to the ocean, Geophysical Research Letters, 33, doi: 10.1029/2005GL024852, 2006.

Fitzwater, S. E., Johnson, K. S., Gordon, R. M., Coale, K. H., and Smith Jr, W. O.: Trace metal concentrations in the Ross Sea and their relationship with nutrients and phytoplankton growth, Deep Sea Research Part II: Topical Studies in Oceanography, 47, 3159-3179, http://dx.doi.org/10.1016/S0967-0645(00)00063-1, 2000.

Fourquez, M., Obernosterer, I., Davies, D. M., Trull, T. W., and Blain, S.: Microbial iron uptake in the naturally fertilized waters in the vicinity of Kerguelen Islands: phytoplankton–bacteria interactions, Biogeosciences Discussions, 11, 15053-15086, 2014.

Geider, R. J., Laroche, J., Greene, R. M., and Olaizola, M.: Response of the Photosynthetic Apparatus of Phaeodactylum-Tricornutum (Bacillariophyceae) to Nitrate, Phosphate, or Iron Starvation, Journal of Phycology, 29, 755-766, 1993.

Gerringa, L. J. A., Alderkamp, A.-C., Laan, P., Thuróczy, C.-E., De Baar, H. J. W., Mills, M. M., van Dijken, G. L., Haren, H. v., and Arrigo, K. R.: Iron from melting glaciers fuels the phytoplankton blooms in Amundsen Sea (Southern Ocean): Iron biogeochemistry, Deep Sea Research Part II: Topical Studies in Oceanography, 71–76, 16-31, http://dx.doi.org/10.1016/j.dsr2.2012.03.007, 2012.

Ginoux, P., Prospero, J. M., Torres, O., and Chin, M.: Long-term simulation of global dust distribution with the GOCART model: correlation with North Atlantic Oscillation, Environmental Modelling And Software, 19, 113-128, 2004.

Ginoux, P., Prospero, J. M., Gill, T. E., Hsu, N. C., and Zhao, M.: Global-scale attribution of anthropogenic and natural dust sources and their emission rates based on MODIS Deep Blue aerosol products, Reviews of Geophysics, 50, 2012.

Gledhill, M., and Van den Berg, C. M. G.: Determination of complexation of iron(III) with natural organic complexing ligands in seawater using cathodic stripping voltammetry, Marine Chemistry, 47, 41-54, 1994.

Gledhill, M., and Buck, K. N.: The organic complexation of iron in the marine environment: a review, Frontiers in microbiology, 3, 2012.

Gobler, C. J., Hutchins, D. A., Fisher, N. S., Cosper, E. M., and Sanudo-Wilhelmy, S. A.: Release and bioavailability of C, N, P, Se and Fe following viral lysis of a marine chrysophyte, Limnology and Oceanography, 42, 1492-1504, 1997.

Grotti, M., Soggia, F., Ianni, C., and Frache, R.: Trace metals distributions in coastal sea ice of Terra Nova Bay, Ross Sea, Antarctica, Antarctic Science, 17, 289-300, doi:10.1017/S0954102005002695, 2005.

Group, S. W.: GEOTRACES–An international study of the global marine biogeochemical cycles of trace elements and their isotopes, Chemie der Erde-Geochemistry, 67, 85-131, 2007.

Guieu, C., Chester, R., Nimmo, M., Martin, J. M., Guerzoni, S., Nicolas, E., Mateu, J., and Keyse, S.: Atmospheric input of dissolved and particulate metals to the northwestern Mediterranean, Deep Sea Research Part II: Topical Studies in Oceanography, 44, 655-674, http://dx.doi.org/10.1016/S0967-0645(97)88508-6, 1997.

Guieu, C., and Martin, J. M.: The level and fate of metals in the Danube River plume, Estuarine, Coastal and Shelf Science, 54, 501-512, 2002.

Hand, J. L., Mahowald, N. M., Chen, Y., Siefert, R. L., Luo, C., Subramaniam, A., and Fung, I.: Estimates of atmospheric-processed soluble iron from observations and a global mineral aerosol model: Biogeochemical implications, Journal Of Geophysical Research-Atmospheres, 109, D17205-D17205, 2004.

Hassler, C. S., Schoemann, V., Nichols, C. M., Butler, E. C. V., and Boyd, P. W.: Saccharides enhance iron availability to Southern Ocean phytoplankton, Proceedings of the National Academy of Sciences of the United States of America, 108, 1076-1081, 2011.

Hatta, M., Measures, C. I., Selph, K. E., Zhou, M., and Hiscock, W. T.: Iron fluxes from the shelf regions near the South Shetland Islands in the Drake Passage during the austral-winter 2006, Deep Sea Research Part II: Topical Studies in Oceanography, 90, 89-101, 10.1016/j.dsr2.2012.11.003, 2013.

Hatta, M., Measures, C. I., Wu, J., Roshan, S., Fitzsimmons, J. N., Sedwick, P., and Morton, P.: An overview of dissolved Fe and Mn distributions during the 2010–2011 U.S. GEOTRACES north Atlantic cruises: GEOTRACES GA03, Deep Sea Research Part II: Topical Studies in Oceanography, http://dx.doi.org/10.1016/j.dsr2.2014.07.005, 2014.

Hawkes, J. A., Connelly, D. P., Rijkenberg, M. J. A., and Achterberg, E. P.: The importance of shallow hydrothermal island arc systems in ocean biogeochemistry, Geophysical Research Letters, 41, 2013GL058817, 10.1002/2013GL058817, 2014.

Heimburger, A., Losno, R., Triquet, S., Dulac, F., and Mahowald, N.: Direct measurements of atmospheric iron, cobalt, and aluminum-derived dust deposition at Kerguelen Islands, Global Biogeochemical Cycles, 26, 2012.

Heimburger, A., Losno, R., Triquet, S., and Nguyen, E. B.: Atmospheric deposition fluxes of 26 elements over the Southern Indian Ocean: time series on Kerguelen and Crozet Islands, Global Biogeochemical Cycles, 2013.

Heller, M. I., and Croot, P. L.: Copper speciation and distribution in the Atlantic sector of the Southern Ocean, Marine Chemistry, http://dx.doi.org/10.1016/j.marchem.2014.09.017, 2014.

Henderson, G. M., Anderson, R. F., Adkins, J., Andersson, P., Boyle, E. A., Cutter, G., de Baar, H., Eisenhauer, A., Frank, M., Francois, R., Orians, K., Gamo, T., German, C., Jenkins, W., Moffett, J., Jeandel, C., Jickells, T., Krishnaswami, S., Mackey, D., Measures, C. I., Moore, J. K., Oschlies, A., Pollard, R., van der Loeff, M. R. D., Schlitzer, R., Sharma, M., von Damm, K., Zhang, J., and Masque, P.: GEOTRACES - An international study of the global marine biogeochemical cycles of trace elements and their isotopes, Chemie der Erde - Geochemistry, 67, 85-131, 2007.

Ho, T.-Y.: Nickel limitation of nitrogen fixation in Trichodesmium, Limnology and Oceanography, 58, 112-120, 2013.

Ho, T. Y., Quigg, A., Finkel, Z. V., Milligan, A. J., Wyman, K., Falkowski, P. G., and Morel, F. M. M.: The elemental composition of some marine phytoplankton, Journal of Phycology, 39, 1145-1159, 2003.

Holm-Hansen, O., Naganobu, M., Kawaguchi, S., Kameda, T., Krasovski, I., Tchernyshkov, P., Priddle, J., Korb, R., Brandon, M., Demer, D., Hewitt, R. P., Kahru, M., and Hewes, C. D.: Factors influencing the distribution, biomass, and productivity of phytoplankton in the Scotia Sea and adjoining waters, Deep Sea Research Part II: Topical Studies in Oceanography, 51, 1333-1350, http://dx.doi.org/10.1016/j.dsr2.2004.06.015, 2004.

Homoky, W. B., Hembury, D. J., Hepburn, L. E., Mills, R. A., Statham, P. J., Fones, G. R., and Palmer, M. R.: Iron and manganese diagenesis in deep sea volcanogenic sediments and the origins of pore water colloids, Geochimica et Cosmochimica Acta, 75, 5032-5048, http://dx.doi.org/10.1016/j.gca.2011.06.019, 2011.

Homoky, W. B., John, S. G., Conway, T. M., and Mills, R. A.: Distinct iron isotopic signatures and supply from marine sediment dissolution, Nat. Commun., 4, 2013.

Hopkinson, B. M., Mitchell, G., Reynolds, R. A., Wang, H., Selph, K. E., Measures, C. I., Hewes, C. D., Holm-Hansen, O., and Barbeau, K. A.: Iron limitation across chlorophyll gradients in the southern Drake Passage: Phytoplankton responses to iron addition and photosynthetic indicators of iron stress, Limnology And Oceanography, 52, 2540-2554, 2007.

Hsu, S.-C., Wong, G. T. F., Gong, G.-C., Shiah, F.-K., Huang, Y.-T., Kao, S.-J., Tsai, F., Candice Lung, S.-C., Lin, F.-J., Lin, I. I., Hung, C.-C., and Tseng, C.-M.: Sources, solubility, and dry deposition of aerosol trace elements over the East China Sea, Marine Chemistry, 120, 116-127, http://dx.doi.org/10.1016/j.marchem.2008.10.003, 2010.

Hutchins, D. A., DiTullio, G. R., and Bruland, K. W.: Iron and regenerated production: Evidence for biological iron recycling in two marine environments, Limnology and Oceanography, 38, 1242-1255, 1993.

Hutchins, D. A., and Bruland, K. W.: Grazer-Mediated Regeneration and Assimilation of Fe, Zn and Mn from Planktonic Prey, Marine Ecology Progress Series, 110, 259-269, 1994.

Jacquet, S., Dehairs, F., Cavagna, A. J., Planchon, F., Monin, L., and André, L.: Early season mesopelagic carbon remineralization and transfer efficiency in the naturally iron-fertilized Kerguelen area, Biogeosciences Discuss., 2014.

Jacquot, J. E., and Moffett, J. W.: Copper distribution and speciation across the International GEOTRACES Section GA03, Deep Sea Research Part II: Topical Studies in Oceanography, http://dx.doi.org/10.1016/j.dsr2.2014.11.013, 2014.

Jickells, T.: Atmospheric inputs of metals and nutrients to the oceans: their magnitude and effects, Marine Chemistry, 48, 199-214, http://dx.doi.org/10.1016/0304-4203(95)92784-P, 1995.

Jickells, T. D., and Spokes, L. J.: Atmospheric iron inputs to the oceans, in: The Biogeochemistry of Iron in Seawater, edited by: Hunter, K. A., and Turner, D. R., John Wiley and Sons Ltd, 85-121, 2001.

Jickells, T. D., An, Z. S., Andersen, K. K., Baker, A. R., Bergametti, G., Brooks, N., Cao, J. J., Boyd, P. W., Duce, R. A., Hunter, K. A., Kawahata, H., Kubilay, N., laRoche, J., Liss, P. S., Mahowald, N., Prospero, J. M., Ridgwell, A. J., Tegen, I., and Torres, R.: Global iron connections between desert dust, ocean biogeochemistry, and climate, Science, 308, 67-71, 2005.

Johnson, K. S., Elrod, V., Fitzwater, S., Plant, J., Boyle, E., Bergquist, B., Bruland, K., Aguilar-Islas, A., Buck, K., and Lohan, M.: Developing standards for dissolved iron in seawater, Eos, Transactions American Geophysical Union, 88, 131-132, 2007.

Jouandet, M. P., Blain, S., Metzl, N., Brunet, C., Trull, T. W., and Obernosterer, I.: A seasonal carbon budget for a naturally iron-fertilized bloom over the Kerguelen Plateau in the Southern Ocean, Deep Sea Research Part II: Topical Studies in Oceanography, 55, 856-867, http://dx.doi.org/10.1016/j.dsr2.2007.12.037, 2008.

Journet, E., Desboeufs, K. V., Caquineau, S., and Colin, J.-L.: Mineralogy as a critical factor of dust iron solubility, Geophysical Research Letters, 35, L07805, 10.1029/2007GL031589, 2008.

Kallos, G., Papadopoulos, A., Katsafados, P., and Nickovic, S.: Transatlantic Saharan dust transport: Model simulation and results, Journal of Geophysical Research: Atmospheres, 111, D09204, 10.1029/2005JD006207, 2006.

Klunder, M. B., Laan, P., Middag, R., De Baar, H. J. W., and Van Ooijen, J. C.: Dissolved iron in the Southern Ocean (Atlantic sector), Deep Sea Research Part II: Topical Studies in Oceanography, 58, 2678-2694, 2011.

Klunder, M. B., Laan, P., De Baar, H. J. W., Neven, I., Middag, R., and Van Ooijen, J.: Dissolved Fe across the Weddell Sea and Drake Passage: impact of DFe on nutrients uptake in the Weddell Sea, Biogeosciences Discuss., 10, 7433-7489, 10.5194/bgd-10-7433-2013, 2013.

Kraemer, S. M.: Iron oxide dissolution and solubility in the presence of siderophores, Aquatic Sciences, 66, 3-18, 2004.

Kremling, K., and Streu, P.: The behaviour of dissolved Cd, Co, Zn, and Pb in North Atlantic near-surface waters (30°N/60°W–60°N/2°W), Deep Sea Research Part I: Oceanographic Research Papers, 48, 2541-2567, http://dx.doi.org/10.1016/S0967-0637(01)00036-X, 2001.

Labatut, M., Lacan, F., Pradoux, C., Chmeleff, J., Radic, A., Murray, J. W., Poitrasson, F., Johansen, A. M., and Thil, F.: Iron sources and dissolved-particulate interactions in the seawater of the Western Equatorial Pacific, iron isotope perspectives, Global Biogeochemical Cycles, 28, 2014GB004928, 10.1002/2014GB004928, 2014.

Lagerstrom, M., Field, M. P., Séguret, M., Fischer, L., Hann, S., and Sherrell, R. M.: Automated on-line flow-injection ICP-MS determination of trace metals (Mn, Fe, Co, Ni, Cu and Zn) in open ocean seawater: Application to the GEOTRACES program, Marine Chemistry, 155, 71-80, 2013.

Lai, X., Norisuye, K., Mikata, M., Minami, T., Bowie, A. R., and Sohrin, Y.: Spatial and temporal distribution of Fe, Ni, Cu and Pb along 140°E in the Southern Ocean during austral summer 2001/02, Marine Chemistry, 111, 171-183, http://dx.doi.org/10.1016/j.marchem.2008.05.001, 2008.

Lam, P. J., and Bishop, J. K. B.: The continental margin is a key source of iron to the HNLC North Pacific Ocean, Geophysical Research Letters, 35, L07608, 10.1029/2008GL033294, 2008.

Landing, W. M., and Bruland, K. W.: Manganese in the North Pacific, Earth and Planetary Science Letters, 49, 45-56, 1980.

Lane, E. S., Semeniuk, D. M., Strzepek, R. F., Cullen, J. T., and Maldonado, M. T.: Effects of iron limitation on intracellular cadmium of cultured phytoplankton: Implications for surface dissolved cadmium to phosphate ratios, Marine Chemistry, 115, 155-162, http://dx.doi.org/10.1016/j.marchem.2009.07.008, 2009.

Lane, T. W., and Morel, F. M. M.: A biological function for cadmium in marine diatoms, Proceedings of the National Academy of Sciences of the United States of America, 97, 4627-4631, 2000.

Lane, T. W., Saito, M. A., George, G. N., Pickering, I. J., Prince, R. C., and Morel, F. à. ü. M. M.: Biochemistry: a cadmium enzyme from a marine diatom, Nature, 435, 42-42, 2005.

Lannuzel, D., Schoemann, V., de Jong, J. T. M., Tison, J., and Chou, L.: Distribution and biogeochemical behaviour of iron in the East Antarctic sea ice, Marine Chemistry, 106, 18-32, 2007.

Lannuzel, D., Schoemann, V., de Jong, J., Chou, L., Delille, B., Becquevort, S., and Tison, J.-L.: Iron study during a time series in the western Weddell pack ice, Marine Chemistry, 108, 85-95, http://dx.doi.org/10.1016/j.marchem.2007.10.006, 2008.

Lannuzel, D., Schoemann, V., de Jong, J., Pasquer, B., van der Merwe, P., Masson, F., Tison, J. L., and Bowie, A.: Distribution of dissolved iron in Antarctic sea ice: Spatial, seasonal, and inter-annual variability, Journal Of Geophysical Research-Biogeosciences, 115, G03022-G03022, 2010.

Lannuzel, D., Bowie, A. R., van der Merwe, P. C., Townsend, A. T., and Schoemann, V.: Distribution of dissolved and particulate metals in Antarctic sea ice, Marine Chemistry, 124, 134-146, 2011.

Lasbleiz, M., Leblanc, K., Blain, S., Ras, J., Cornet-Barthaux, V., Hélias Nunige, S., and Quéguiner, B.: Pigments, elemental composition (C, N, P, Si) and stoichiometry of particulate matter, in the naturally iron fertilized region of Kerguelen in the Southern Ocean, Biogeosciences Discuss., 11, 8259-8324, 10.5194/bgd-11-8259-2014, 2014.

Laws, E. A., Falkowski, P. G., Smith, W. O., Ducklow, H., and McCarthy, J. J.: Temperature effects on export production in the open ocean, Global Biogeochemical Cycles, 14, 1231-1246, 2000.

Lee, J.-M., Boyle, E. A., Echegoyen-Sanz, Y., Fitzsimmons, J. N., Zhang, R., and Kayser, R. A.: Analysis of trace metals (Cu, Cd, Pb, and Fe) in seawater using single batch nitrilotriacetate resin extraction and isotope dilution inductively coupled plasma mass spectrometry, Analytica Chimica Acta, 686, 93-101, 2011.

Lin, H., Rauschenberg, S., Hexel, C. R., Shaw, T. J., and Twining, B. S.: Free-drifting icebergs as sources of iron to the Weddell Sea, Deep Sea Research Part II: Topical Studies in Oceanography, 58, 1392-1406, http://dx.doi.org/10.1016/j.dsr2.2010.11.020, 2011.

Lin, H., and Twining, B. S.: Chemical speciation of iron in Antarctic waters surrounding free-drifting icebergs, Marine Chemistry, 128-129, 81-91, 2012.

Lohan, M. C., Aguilar-Islas, A. M., Franks, R. P., and Bruland, K. W.: Determination of iron and copper in seawater at pH 1.7 with a new commercially available chelating resin, NTA Superflow, Analytica Chimica Acta, 530, 121-129, http://dx.doi.org/10.1016/j.aca.2004.09.005, 2005.

Lohan, M. C., and Bruland, K. W.: Elevated Fe(II) and Dissolved Fe in Hypoxic Shelf Waters off Oregon and Washington: An Enhanced Source of Iron to Coastal Upwelling Regimes, Environmental Science & Technology, 42, 6462-6468, 10.1021/es800144j, 2008.

Löscher, B. M.: Relationships among Ni, Cu, Zn, and major nutrients in the Southern Ocean, Marine Chemistry, 67, 67-102, http://dx.doi.org/10.1016/S0304-4203(99)00050-X, 1999.

Luther III, G. W., Madison, A. S., Mucci, A., Sundby, B., and Oldham, V. E.: A kinetic approach to assess the strengths of ligands bound to soluble Mn(III), Marine Chemistry, 173, 93-99, http://dx.doi.org/10.1016/j.marchem.2014.09.006, 2015.

Mackie, D. S., Boyd, P. W., Hunter, K. A., and McTainsh, G. H.: Simulating the cloud processing of iron in Australian dust: pH and dust concentration, Geophysical Research Letters, 32, L06809-L06809, 2005.

Madison, A. S., Tebo, B. M., Mucci, A., Sundby, B., and Luther, G. W.: Abundant porewater Mn (III) is a major component of the sedimentary redox system, science, 341, 875-878, 2013.

Mahowald, N. M., and Luo, C.: A less dusty future?, Geophysical Research Letters, 30, 1903-1903, 2003.

Mahowald, N. M., Baker, A. R., Bergametti, G., Brooks, N., Duce, R. A., Jickells, T. D., Kubilay, N., Prospero, J. M., and Tegen, I.: Atmospheric global dust cycle and iron inputs to the ocean, Global Biogeochemical Cycles, 19, GB4025-GB4025, 2005.

Maldonado, M. T., Allen, A. E., Chong, J. S., Lin, K., Leus, D., Karpenko, N., and Harris, S. L.: Copper-dependent iron transport in coastal and oceanic diatoms, Limnology And Oceanography, 51, 1729-1743, 2006.

Maranger, R., Bird, D. F., and Price, N. M.: Iron acquisition by photosynthetic marine phytoplankton from ingested bacteria, Nature, 396, 248-251, 1998.

Maring, H., Savoie, D. L., Izaguirre, M. A., Custals, L., and Reid, J. S.: Mineral dust aerosol size distribution change during atmospheric transport, Journal of Geophysical Research: Atmospheres, 108, 8592, 10.1029/2002JD002536, 2003.

Martin, J. H.: Glacial-interglacial CO2 change: the iron hypothesis, Paleoceanography, vol.5, no.1, 1-13, 1990.

Martin, J. H., Coale, K. H., Johnson, K. S., Fitzwater, S. E., Gordon, R. M., Tanner, S. J., Hunter, C. N., Elrod, V. A., Nowiicki, J. L., Coley, T. L., Barber, R. T., Lindley, S., Watson, A. J., Van Scoy, K., Law, C. S., Liddicoat, M. I., Ling, R., Stanton, T., Stockel, J., Collins, C., Anderson, A., Bidigare, R., Ondrusek, M., Latasa, M., Millero, F. J., Lee, K., Yao, W., Zhang, J. Z., Friederich, G., Sakamoto, C., Chavez, F., Buck, K., Kolber, Z., Greene, R., Falkowski, P., Chisholm, S. W., Hoge, F., Swift, R., Yungel, J., Turner, S., Nightingale, P., Hatton, A., Liss, P., and Tindale, N. W.: Testing the iron hypothesis in ecosystems of the equatorial Pacific Ocean, Nature, 371, 123-129, 1994.

McLennan, S. M.: Relationships between the trace element composition of sedimentary rocks and upper continental crust, Geochemistry, Geophysics, Geosystems, 2, 2001.

Measures, C. I., Landing, W. M., Brown, M. T., and Buck, C. S.: A commercially available rosette system for trace metal-clean sampling, Limnology and Oceanography-Methods, 6, 384-394, 2008.

Measures, C. I., Brown, M. T., Selph, K. E., Apprill, A., Zhou, M., Hatta, M., and Hiscock, W. T.: The influence of shelf processes in delivering dissolved iron to the HNLC waters of the Drake Passage, Antarctica, Deep Sea Research Part II: Topical Studies in Oceanography, 90, 77-88, 10.1016/j.dsr2.2012.11.004, 2013.

Middag, R., de Baar, H. J. W., Laan, P., Cai, P. H., and van Ooijen, J. C.: Dissolved manganese in the Atlantic sector of the Southern Ocean, Deep-Sea Research Part II-Topical Studies In Oceanography, 58, 2661-2677, 10.1016/j.dsr2.2010.10.043, 2011a.

Middag, R., de Baar, H. J. W., Laan, P., and Klunder, M. B.: Fluvial and hydrothermal input of manganese into the Arctic Ocean, Geochimica Et Cosmochimica Acta, 75, 2393-2408, 2011b.

Middag, R., de Baar, H. J. W., Laan, P., and Huhn, O.: The effects of continental margins and water mass circulation on the distribution of dissolved aluminum and manganese in Drake Passage, Journal Of Geophysical Research-Oceans, 117, C01019-C01019, 2012.

Millero, F. J., Sotolongo, S., and Izaguirre, M.: The oxidation kinetics of Fe(II) in seawater, Geochimica et Cosmochimica Acta, 51, 793-801, 1987.

Millero, F. J., and Sotolongo, S.: The oxidation of Fe(II) with H_2O_2 in seawater, Geochimica et Cosmochimica Acta, 53, 1867-1873, 1989.

Milliman, J. D., and Meade, R. H.: World-wide delivery of river sediment to the oceans, The Journal of Geology, 1-21, 1983.

Milne, A., Landing, W., Bizimis, M., and Morton, P.: Determination of Mn, Fe, Co, Ni, Cu, Zn, Cd and Pb in seawater using high resolution magnetic sector inductively coupled mass spectrometry (HR-ICP-MS), Analytica Chimica Acta, 665, 200-207, 2010.

Minami, T., Konagaya, W., Zheng, L., Takano, S., Sasaki, M., Murata, R., Nakaguchi, Y., and Sohrin, Y.: An off-line automated preconcentration system with ethylenediaminetriacetate chelating resin for the determination of trace metals in seawater by high-resolution inductively coupled plasma mass spectrometry, Analytica chimica acta, 854, 183-190, 2015.

Mioni, C. E., Handy, S. M., Ellwood, M. J., Twiss, M. R., McKay, R. M. L., Boyd, P. W., and Wilhelm, S. W.: Tracking changes in bioavailable Fe within high nitrate low chlorophyll oceanic waters: A first estimate using a heterotrophic bacterial bioreporter, Global Biogeochemical Cycles, 19, 2005.

Moffett, J. W., and Zika, R. G.: Reaction Kinetics of Hydrogen Peroxide with Copper and Iron in Seawater, Environment and Science Technology, 21, 804-810, 1987.

Moffett, J. W., and Ho, J.: Oxidation of cobalt and manganese in seawater via a common microbially catalyzed pathway, Geochimica et Cosmochimica Acta, 60, 3415-3424, 1996.

Moore, C. M., Mills, M. M., Achterberg, E. P., Geider, R. J., LaRoche, J., Lucas, M. I., McDonagh, E. L., Pan, X., Poulton, A. J., Rijkenberg, M. J. A., Suggett, D. J., Ussher, S. J., and Woodward, E. M. S.: Large-scale distribution of Atlantic nitrogen fixation controlled by iron availability, Nature Geoscience, 2, 867-871, 2009.

Moore, J. K., Doney, S. C., and Lindsay, K.: Upper ocean ecosystem dynamics and iron cycling in a global three-dimensional model, Global Biogeochemical Cycles, 18, GB4028-GB4028, 2004.

Moore, J. K., and Braucher, O.: Sedimentary and mineral dust sources of dissolved iron to the world ocean, Biogeosciences, 5, 631-656, 2008.

Morel, F. M. M., and Price, N. M.: The biogeochemical cycles of trace metals in the oceans, Science, 300, 944-947, 2003.

Morris, P. J., and Charette, M. A.: A synthesis of upper ocean carbon and dissolved iron budgets for Southern Ocean natural iron fertilisation studies, Deep Sea Research Part II: Topical Studies in Oceanography, 90, 147-157, http://dx.doi.org/10.1016/j.dsr2.2013.02.001, 2013.

Mosseri, J., Quéguiner, B., Armand, L., and Cornet-Barthaux, V.: Impact of iron on silicon utilization by diatoms in the Southern Ocean: A case study of Si/N cycle decoupling in a naturally iron-enriched area, Deep Sea Res., 55, 801-819, 2008.

Ndung'u, K., Franks, R. P., Bruland, K. W., and Flegal, A. R.: Organic complexation and total dissolved trace metal analysis in estuarine waters: comparison of solvent-extraction graphite furnace atomic absorption spectrometric and chelating resin flow injection inductively coupled plasma-mass spectrometric analysis, Analytica Chimica Acta, 481, 127-138, 2003.

Ndung'u, K., Franks, R. P., Bruland, K. W., and Flegal, A. R.: Organic complexation and total dissolved trace metal analysis in estuarine waters: comparison of solvent-extraction graphite furnace atomic absorption spectrometric and chelating resin flow injection inductively coupled plasma-mass spectrometric analysis, Analytica Chimica Acta, 481, 127-138, 2003.

Nicol, S., Bowie, A., Jarman, S., Lannuzel, D., Meiners, K. M., and van der Merwe, P.: Southern Ocean iron fertilization by baleen whales and Antarctic krill, Fish and Fisheries, 11, 203-209, 2010.

Nielsdóttir, M. C., Bibby, T. S., Moore, C. M., Hinz, D. J., Sanders, R., Whitehouse, M., Korb, R., and Achterberg, E. P.: Seasonal and spatial dynamics of iron availability in the Scotia Sea, Marine Chemistry, 130–131, 62-72, 10.1016/j.marchem.2011.12.004, 2012.

Nishioka, J., Obata, H., and Tsumune, D.: Evidence of an extensive spread of hydrothermal dissolved iron in the Indian Ocean, Earth and Planetary Science Letters, 361, 26-33, http://dx.doi.org/10.1016/j.epsl.2012.11.040, 2013.

Noble, A. E., Saito, M. A., Maiti, K., and Benitez-Nelson, C. R.: Cobalt, manganese, and iron near the Hawaiian Islands: A potential concentrating mechanism for cobalt within a cyclonic eddy and implications for the hybrid-type trace metals, Deep Sea Research Part II: Topical Studies in Oceanography, 55, 1473-1490, http://dx.doi.org/10.1016/j.dsr2.2008.02.010, 2008.

Noble, A. E., Lamborg, C. H., Ohnemus, D. C., Lam, P. J., Goepfert, T. J., Measures, C. I., Frame, C. H., Casciotti, K. L., DiTullio, G. R., Jennings, J., and Saito, M. A.: Basin-scale inputs of cobalt, iron, and manganese from the Benguela-Angola front to the South Atlantic Ocean, Limnology and Oceanography, 57, 989-1010, 2012.

Noble, A. E., Echegoyen-Sanz, Y., Boyle, E. A., Ohnemus, D. C., Lam, P. J., Kayser, R., Reuer, M., Wu, J., and Smethie, W.: Dynamic variability of dissolved Pb and Pb isotope composition from the US north Atlantic GEOTRACES transect, Deep Sea Research Part II: Topical Studies in Oceanography, 2014.

Nuester, J., Vogt, S., Newville, M., Kustka, A. B., and Twining, B. S.: The unique biogeochemical signature of the marine diazotroph Trichodesmium, Frontiers in Microbiology, 3, DOI:10.3389/fmicb.2012.00150-DOI:00110.03389/fmicb.02012.00150, 2012.

O'Sullivan, J. E., Watson, R. J., and Butler, E. C. V.: An ICP-MS procedure to determine Cd, Co, Cu, Ni, Pb and Zn in oceanic waters using in-line flow-injection with solid-phase extraction for preconcentration, Talanta, DOI:--DOI: 10.1016/j.talanta.2013.1006.1054-DOI: 1010.1016/j.talanta.2013.1006.1054, 2013.

Obata, H., Karatani, H., and Nakayama, E.: Automated determination of iron in seawater by chelating resin concentration and chemiluminescence detection, Analytical Chemistry, 65, 1524-1528, 1993.

Park, H., Song, B., and Morel, F. M. M.: Diversity of the cadmium-containing carbonic anhydrase in marine diatoms and natural waters, Environmental Microbiology, 9, 403-413, 2007.

Park, Y. H., Durand, I., Kestenare, E., Rougier, G., Zhou, M., d'Ovidio, F., Cotté, C., and Lee, J. H.: Polar Front around the Kerguelen Islands: An up-to-date determination and associated circulation of surface/subsurface waters, Journal of Geophysical Research: Oceans, 119, 6575-6592, 2014.

Peers, G., and Price, N. M.: A role for manganese in superoxide dismutases and growth of iron-deficient diatoms, Limnology and Oceanography, 49, 1774-1783, 2004.

Peers, G., Quesnel, S. A., and Price, N. M.: Copper requirements for iron acquisition and growth of coastal and oceanic diatoms, Limnology and Oceanography, 50, 1149-1158, 2005.

Peers, G., and Price, N. M.: Copper-containing plastocyanin used for electron transport by an oceanic diatom, Nature, 441, 341-344, 2006.

Planquette, H., Statham, P. J., Fones, G. R., Charette, M. A., Moore, C. M., Salter, I., Nédélec, F. H., Taylor, S. L., French, M., Baker, A. R., Mahowald, N., and Jickells, T. D.: Dissolved iron in the vicinity of the Crozet Islands, Southern Ocean, Deep Sea Research Part II: Topical Studies in Oceanography, 54, 1999-2019, http://dx.doi.org/10.1016/j.dsr2.2007.06.019, 2007.

Planquette, H., Sanders, R. R., Statham, P. J., Morris, P. J., and Fones, G. R.: Fluxes of particulate iron from the upper ocean around the Crozet Islands: A naturally iron-fertilized environment in the Southern Ocean, Global Biogeochemical Cycles, 25, GB2011-GB2011, 2011.

Planquette, H., and Sherrell, R. M.: Sampling for particulate trace element determination using water sampling bottles: methodology and comparison to in situ pumps, Limnology And Oceanography-methods, 10, 367-388, 2012.

Pollard, R., Sanders, R., Lucas, M., and Statham, P.: The Crozet Natural Iron Bloom and Export Experiment (CROZEX), Deep Sea Research Part II: Topical Studies in Oceanography, 54, 1905-1914, http://dx.doi.org/10.1016/j.dsr2.2007.07.023, 2007a.

Pollard, R. T., Venables, H. J., Read, J. F., and Allen, J. T.: Large-scale circulation around the Crozet Plateau controls an annual phytoplankton bloom in the Crozet Basin, Deep Sea Research Part II: Topical Studies in Oceanography, 54, 1915-1929, 2007b.

Pollard, R. T., Salter, I., Sanders, R. J., Lucas, M. I., Moore, C. M., Mills, R. A., Statham, P. J., Allen, J. T., Baker, A. R., Bakker, D. C. E., Charette, M. A., Fielding, S., Fones, G. R., French, M., Hickman, A. E., Holland, R. J., Hughes, J. A., Jickells, T. D., Lampitt, R. S., Morris, P. J., Nedelec, F. H., Nielsdottir, M., Planquette, H., Popova, E. E., Poulton, A. J., Read, J. F., Seeyave, S., Smith, T., Stinchcombe, M., Taylor, S., Thomalla, S., Venables, H. J., Williamson, R., and Zubkov, M. V.: Southern Ocean deep-water carbon export enhanced by natural iron fertilization, Nature, 457, 577-U581, 2009.

Poorvin, L., Rinta-Kanto, J. M., Hutchins, D. A., and Wilhelm, S. W.: Viral release of iron and its bioavailability to marine plankton, Limnology and Oceanography, 49, 1734-1741, 2004.

Price, N. M., and Morel, F. M. M.: Cadmium and cobalt substitution for zinc in a marine diatom, Nature, 344, 658-660, 1990.

Price, N. M., and Morel, F. M. M.: Colimitation of phytoplankton growth by nickel and nitrogen, Limnology And Oceanography, 36, 1071-1077, 1991.

Prospero, J. M., Ginoux, P., Torres, O., Nicholson, S. E., and Gill, T. E.: Environmental characterization of global sources of atmospheric soil dust identified with the Nimbus 7 Total Ozone Mapping Spectrometer (TOMS) absorbing aerosol product, Reviews Of Geophysics, 40, 1002-1002, 2002.

Quéguiner, B.: Iron fertilization and the structure of planktonic communities in high nutrient regions of the Southern Ocean, Deep Sea Research Part II: Topical Studies in Oceanography, 90, 43-54, http://dx.doi.org/10.1016/j.dsr2.2012.07.024, 2013.

Quéroué, F., Townsend, A. T., van der Merwe, P., Lannuzel, D., Sarthou, G., Bucciarelli, E., and Bowie, A. R.: Advances in the offline trace metal extraction of Mn, Co, Ni, Cu, Cd, and Pb from open ocean seawater samples with determination by Sector Field ICP-MS analysis, Analytical Methods, 6, 2837-2847, 10.1039/C3AY41312H, 2014.

Quéroué, F., Sarthou, G., Planquette, H. F., Bucciarelli, E., Chever, F., van der Merwe, P., Lannuzel, D., Townsend, A. T., Cheize, M., and Blain, S.: High variability of dissolved iron concentrations in the vicinity of Kerguelen Island (Southern Ocean), Biogeosciences Discussions, 12, 231-270, 2015.

Radic, A., Lacan, F., and Murray, J. W.: Iron isotopes in the seawater of the equatorial Pacific Ocean: New constraints for the oceanic iron cycle, Earth and Planetary Science Letters, 306, 1-10, http://dx.doi.org/10.1016/j.epsl.2011.03.015, 2011.

Raiswell, R., Tranter, M., Benning, L. G., Siegert, M., De'ath, R., Huybrechts, P., and Payne, T.: Contributions from glacially derived sediment to the global iron (oxyhydr)oxide cycle: Implications for iron delivery to the oceans, Geochimica et Cosmochimica Acta, 70, 2765-2780, http://dx.doi.org/10.1016/j.gca.2005.12.027, 2006.

Raiswell, R., and Canfield, D. E.: The iron biogeochemical cycle past and present, Geochemical Perspectives, 1, 1-2, 2012.

Ratnarajah, L., Bowie, A. R., Lannuzel, D., Meiners, K. M., and Nicol, S.: The Biogeochemical Role of Baleen Whales and Krill in Southern Ocean Nutrient Cycling, PloS one, 9, e114067, 2014.

Remenyi, T., Nesterenko, P., Bowie, A., Butler, E., and Haddad, P.: Reversed phase high performance liquid chromatographic determination of dissolved aluminium in open ocean seawater, Limnology and Oceanography-Methods, 10, 832-839, 2012.

Rodushkin, I., and Ruth, T.: Determination of trace metals in estuarine and sea-water reference materials by high resolution inductively coupled plasma mass spectrometry, Journal of Analytical Atomic Spectrometry, 12, 1181-1185, 1997.

Rouxel, O., Shanks Iii, W. C., Bach, W., and Edwards, K. J.: Integrated Fe- and S-isotope study of seafloor hydrothermal vents at East Pacific Rise 9–10°N, Chemical Geology, 252, 214-227, http://dx.doi.org/10.1016/j.chemgeo.2008.03.009, 2008.

Rue, E. L., and Bruland, K. W.: Complexation of iron(III) by natural organic ligands in the Central North Pacific as determined by a new competitive ligand equilibration/adsorptive cathodic stripping voltammetric method, Marine Chemistry, 50, 117-138, 1995.

Sackett, O., Armand, L., Beardall, J., Hill, R., Doblin, M., Connelly, C., Howes, J., Stuart, B., Ralph, P., and Heraud, P.: Taxon-specific responses of Southern Ocean diatoms to Fe

enrichment revealed by synchrotron radiation FTIR microspectroscopy, Biogeosciences, 11, 5795-5808, 2014.

Saito, M. A., and Moffett, J. W.: Complexation of cobalt by natural organic ligands in the Sargasso Sea as determined by a new high-sensitivity electrochemical cobalt speciation method suitable for open ocean work, Marine Chemistry, 75, 49-68, http://dx.doi.org/10.1016/S0304-4203(01)00025-1, 2001.

Saito, M. A., Moppett, J. W., Chisholm, S. W., and Waterbury, J. B.: Cobalt limitation and uptake in Prochlorococcus, Limnology and Oceanography, 47, 1629-1636, 2002.

Saito, M. A., and Goepfert, T. J.: Zinc-cobalt colimitation of Phaeocystis antarctica, Limnology and Oceanography, 53, 266-275, 2008.

Saito, M. A., Noble, A. E., Tagliabue, A., Goepfert, T. J., Lamborg, C. H., and Jenkins, W. J.: Slow-spreading submarine ridges in the South Atlantic as a significant oceanic iron source, Nature Geoscience, 6, 775-779, 2013.

Sanial, V., van Beek, P., Lansard, B., Souhaut, M., Kestenare, E., d'Ovidio, F., Zhou, M., and Blain, S.: Use of Ra isotopes to deduce rapid transfer of sediment-derived inputs off Kerguelen, Biogeosciences Discussions, 11, 14023-14061, 2014.

Sarthou, G., Baker, A. R., Blain, S., Achterberg, E. P., Boye, M., Bowie, A. R., Croot, P., Laan, P., de Baar, H. J. W., Jickells, T. D., and Worsfold, P. J.: Atmospheric iron deposition and sea-surface dissolved iron concentrations in the eastern Atlantic Ocean, Deep-Sea Research Part I-oceanographic Research Papers, 50, 1339-1352, 2003.

Sarthou, G., Vincent, D., Christaki, U., Obernosterer, I., Timmermans, K. R., and Brussaard, C. P. D.: The fate of biogenic iron during a phytoplankton bloom induced by natural fertilisation: Impact of copepod grazing, Deep-Sea Research Part II-topical Studies In Oceanography, 55, 734-751, 2008.

Sarthou, G.: Le cycle biogéochimique du fer en milieu océanique, Habilitation à Diriger les Recherche, Université de Bretagne Occidentale, 175 pp., 2009.

Schlitzer, R.: eGEOTRACES, Electronic Atlas of GEOTRACES Sections and Animated 3D Scenes, http://www.egeotraces.org, 2014.

Schroth, A. W., Crusius, J., Sholkovitz, E. R., and Bostick, B. C.: Iron solubility driven by speciation in dust sources to the ocean, Nature Geoscience, 2, 337-340, 2009.

Schulz, M., Prospero, J. M., Baker, A. R., Dentener, F., Ickes, L., Liss, P. S., Mahowald, N. M., Nickovic, S., Garcia-Pando, C. P., and Rodríguez, S.: Atmospheric transport and deposition of mineral dust to the ocean: implications for research needs, Environmental science & technology, 46, 10390-10404, 2012.

Sedwick, P. N., Sholkovitz, E. R., and Church, T. M.: Impact of anthropogenic combustion emissions on the fractional solubility of aerosol iron: Evidence from the Sargasso Sea, Geochemistry, Geophysics, Geosystems, 8, 2007.

Semeniuk, D. M., Bundy, R. M., Payne, C. D., Barbeau, K. A., and Maldonado, M. T.: Acquisition of organically complexed copper by marine phytoplankton and bacteria in the northeast subarctic Pacific Ocean, Marine Chemistry, 173, 222-233, http://dx.doi.org/10.1016/j.marchem.2015.01.005, 2015.

Severmann, S., Johnson, C. M., Beard, B. L., German, C. R., Edmonds, H. N., Chiba, H., and Green, D. R. H.: The effect of plume processes on the Fe isotope composition of hydrothermally derived Fe in the deep ocean as inferred from the Rainbow vent site, Mid-Atlantic Ridge, 36 14′ N, Earth and Planetary Science Letters, 225, 63-76, 2004.

Sharma, M., Polizzotto, M., and Anbar, A. D.: Iron isotopes in hot springs along the Juan de Fuca Ridge, Earth and Planetary Science Letters, 194, 39-51, http://dx.doi.org/10.1016/S0012-821X(01)00538-6, 2001.

Shelley, R. U., Zachhuber, B., Sedwick, P. N., Worsfold, P. J., and Lohan, M. C.: Determination of total dissolved cobalt in UV-irradiated seawater using flow injection with chemiluminescence detection, Limnology And Oceanography-Methods, 8, 352-362, 2010.

Shelley, R. U., Sedwick, P. N., Bibby, T. S., Cabedo-Sanz, P., Church, T. M., Johnson, R. J., Macey, A. I., Marsay, C. M., Sholkovitz, E. R., and Ussher, S. J.: Controls on dissolved cobalt in surface waters of the Sargasso Sea: Comparisons with iron and aluminum, Global Biogeochemical Cycles, 26, 2012.

Slemons, L., Gorgues, T., Aumont, O., Menkes, C., and Murray, J. W.: Biogeochemical impact of a model western iron source in the Pacific Equatorial Undercurrent, Deep Sea Research Part I: Oceanographic Research Papers, 56, 2115-2128, http://dx.doi.org/10.1016/j.dsr.2009.08.005, 2009.

Smith Jr, K. L.: Free-drifting icebergs in the Southern Ocean: An overview, Deep Sea Research Part II: Topical Studies in Oceanography, 58, 1277-1284, http://dx.doi.org/10.1016/j.dsr2.2010.11.003, 2011.

Smith Jr, W. O., Sedwick, P. N., Arrigo, K. R., Ainley, D. G., and Orsi, A. H.: The Ross Sea in a sea of change, Oceanography, 25, 2012.

Smith, K. L., Robison, B. H., Helly, J. J., Kaufmann, R. S., Ruhl, H. A., Shaw, T. J., Twining, B. S., and Vernet, M.: Free-Drifting Icebergs: Hot Spots of Chemical and Biological Enrichment in the Weddell Sea, Science, 317, 478-482, 2007.

Smith, L. V., McMinn, A., Martin, A., Nicol, S., Bowie, A. R., Lannuzel, D., and van der Merwe, P.: Preliminary investigation into the stimulation of phytoplankton photophysiology and growth by whale faeces, Journal of Experimental Marine Biology and Ecology, 446, 1-9, http://dx.doi.org/10.1016/j.jembe.2013.04.010, 2013.

Spokes, L. J., Jickells, T. D., and Lim, B.: Solubilization of Aerosol Trace-metals By Cloud Processing - A Laboratory Study, Geochimica Et Cosmochimica Acta, 58, 3281-3287, 1994.

Statham, P. J., Yeats, P. A., and Landing, W. M.: Manganese in the eastern Atlantic Ocean: processes influencing deep and surface water distributions, Marine Chemistry, 61, 55-68, 1998.

Statham, P. J., German, C. R., and Connelly, D. P.: Iron(II) distribution and oxidation kinetics in hydrothermal plumes at the Kairei and Edmond vent sites, Indian Ocean, Earth and Planetary Science Letters, 236, 588-596, 2005.

Statham, P. J., Skidmore, M., and Tranter, M.: Inputs of glacially derived dissolved and colloidal iron to the coastal ocean and implications for primary productivity, Global Biogeochemical Cycles, 22, GB3013, 10.1029/2007GB003106, 2008.

Sullivan, C. W., Arrigo, K. R., McClain, C. R., Comiso, J. C., and Firestone, J.: Distributions of phytoplankton blooms in the Southern Ocean, Science, 262, 1832-1837, 1993.

Sunda, W. G., Huntsman, S. A., and Harvey, G. R.: Photo-Reduction of Manganese Oxides in Seawater and Its Geochemical and Biological Implications, Nature, 301, 234-236, 1983.

Sunda, W. G., and Huntsman, S. A.: Effect of Sunlight on Redox Cycles of Manganese in the Southwestern Sargasso Sea, Deep-Sea Research Part a-Oceanographic Research Papers, 35, 1297-1317, 1988.

Sunda, W. G.: Trace metal interactions with marine phytoplankton, Biological Oceanography, 6, 411-442, 1989.

Sunda, W. G., and Huntsman, S. A.: Diel Cycles in Microbial Manganese Oxidation and Manganese Redox Speciation in Coastal Waters of the Bahama-Islands, Limnology and Oceanography, 35, 325-338, 1990.

Sunda, W. G., and Huntsman, S. A.: Photoreduction of manganese oxides in seawater, Marine Chemistry, 46, 133-152, 1994.

Sunda, W. G., and Huntsman, S. A.: Cobalt and zinc interreplacement in marine phytoplankton: Biological and geochemical implications, Limnology and Oceanography, 1404-1417, 1995.

Tagliabue, A., Bopp, L., Dutay, J. C., Bowie, A. R., Chever, F., Jean-Baptiste, P., Bucciarelli, E., Lannuzel, D., Remenyi, T., Sarthou, G., Aumont, O., Gehlen, M., and Jeandel, C.: Hydrothermal contribution to the oceanic dissolved iron inventory, Nature Geoscience, 3, 252-256, 2010.

Tagliabue, A., Aumont, O., and Bopp, L.: The impact of different external sources of iron on the global carbon cycle, Geophysical Research Letters, 41, 920-926, 2014.

Taylor, S. R.: Abundance of chemical elements in the continental crust: a new table, Geochimica Et Cosmochimica Acta, 28, 1273-1285, 1964.

Taylor, S. R., and McLennan, S. M.: The geochemical evolution of the continental crust, Reviews of Geophysics, 33, 241-265, 10.1029/95RG00262, 1995.

Tebo, B. M., Clement, B. G., and Dick, G. J.: Biotransformations of manganese, Manual of Environmental Microbiology, 3, 1223-1238, 2007.

Tegen, I.: Modeling the mineral dust aerosol cycle in the climate system, Quaternary Science Reviews, 22, 1821-1834, 2003.

Thuróczy, C.-E., Alderkamp, A.-C., Laan, P., Gerringa, L. J. A., Mills, M. M., Van Dijken, G. L., De Baar, H. J. W., and Arrigo, K. R.: Key role of organic complexation of iron in sustaining phytoplankton blooms in the Pine Island and Amundsen Polynyas (Southern Ocean), Deep Sea Research Part II: Topical Studies in Oceanography, 71–76, 49-60, http://dx.doi.org/10.1016/j.dsr2.2012.03.009, 2012.

Tovar-Sanchez, A., Duarte, C. M., Hernández-León, S., and Sañudo-Wilhelmy, S. A.: Krill as a central node for iron cycling in the Southern Ocean, Geophysical Research Letters, 34, L11601, 10.1029/2006GL029096, 2007.

Trouwborst, R. E., Clement, B. G., Tebo, B. M., Glazer, B. T., and Luther, G. W.: Soluble Mn (III) in suboxic zones, Science, 313, 1955-1957, 2006.

Tsuda, A., Saito, H., Nishioka, J., Ono, T., Noiri, Y., and Kudo, I.: Mesozooplankton response to iron enrichment during the diatom bloom and bloom decline in SERIES (NE Pacific), Deep Sea Research Part II: Topical Studies in Oceanography, 53, 2281-2296, http://dx.doi.org/10.1016/j.dsr2.2006.05.041, 2006.

Turner, A., and Martino, M.: Modelling the equilibrium speciation of nickel in the Tweed Estuary, UK: Voltammetric determinations and simulations using WHAM, Marine Chemistry, 102, 198-207, http://dx.doi.org/10.1016/j.marchem.2006.04.002, 2006.

Turner, D. R., Whitfield, M., and Dickson, A. G.: The equilibrium speciation of dissolved components in freshwater and seawater at 25°C and 1 atm pressure, Geochimica et Cosmochimica Acta, 45, 855-881, 1981.

Twining, B. S., and Baines, S. B.: The trace metal composition of marine phytoplankton, Annual review of marine science, 5, 191-215, 2013.

Twining, B. S., Nodder, S. D., King, A. L., Hutchins, D. A., LeCleir, G. R., DeBruyn, J. M., Maas, E. W., Vogt, S., Wilhelm, S. W., and Boyd, P. W.: Differential remineralization of major and trace elements in sinking diatoms, Limnology and Oceanography, 59, 689-704, 2014.

Ussher, S. J., Achterberg, E. P., Powell, C., Baker, A. R., Jickells, T. D., Torres, R., and Worsfold, P. J.: Impact of atmospheric deposition on the contrasting iron biogeochemistry of the North and South Atlantic Ocean, Global Biogeochem. Cycles, n/a-n/a, 2013.

van der Merwe, P., Lannuzel, D., Nichols, C. A. M., Meiners, K., Heil, P., Norman, L., Thomas, D. N., and Bowie, A. R.: Biogeochemical observations during the winter-spring transition in East Antarctic sea ice: Evidence of iron and exopolysaccharide controls, Marine Chemistry, 115, 163-175, 2009.

van der Merwe, P., Lannuzel, D., Bowie, A. R., and Meiners, K. M.: High temporal resolution observations of spring fast ice melt and seawater iron enrichment in East Antarctica, Journal Of Geophysical Research-Biogeosciences, 116, G03017-G03017, 2011.

van der Merwe, P., Bowie, A. R., Quéroué, F., Armand, L., Blain, S., Chever, F., Davies, D., Dehairs, F., Planchon, F., and Sarthou, G.: Sourcing the iron in the naturally-fertilised bloom around the Kerguelen Plateau: particulate trace metal dynamics, Biogeosciences Discussions, 11, 13389-13432, 2014.

van der Merwe, P., Bowie, A. R., Quéroué, F., Armand, L., Blain, S., Chever, F., Davies, D., Dehairs, F., Planchon, F., Sarthou, G., Townsend, A. T., and Trull, T. W.: Sourcing the iron in the naturally fertilised bloom around the Kerguelen Plateau: particulate trace metal dynamics, Biogeosciences, 12, 739-755, 10.5194/bg-12-739-2015, 2015.

Vega, M., and van den Berg, C. M. G.: Determination of cobalt in seawater by catalytic adsorptive cathodic stripping voltammetry, Analytical Chemistry, 69, 874-881, 1997.

Wagener, T., Guieu, C., Losno, R., Bonnet, S., and Mahowald, N.: Revisiting atmospheric dust export to the Southern Hemisphere ocean: Biogeochemical implications, Global Biogeochemical Cycles, 22, GB2006-GB2006, 2008.

Witt, M., Baker, A. R., and Jickells, T. D.: Atmospheric trace metals over the Atlantic and South Indian Oceans: Investigation of metal concentrations and lead isotope ratios in coastal and remote marine aerosols, Atmospheric Environment, 40, 5435-5451, 2006.

Wolfe-Simon, F., Grzebyk, D., Schofield, O., and Falkowski, P. G.: The role and evolution of superoxide dismutases in algae, Journal Of Phycology, 41, 453-465, 2005.

Wolfe-Simon, F., Starovoytov, V., Reinfelder, J. R., Schofield, O., and Falkowski, P. G.: Localization and role of manganese superoxide dismutase in a marine diatom, Plant Physiology, 142, 1701-1709, 2006.

Wu, J., Boyle, E., Sunda, W., and Wen, L.-S.: Soluble and colloidal iron in the oligotrophic North Atlantic and North Pacific, Science, 293, 847-849, 2001.

Wu, J., Wells, M. L., and Rember, R.: Dissolved iron anomaly in the deep tropical–subtropical Pacific: Evidence for long-range transport of hydrothermal iron, Geochimica et Cosmochimica Acta, 75, 460-468, 2011.

Wu, J. F., and Boyle, E. A.: Low blank preconcentration technique for the determination of lead, copper, and cadmium in small-volume seawater samples by isotope dilution ICPMS, Analytical Chemistry, 69, 2464-2470, 1997.

Wuttig, K., Wagener, T., Bressac, M., Dammshauser, A., Streu, P., Guieu, C., and Croot, P. L.: Impacts of dust deposition on dissolved trace metal concentrations (Mn, Al and Fe) during a mesocosm experiment, Biogeosciences, 10, 2583-2600, 2013.

Xu, Y., and Wang, W.-X.: Fates of diatom carbon and trace elements by the grazing of a marine copepod, Marine ecology. Progress series, 254, 225-238, 2003.

Xu, Y., and Morel, F. M. M.: Cadmium in Marine Phytoplankton, in: Cadmium: From Toxicity to Essentiality, Springer, 509-528, 2013.

Xue, H. B., Jansen, S., Prasch, A., and Sigg, L.: Nickel Speciation and Complexation Kinetics in Freshwater by Ligand Exchange and DPCSV, Environmental Science & Technology, 35, 539-546, 10.1021/es0014638, 2001.

Yeats, P. A., and Bewers, J. M.: Manganese in the western north Atlantic Ocean, Marine Chemistry, 17, 255-263, 1985.

Zhang, W., and Wang, W.-X.: Colloidal organic carbon and trace metal (Cd, Fe, and Zn) releases by diatom exudation and copepod grazing, Journal of experimental marine biology and ecology, 307, 17-34, 2004.

Zhou, M., Zhu, Y., d'Ovidio, F., Park, Y.-H., Durand, I., Kestenare, E., Sanial, V., Van-Beek, P., Queguiner, B., Carlotti, F., and Blain, S.: Surface currents and upwelling in Kerguelen Plateau regions, Biogeosciences Discuss., 2014.

Zhu, X. R., Prospero, J. M., and Millero, F. J.: Diel variability of soluble Fe(II) and soluble total Fe in North African dust in the trade winds at Barbados, Journal Of Geophysical Research-Atmospheres, 102, 21297-21305, 1997.